Appendix 7-A

Dredge Modelling

WorleyParsons
resources & energy

EcoNomics™

RIO TINTO ALCAN

South of Embley Project

Marine Environmental Modelling of Dredging Methods for the Proposed Port

301001-01069 – 00-EN-REP-0014

Updated 13 February 2013

Level 3, 60 Albert Street
Brisbane QLD 4000
Australia
Telephone: +61 7 3239 7400
Facsimile: +61 7 3221 7791
www.worleyparsons.com
ABN 61 001 279 812

SYNOPSIS

Rio Tinto Alcan (RTA) has requested WorleyParsons to conduct studies to investigate options for the development of a new port facility approximately 40km south of Weipa on the eastern side of the Gulf of Carpentaria. The port will form part of the infrastructure required to service a potential bauxite mining operation currently under investigation by RTA.

This study presents a comparative assessment of the impact of two separate dredging methodologies considered for the proposed port construction.

Disclaimer

PROJECT 301001-01069 - SOUTH OF EMBLEY PROJECT

REV	DESCRIPTION	ORIG	REVIEW	WORLEY-PARSONS APPROVAL	DATE	CLIENT APPROVAL	DATE
A	Issued for Internal Review	M Zed	C Ryan	A Butcher	29-Aug-12	N/A	
0	Issued as Final	M Zed	D Parry	A Butcher	5-Sep-12		N/A
1	Reissued as Final	M Zed	D Parry	A Butcher	12-Oct-12		N/A
2	Reissued as Final	M Zed	D Parry	A Butcher	26-Oct-12		N/A
3	Reissued as Final	M Zed	D Parry	A Butcher	7-Nov-12		
4	Data updates	M Zed	D Parry	A Butcher	31-Jan-13		
5	Data updates	M Zed	D Parry	A Butcher	13-Feb-13		

EXECUTIVE SUMMARY

Rio Tinto Alcan (RTA) has requested WorleyParsons to conduct studies that investigate options for the development of a new marine port facility approximately 40 km south of Weipa, which is located on the eastern side of the Gulf of Carpentaria.

This report assesses the potential marine and coastal impacts of two separate dredging methodologies (including disposal) considered for initial capital dredging of the proposed South of Embley (SoE) Port facility.

The study approach was developed around investigations in relation to quantifying the potential impacts of dredging and spoil disposal on water quality, through assessment of total suspended sediment concentration (TSS), and sedimentation. This was achieved through utilisation of numerical models of hydrodynamic and coastal processes, in addition to short term data collection at the site that included currents, water depth, wave conditions, and turbidity.

The accuracy of the results obtained in this study has been ensured through detailed interrogation of all datasets utilised in the model development and supported through the high level of skill provided in the hydrodynamic and wave model forcing functions. The entire dredging program was modelled under two separate dredging options, following the validation of the sediment transport model for the region, inclusive of expected downtime of dredging operations and variable meteorological and oceanographic forcing over the respective dredging programs.

Key results from the marine environmental modelling of the Port's initial capital dredging and spoil disposal operations are as follows:

Suspended Sediment Concentration

The TSS resulting from the dredging operations was characterised through analysis of the median and 80th percentile maps, timeseries at sensitive receptor sites and exceedance of set concentration limits as a percentage of the total dredging duration. This multi-faceted approach to the analysis enabled the plume behavior to be defined and characterised in detail across the two dredging options.

The main findings of the sediment fate model are listed below.

- The turbid plume generated by Port area initial capital dredging extends generally parallel to the coast, from beyond Pera Head and Thud Point in the south (migrating during flood tide) to Boyd Point in the north (migrating during ebb tide).
- The net south-west tidal current direction causes suspended material to accumulate between the proposed Port and Pera Head, with the plume extending up to 27 km south of the proposed development (at concentrations >2 mg/L above background).
- Periods of elevated TSS concentration generally coincide with the TSHD and CSD operating in the inshore area during dredging of the top layer of sediments, as a result of the higher content of fines in this layer. Whilst Boyd Point experiences higher instantaneous TSS levels (due to its closer proximity to the dredging operations), Pera Head is predicted to receive more consistently elevated TSS levels due to the net migration south.
- Comparatively, the CSD and TSHD option is shown to produce a larger plume in the nearshore than the CSD and SHB option. This is the result of the multiple discharge sources acting

simultaneously and additional discharge from the CSD diffuser contributing to the larger plume present under this dredging methodology.

- The CSD and TSHD option not only produces higher instantaneous and daily average concentrations, but also a more prolonged plume in this vicinity due to the longer dredging operations.
- Offshore at the Nine Mile Reef receptor sites, concentrations are shown to be consistently low under both dredging options, with the instantaneous depth-averaged TSS less than 5 mg/L, and daily average less than 3 mg/L, under both dredging methodologies.
- Due to the larger hopper volume of material being dumped by the TSHD, the instantaneous TSS concentrations at the proposed new spoil ground (offshore) are higher under the CSD and TSHD case; however, the daily-averaged TSS is comparable amongst both cases due to the more frequent SHB dumping.
- Depth-variation in TSS is significant for both dredging options, with peak daily near-seabed TSS concentrations often double those near the surface.

Total Sedimentation

Sedimentation predicted in the dredge dispersion model was assessed through analysing the mean daily deposition rate over the entire model simulation. In this analysis the deposition rate over the dredging period combining all particle classes was selected as it presented the most indicative level of expected deposition over the dredging program.

Key findings from the analysis of the sedimentation predicted by the model were:

- Areas between Pera Head and Boyd Point are expected to experience the highest deposition rates under both dredging options, with rates outside of this area expected to be negligible compared to the background rates at Pera Head of 17 mg/cm^2/day and 63 mg/cm^2/day in the dry and wet seasons, respectively;
- At both the nearshore and offshore locations, sedimentation is predicted to be lower under the CSD and SHB dredging option;
- Model predictions near the reef areas immediately offshore from Pera Head show the median above-ambient deposition as less than 2.0 mg/cm^2/day under the CSD and TSHD case, and less than 0.8 mg/cm^2/day under the CSD and SHB case;
- The highest sedimentation rates, in excess of 7.5 mg/cm^2/day above background for the CSD and TSHD case, are in the immediate vicinity (within 500 m) of the dredge footprint. Sedimentation rates of approximately 5.0 mg/cm^2/day are expected under the CSD and SHB option;
- The reef colony immediately south of the dredge area (approximately 1 km to the southwest) is the only site expected to receive a daily sedimentation rate in excess of 5.0 mg/cm^2/day for more than 80 % of the dredging operation for the CSD and TSHD case, and below 3.0 mg/cm^2/day for the CSD and SHB option;
- Variable conditions at the proposed new spoil ground (offshore) during the separate SHB disposals result in a low mean daily sedimentation, where as the TSHD disposal, given its

larger load and disposal over a short timeframe, results in a larger level of sedimentation, of up to 3 mg/cm^2/day as depicted in the 80th percentile; and

- Deposition rates above background (0.5 to 2 mg/cm^2/day) would not extend beyond 4km outside the proposed new spoil ground area for either dredging methodologies. The increase in deposition outside the proposed new spoil ground area is expected to be negligible compared to the mean background rates in the area of 47 mg/cm^2/day and 31 mg/cm^2/day for dry and wet season, respectively.

While the suspended sediment concentrations and sedimentation rates are lower for the CSD and SHB compared to the CSD and TSHD method, both methods result in suspended sediment plumes and sedimentation rates that are within the range of the relatively high and variable background at the proposed Port and new spoil disposal site.

Estimated Maintenance Dredging Requirements

The predicted average siltation depth in the berth pockets, departure area, and departure channel in an average year varies from 0.35 m to 0.87 m. The predicted total annual volume required for maintenance dredging is 420,000 m^3 for the 2.6 million m^3 dredge volume case. This was calculated for a typical year of wave and wind conditions and, as such, it is expected that a potentially significant year to year variation in the wave climate based on the frequency of storms may lead to higher or lower siltation levels.

CONTENTS

GLOSSARY

RTA	Rio Tinto Alcan
SoE	South of Embley
CD	Chart Datum
EPA	Queensland Environmental Protection Agency
BoM	Bureau of Meteorology
LAT	Lowest Astronomical Tide
GA	GeoScience Australia
HAT	Highest Astronomical Tide
AHD	Australian Height Datum
H_{sig} (or H_s)	Significant wave height. Average of the highest one-third of waves in each recording cycle.
T_{peak} (or T_p)	Peak energy wave period.
Pdir	Peak energy wave direction
PSD	Particle Size Distribution
ADCP	Acoustic Doppler Current Profiler
TSS	Total Suspended Solids
TC	Tropical Cyclone
ntu	Nephelometric turbidity units
mg/l	milligrams per litre

1 INTRODUCTION

RTA requested WorleyParsons to undertake marine component studies in relation to an EIS for the development of a new Port facility approximately 40km south of Weipa on the eastern side of the Gulf of Carpentaria.

The Port facility forms part of the infrastructure required to service a potential bauxite mining operation currently under investigation by RTA. Based on the most recently proposed design scenario, construction of the Port facility includes initial capital dredging of approximately 2.6 million m^3 of material (Figure 1-1). This design involves dredging the departure area to approximately 17.8 m below Lowest Astronomical Tide (LAT) (declared depth of 17.3 mLAT), a single Capesize berth pocket to 20.2 mLAT (declared depth 19.7 mLAT) and DPPV berth pocket to 14.9 mLAT (14.4 mLAT).

This assessment describes the existing physical marine environment including water quality and sediment properties in the vicinity of the Project area, the associated environmental values, and any potential impacts associated with the proposed Project.

The general study area, illustrated in Figure 1-2, used to describe the existing marine environment and predict the environmental impacts from the proposed Project includes:

- Albatross Bay (including rivers and creeks) bound by Jantz Point in the north and Pera Head in the south; and
- An area extending 16 km westward, offshore from Albatross Bay.

This area includes all components of the Project including the proposed Port site, the proposed new spoil ground, offshore of Boyd Point, the existing Albatross Bay spoil ground and the proposed location of the barge and ferry facilities at Hornibrook Point, Humbug terminal and Hey River terminal, in the Embley River. The proposed Port site and the proposed new spoil ground offshore from Boyd Point are specifically examined in this report.

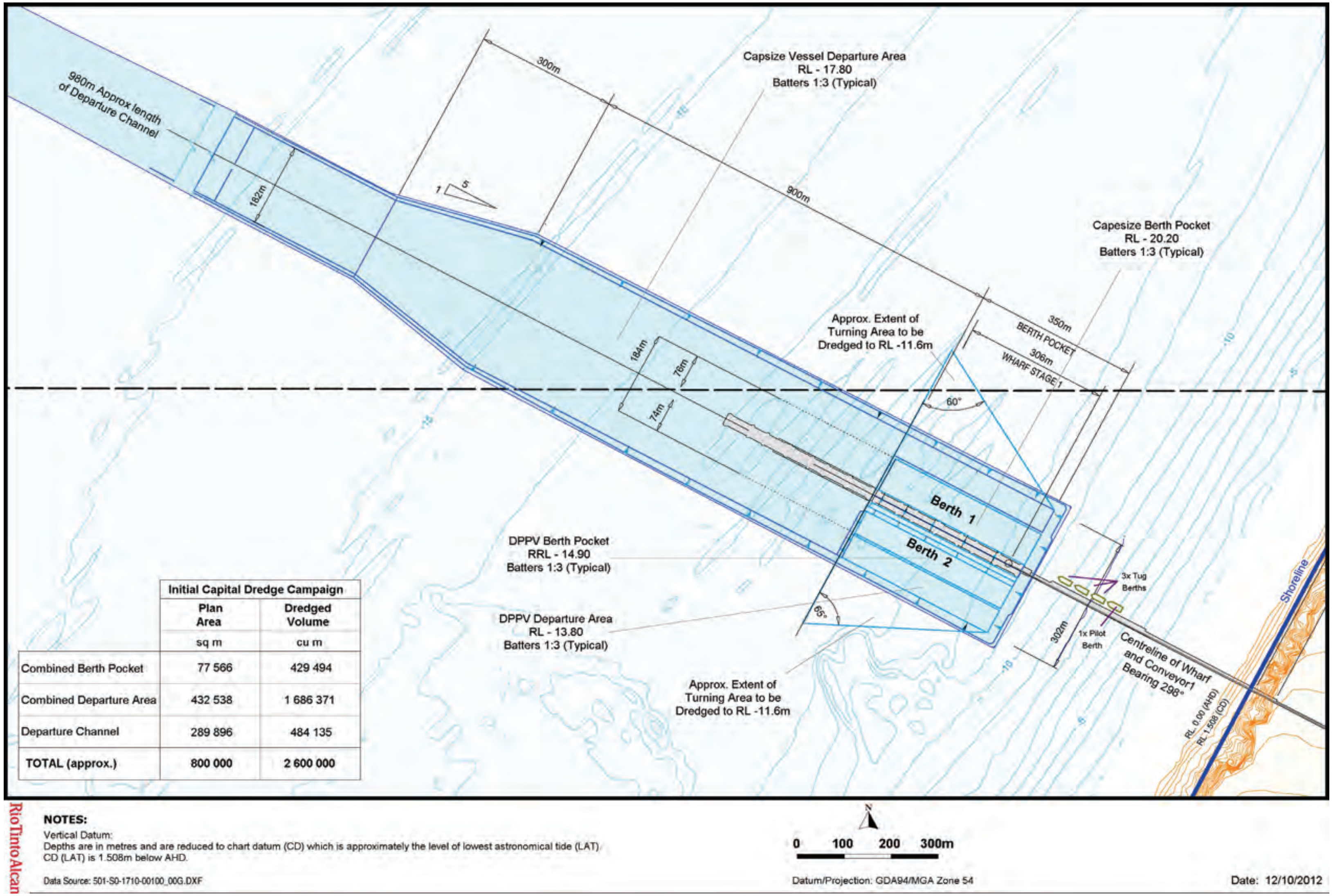

Initial Capital Dredge Campaign	Plan Area	Dredged Volume
	sq m	cu m
Combined Berth Pocket	77 566	429 494
Combined Departure Area	432 538	1 686 371
Departure Channel	289 896	484 135
TOTAL (approx.)	800 000	2 600 000

Figure 1-1 SoE Port Facility dredge and berth design for 2.6 Mm3 layout (Drawing No. 25403-501-S0-1721-00100-RevC dated 22 December 2011). Dashed line is ML7024 lease boundary.

Figure 1-2 Locality plan – Proposed Boyd (SoE) Port site and proposed new spoil ground in relation to the existing Albatross Bay (Port of Weipa) spoil ground

1.1 Scope of Works

This report assesses the potential marine and coastal impacts of two separate dredging methodologies (including spoil disposal) considered for initial capital dredging for the proposed Port facility.

The study approach was developed around investigations in relation to quantifying the potential impacts of dredging and spoil disposal on water quality, through assessment of total suspended sediment concentration (TSS), and sedimentation. This was achieved through utilisation of state-of-the-art numerical models of hydrodynamic and coastal processes in addition to short term data collection at the site that included currents, water depth, wave conditions, and turbidity.

Coastal processes at the site are dependent upon currents, waves, and sediments that are specific to the Boyd Point area. Measurements and observations of coastal parameters are more regular in Albatross Bay where existing port operations are of interest, or within deeper waters of the Gulf of Carpentaria where research programs have been undertaken. Although some local data was collected as part of this study, numerical modelling has been utilised extensively to provide currents, water levels, and wave conditions for the type of investigation being conducted.

As the sediment transport model represents the integration of numerous modules with physical site data, it is necessary to clarify the overall strategy employed in the modelling process. To aid in this, the diagram shown in Figure 1-3 illustrates the integration of the various elements employed in the modelling process and their relation to the environmental impact assessment.

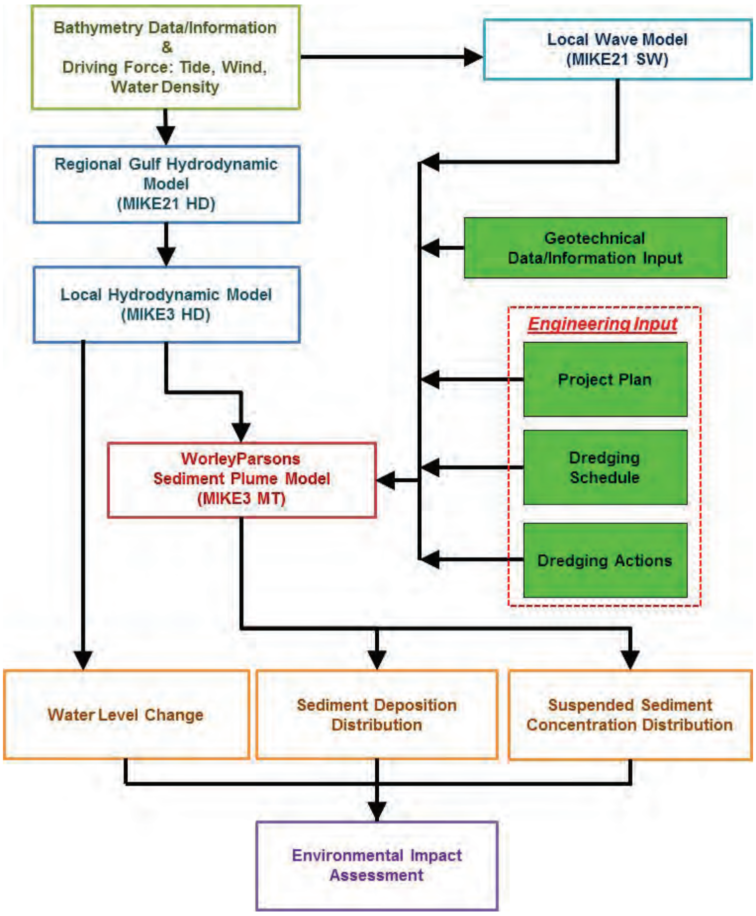

Figure 1-3 Schematic of the sediment dispersion modelling process.

As illustrated in the schematic, the sediment dispersion study involved using wave, gulf-scale hydrodynamic and local three-dimensional hydrodynamic models within the oceanographic setting of the Gulf. The models need to both resolve the complex bathymetry and be capable of accurately representing metocean conditions in the nearshore areas of the proposed development. Wetting and drying of the inter-tidal flats also needs to be properly represented in the model.

For sediment plume modelling studies, it is important that the model domain is sufficient to encompass the total area affected by the sediment plumes arising from the proposed dredging. The total area affected not only includes the initial extent of the sediment plume and deposition, but also areas affected following the reworking of sediments, which occurs through re-suspension and subsequent transport. As such, it is necessary to ensure that accurate wave and hydrodynamic inputs are used to force the sediment transport model. For correct characterisation of the wave and hydrodynamic climate, the domain of the study must be large enough to properly capture wind energy transfer to the sea surface over long fetches, of the order of 50-100 km.

The sediment transport model must account for the particle-size specific sinking, sedimentation and re-suspension of sediments given the range of current and wave conditions indicated for the area, as derived by the hydrodynamic and wave models. The model must also account for the effects of sediment cohesion (i.e. clumping) on sinking rates of fine particles and the effects of sedimentation history, burial and armouring on re-suspension rates. In consideration of this, detailed site-specific geotechnical information is a necessary input for the sediment transport model. The sediment transport model should also be able to simulate any possible hydrodynamic changes as a result of morphological variation during the simulation.

Other necessary inputs are specific to the Project and relate to the dredging operation itself. Details of the dredge vessel to be utilised, transport and disposal plans for the removed material, schedule and production rates are all necessary inputs for the model.

All of these requirements have been considered in selecting the optimal models to employ for this study.

2 METOCEAN

2.1 General Oceanography

Within the Gulf of Carpentaria, complex hydrodynamics result from a combination of tidal dynamics, meteorology and the fact that the Gulf effectively acts as an enclosed body of water receiving an exchange of water at its northern entrances. Of the two entrances to the Gulf to the North, the Arafura Sea is dominant since the Torres Strait is shallow and contains numerous reefs, shoals, and islands.

Much of the Gulf is reasonably shallow. A deeper area exists near the centre with no prominent shoals or reefs. The average depth within the Gulf is approximately 42m, with the deeper, central parts averaging approximately 65m. A few large islands are located in the south.

Tidal signals around the Gulf of Carpentaria are semi-diurnal in the north, decreasing rapidly towards a diurnal signal in the south to locations such as Karumba where diurnal constituents K1 and O1 dominate. Weipa tide signals are mixed but mainly diurnal (see Section 2.2). In the Gulf, a tidal wave enters from the north-west and propagates clockwise around the Gulf about its amphidrome (the nodal point about which the tide rotates).

Seasonal fluctuations in sea level occur in the Gulf of Carpentaria and these are primarily due to trade winds and forcing from the Arafura Sea (Wolanski, 1993). Circulations and gyres within the Gulf can also be setup by tropical cyclones during the wet season that apply significant wind stress to the sea surface and provide sufficient energy for mixing over the water depth.

2.2 Tidal Planes

Figure 2-1and Figure 2-2 show that the tidal signal at Weipa is predominantly diurnal with short periods of semi-diurnal tides at times of neaps. Figure 2-1 clearly shows the two tides each day during the neap phase that transform to the diurnal signal going into the spring tide, while Figure 2-2 provides a four month overview of the signal showing inequality of successive spring tide ranges. Careful examination of Figure 2-2 also reveals the changing length of the semi-diurnal signal and its asymmetry about the neap-spring tide junction.

The relative importance of diurnal and semidiurnal tidal constituents can be expressed in terms of the following Form Factor ‘F’, where the amplitude of the constituent is given by ‘H’.

$$F = \left(\frac{H_{K1} + H_{O1}}{H_{M2} + H_{S2}} \right)$$

For Weipa the Form Factor is 1.53 which identifies the tidal variation as mixed, mainly diurnal (F > 1.5).

Table 2-1 is a summary of tidal planes at Weipa and is referred to Australian Height Datum (AHD). At Weipa (Humbug Point) this is 1.752 m above Lowest Astronomical Tide (LAT) and at Boyd Point it is 1.508m above LAT.

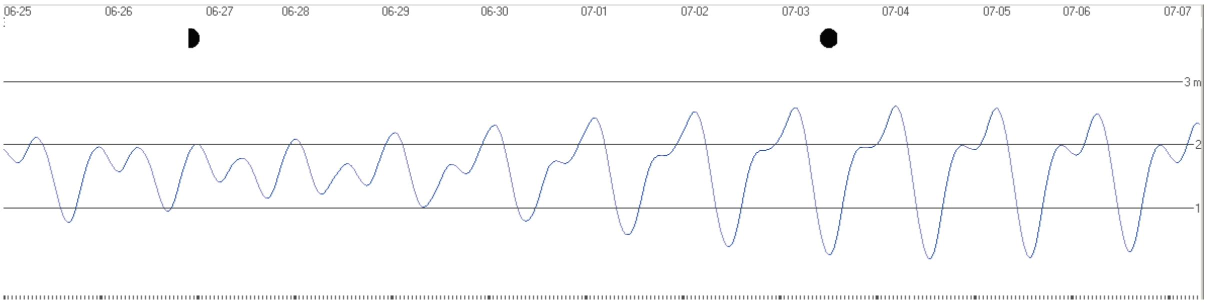

Figure 2-1 Weipa tidal signal (prediction 25 June to 7 July 2008)

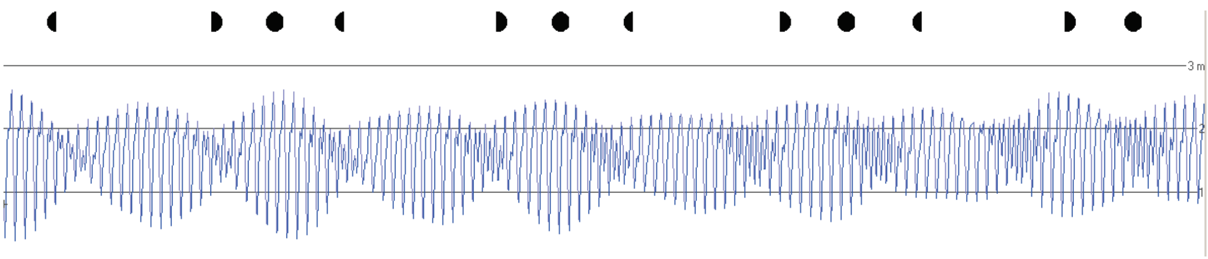

Figure 2-2 Weipa tidal signal (prediction 5 June to 6 October 2008)

Table 2-1 Tidal Planes at Weipa

Tidal Plane	Weipa (m)	Boyd Pt (m)
HAT (Highest Astronomical Tide)	3.38	3.09
MHHW (Mean High High-Water)	3.0	2.73
MLHW (Mean Low High-Water)	2.2	2.17
MSL (Mean Sea Level)	1.85	1.76
MHLW (Mean High Low-Water)	1.5	1.35
MLLW (Mean Low Low-Water)	0.7	0.8
LAT (Lowest Astronomical Tide)	0.0	0.0

Figure 2-3 contains information on the tidal phase-lags at the standard port (▲ Weipa), and the secondary ports (● such as Archer River, and Pennefather River). A negative time of -1:07 at the secondary port of Pennefather River refers to the tide occurring one hour and seven minutes before Weipa and a positive time of +0:30 at Archer River refers to the tide occurring thirty minutes after Weipa.

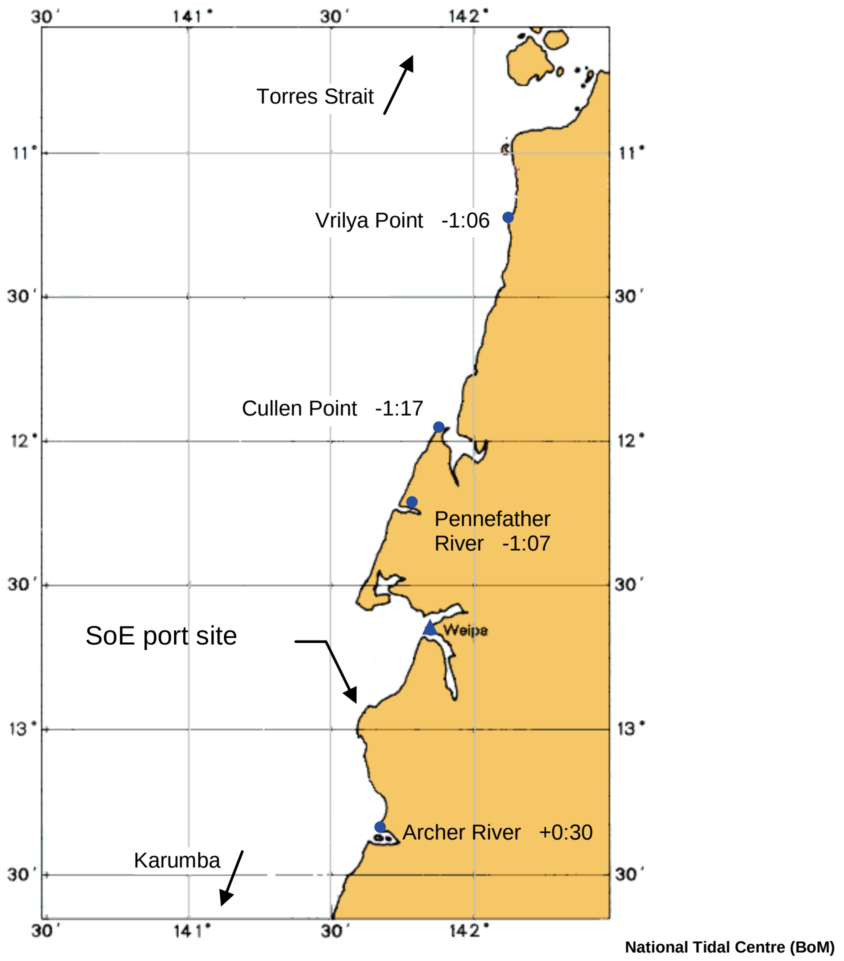

Figure 2-3 Weipa tide phase

Figure 2-4 is a typical spectrum of the tidal observations and of the non-tidal residuals at Weipa (ICSM, 2008). It shows that there is additional energy in the residuals at the same frequency as the observations, which means that additional constituents could be chosen to better match the observations, i.e. the prediction does not fully explain the tidal observations. This would be subject to sufficient data being available to resolve additional tidal constituents that could then be incorporated into the prediction.

Additional energy across all frequency bands in the non-tidal residuals could also be attributed to meteorological forcing.

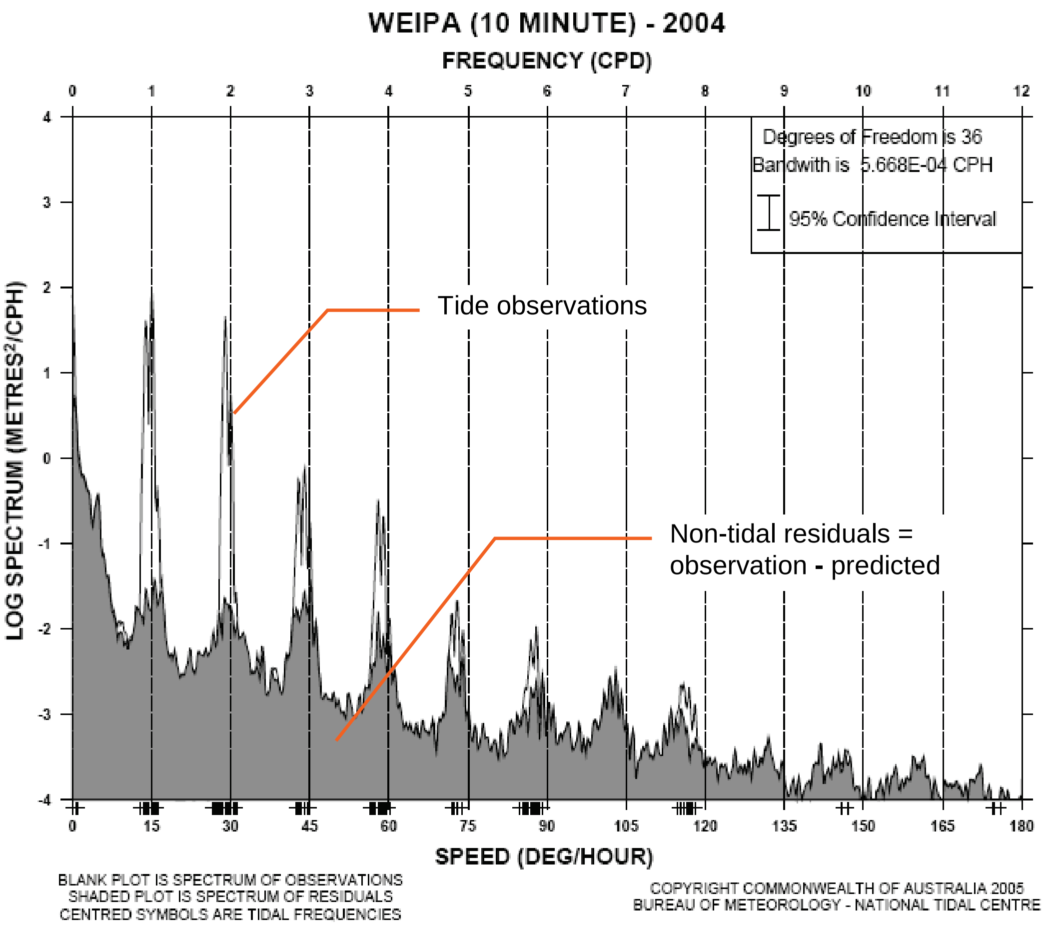

Figure 2-4 Weipa tide energy spectra

2.3 Meteorology

The Weipa region has a tropical monsoonal climate with a distinct wet (December to April) and dry (May to November) season. The region typically experiences light to moderate southeast to east winds during the dry season and light tending to moderate northwest to westerly winds during the wet season. Fresh winds occur with the active monsoon (see Figure 2-5), however, strong or gale force winds normally only occur with tropical cyclones. The average annual rainfall is greater than 2m, with most falling between December and April as indicated in Table 2-2.

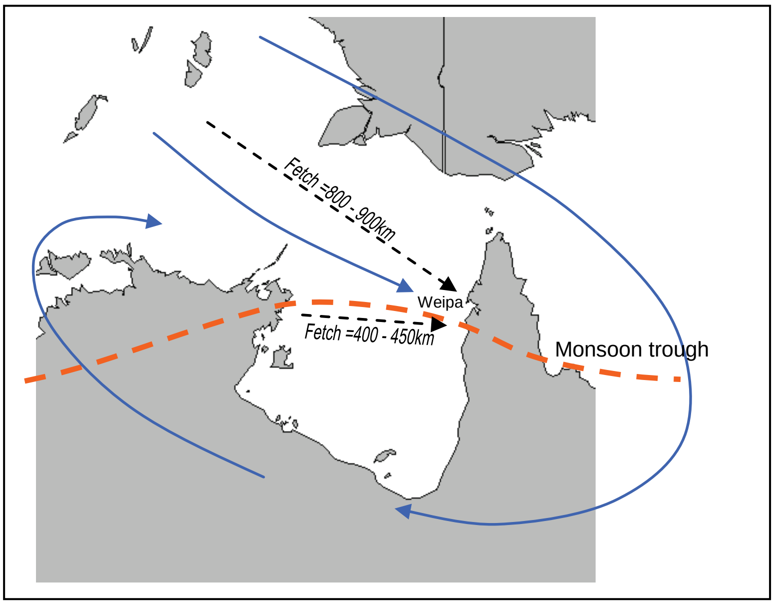

Figure 2-5 Active monsoon across the Gulf of Carpentaria

Table 2-2 Mean air temperature and rainfall, Weipa Aero

	Jan	Feb	Mar	Apr	May	Jun	Jul	Aug	Sep	Oct	Nov	Dec
Mean Max. °C	32.0	31.3	31.8	32.3	31.9	31.1	30.9	31.8	34.2	35.5	35.6	33.7
Mean Min. °C	24.2	24.1	23.8	22.8	21.3	19.8	18.7	18.4	19.5	21.7	23.4	24.2
Mean Rain mm	445.2	565.4	432.7	93.2	23.3	4.6	1.2	7.6	1.9	15.9	94.0	279.4

Wind data was obtained from the Bureau of Meteorology (BoM) site "WEIPA AERO" (station 027045) for the 12 year period from 12 October 1995 to 27 February 2008. The Automatic Weather Station (AWS) is situated approximately 60kms from the study site at an elevation of 18m. A frequency analysis for all hourly data, 9am data, and 3pm data was carried out and results presented in Figure 2-6.

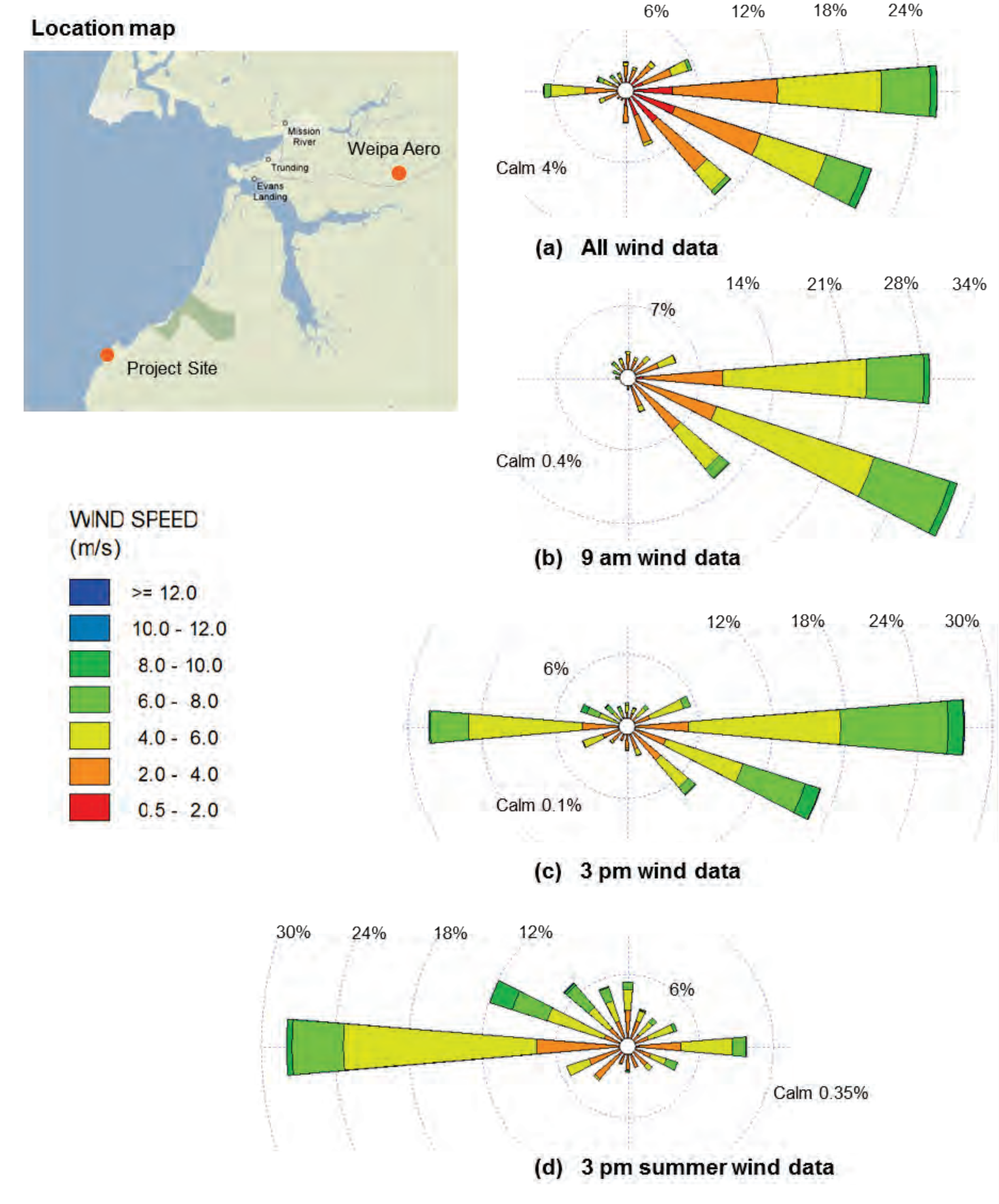

Figure 2-6 Wind Roses for Weipa Aero (based on hourly records from October 1995 to February 2008).

The wind roses presented in Figure 2-6 indicate:

- easterly and south-easterly winds occur with the highest frequency; and
- westerly winds associated with the afternoon sea breezes that are more prevalent in the summer months (December through to the end of February).

A frequency analysis of seasonal wind directions is provided in Table 2-3 that quantitatively shows, in the wet season, easterly winds are overall more prevalent, although in the afternoons the westerly breezes tend to dominate. The dominance of easterlies is also apparent across the dry season, with over 50 % directional occurrence from the E and ESE directions.

Table 2-3 Seasonal wind frequency for Weipa Aero

All wind speeds	Wet season (Dec – Apr)	Wet Season 3pm data	Dry Season (May-Nov)
East	20.1%	15.8%	29.2%
East South East	15.5%	9.9%	25.1
West	8.5%	21.9%	5.5%
All other directions (includes missing data & calms)	55.9%	52.4%	40.2%

2.4 Waves

During the dry season (May to November) smooth waters will be typically present at the Project site. Wind strength and direction (refer to Figure 2-6) from westerly afternoon summer sea breezes result in the only conditions favourable for generation of *local* seas.

Large swell waves, in excess of 2.0 m, are rare since the Gulf of Carpentaria is a semi-enclosed body of water, however, occasional significant swells do reach Weipa during periods of sustained high westerly winds across the long fetch of the Gulf and those that originate in the Arafura Sea. Monsoon winds are normally associated with the longer fetch distances (see Figure 2-5).

The Queensland Environmental Protection Agency (EPA, and now Department of Environment & Heritage Protection (DEHP)) has operated a wave buoy site in Albatross Bay since 1978 that is located as shown in Figure 2-7. The WaveRider® buoy system was deployed in 6.8m water depth relative to AHD from December 1978 to July 1994 and relocated into 5.3m water depth relative to AHD from July 1994 to present. The location itself is partially sheltered from waves incident from the north and northwest as indicated in the figure.

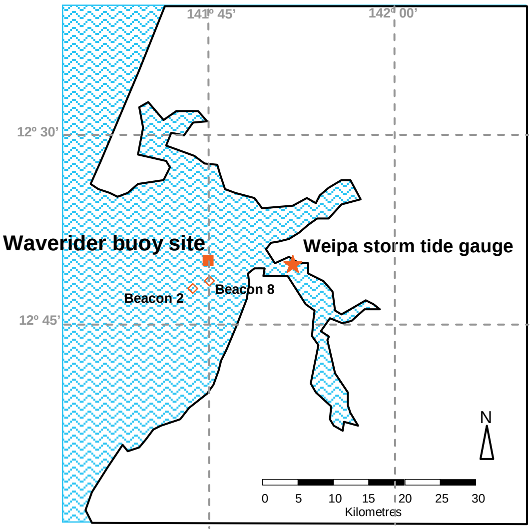

Figure 2-7 Location of Weipa WaveRider buoy

In recent years, the data at this site has included directional wave records. It is exposed to wave directions from Gulf waters through a north-west to south-west sector and in significant storm events that affect Albatross Bay, the buoy could be subject to breaking waves.

Recorded data from this site indicates significant wave heights (H_{sig}) are below 1 m over 95 % of the time on an annual basis, with less than 1 % of records above 1.0 m during the dry season as indicated in Figure 2-8.

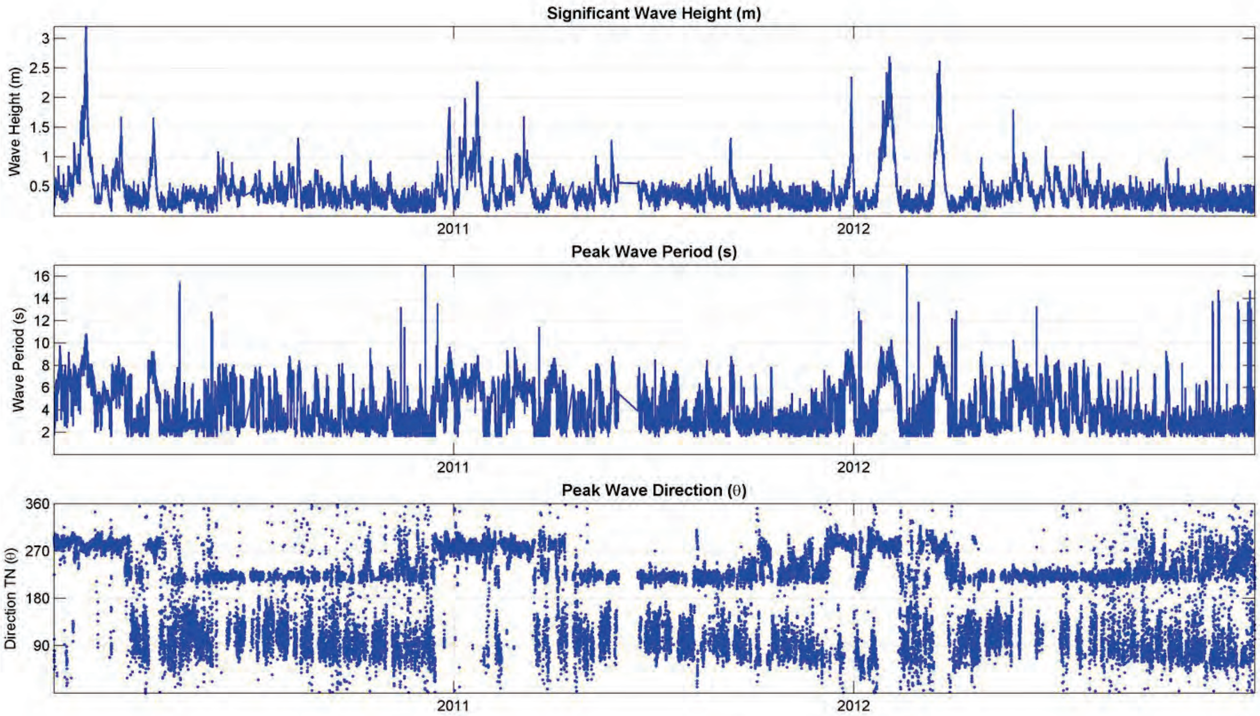

Figure 2-8 Measurements at Weipa WaveRider Buoy over 2010 to 2012 deployment.

2.5 Currents

Current data at the proposed Port site was collected over almost two years. Measurements by Oceanographic Field Services Pty Ltd were undertaken with an Acoustic Doppler Current Profiler (ADCP) located in 14m of water at Boyd Point over the 2006-07 and 2007-08 seasons. The ADCP recorded at 6 minute intervals and currents were measured at every half-metre bin over the water column depth. Figure 2-9 shows a sample of the current speed and direction measured by the ADCP at Boyd Point.

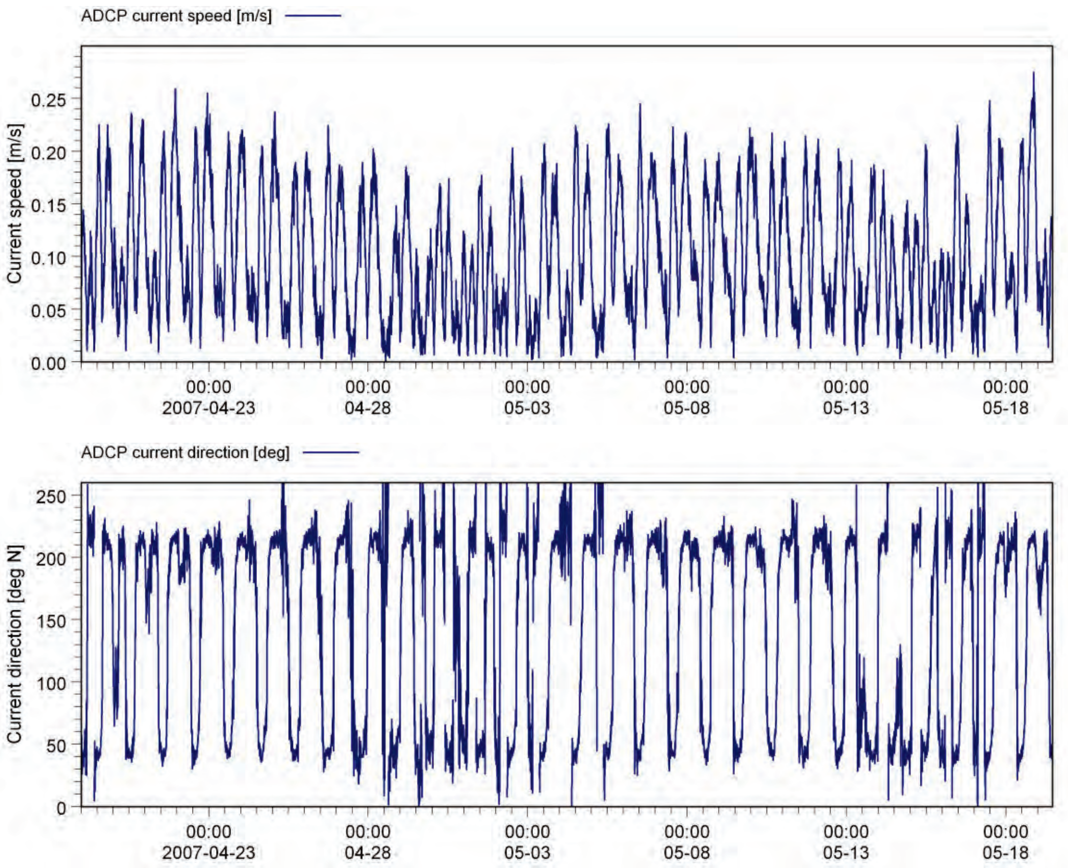

Figure 2-9 Depth-averaged measured current speed (top) and direction (bottom) at study site as measured by ADCP

Current speed was relatively uniform over depth. Average peak spring tide currents were 0.25 m/s and average peak neap tide currents were 0.15 m/s. Currents are predominantly aligned with the coast, typically between 210° and 220°N during flood tides and between 30° and 40°N during ebb tides.

2.6 Temperature and Salinity

Sea water temperature was measured by sensors on the ADCP instrument at the Boyd Point site during the period from August 2006 to March 2008 and averaged values calculated for each month of deployment. Variation in average seawater temperature is approximately 5ºC over the year and ranges between 25ºC and 30ºC with the warmer conditions occurring in the summer months as shown in Figure 2-10. This temperature variation is consistent with Roelofs et al. (2006) who presented water temperature measurements from within Albatross Bay (Evan's Landing) obtained during 2004/05 at intertidal zones. Further to this, Somers & Long (1994) saw similar variations for surface water temperatures, with averages ranging from approximately 24.4^{O}C in July to 31.6^{O}C in November. Somers & Long also found that in the nearshore area, for waters generally less than 35 m depth, there was little vertical stratification present, which agrees with the seabed temperature observations by the ADCP and surface measurements by both Roelofs et al. (2006) and Somers & Long (1994).

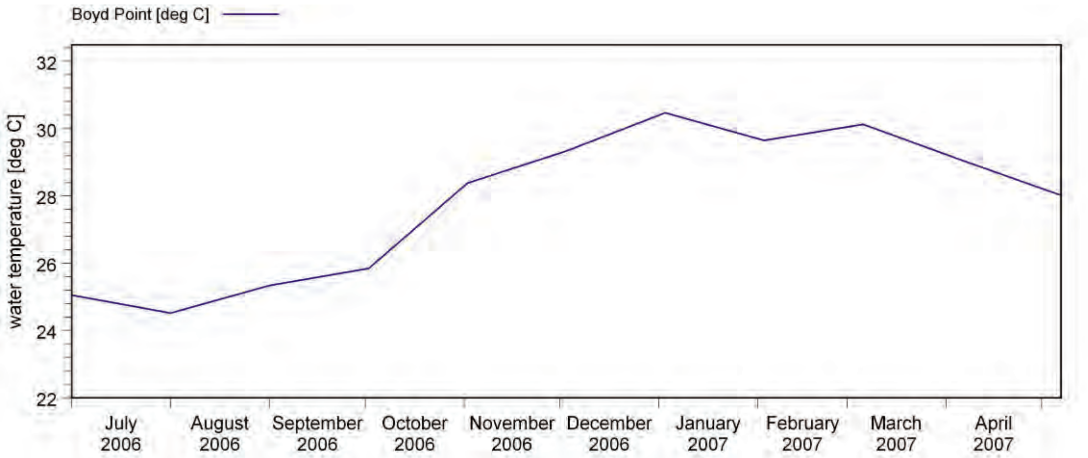

Figure 2-10 Average seawater temperature variation

Salinity in the shallower depths of the Gulf of Carpentaria is typically within the range 33 to 34 PSU with little variation over depth. However, during the peak of the wet season surface salinities may drop as low as 27 PSU (Harris et. al. 2006).

2.7 Sediment Data

Sediment characteristics at the site were identified from vibrocoring undertaken by WorleyParsons and geotechnical work carried out by Coffey Geotechnics Pty Ltd. The location of the relevant sediment samples and boreholes are shown on Figure 2-11. It is noted that all of these seabed investigations were undertaken for previous iterations of the proposed design that were based on a shorter departure channel design and shallower dredged depths.

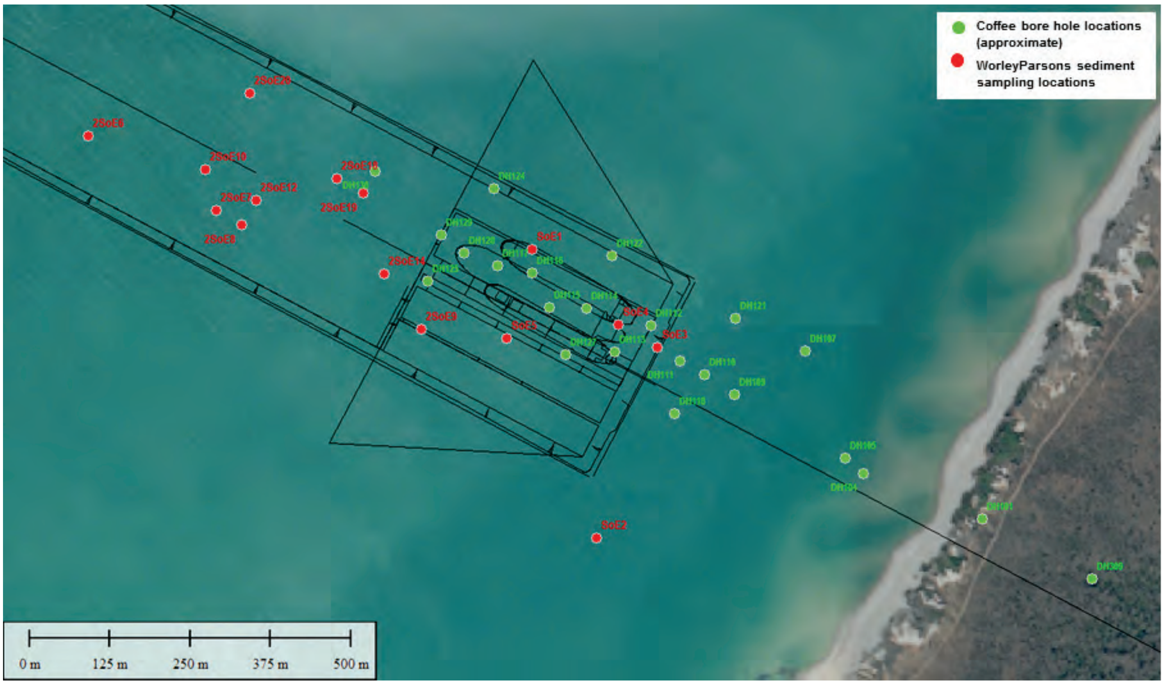

Figure 2-11 Borehole and sediment sampling locations. Red (WorleyParsons) Green (Coffey Geotechnics)

2.7.1 WorleyParsons Vibrocoring 2007

Seabed sediment sampling was conducted by WorleyParsons Services Pty Ltd during October 2007 and nine sediment samples were obtained using a vibrocorer at five sites within the proposed Port area. The sediment particle size distribution (PSD) analysis of samples has been used to describe the bed material. Due to the presence of stiff clays, vibrocoring was restricted to a depth of approximately 1m and at each site an ‘upper’ and ‘lower’ sample was obtained over a depth range of 0 – 0.5m (upper) and 0.5 – 1m (lower), respectively (refusal at 0.5m resulted in only one layer being reported from SoE4).

Figure 2-12 presents percentage fraction PSD results for each vibrocore sediment sample and PSD results are summarised for each location in Table 2-4. As identified in Table 2-4, the deeper waters of the site contain higher fractions of clay and silt material. The remaining material is predominantly sand with a small fraction of gravel. The percentage of sand and gravel is higher for samples collected closer to shore.

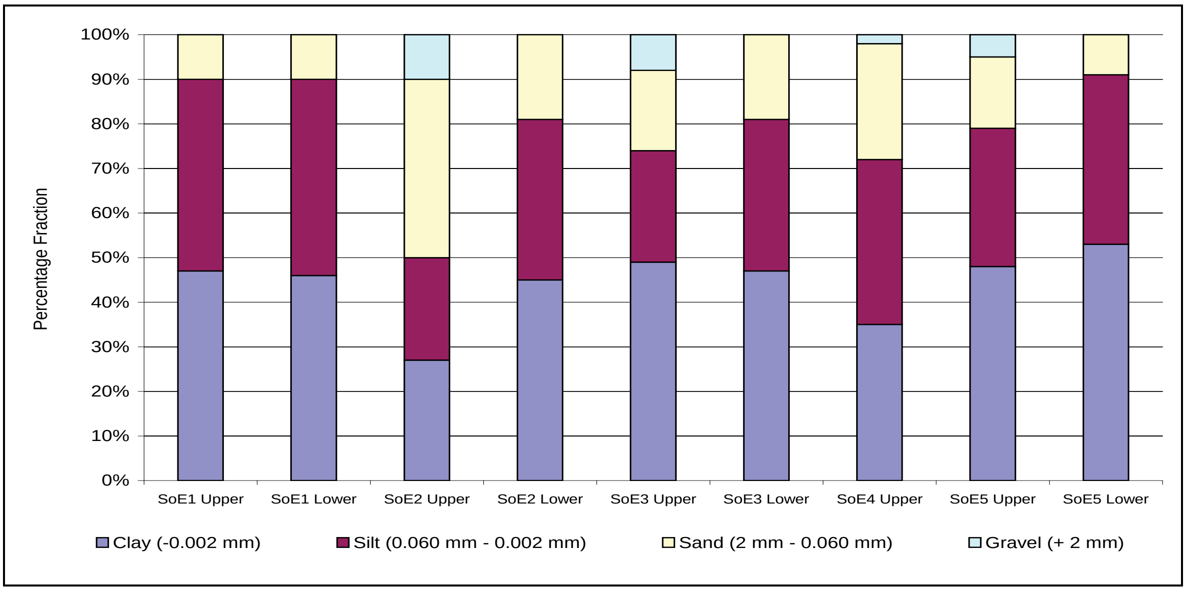

Figure 2-12 Vibrocore sediment sample particle size distribution as percentage fraction

The percentage of clay and silt materials decreases towards shore where wave breaking and turbulent processes assist to sort bed material resulting in coarser sediment grains towards shore. During storms, finer sediments are suspended and transported seaward, eventually settling offshore. Coarser materials (sands and gravel) are more resistant to movement and are not transported in the offshore direction, but remain as the majority of upper beach material (see Figure 2-13).

Table 2-4 Summary statistics of PSD at the proposed port site (9 samples).

	Percent Clay (-0.002 mm)	Percent Silt (0.060 mm - 0.002 mm)	Percent Sand (2 mm - 0.060 mm)	Percent Gravel (> 2 mm)
Mean %	44.11	34.56	18.56	2.78
Std Dev	8.02	7.23	9.75	3.93
Min %	27.00	23.00	9.00	0.00
Max %	53.00	44.00	40.00	10.00

Beach sediments were collected in a separate phase of the field work and analysed to provide particle size distributions and sand grain fall velocities. Figure 2-13 shows the composition of the upper beach sediments and the individual sand grains that are a mixture of well sorted calcareous and silica material containing 11% gravel, 88% sand, and less than 1% clay. The size distribution is shown in Figure 2-14.

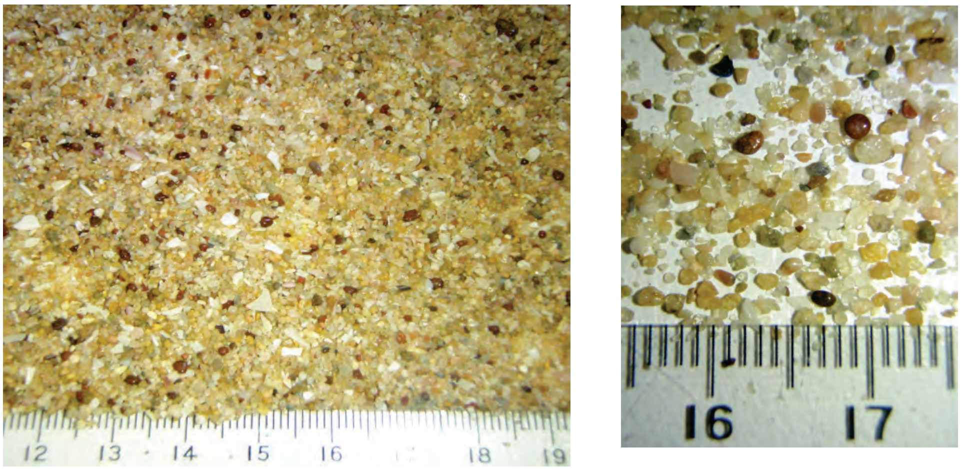

Figure 2-13 Upper beach sediment and individual grains

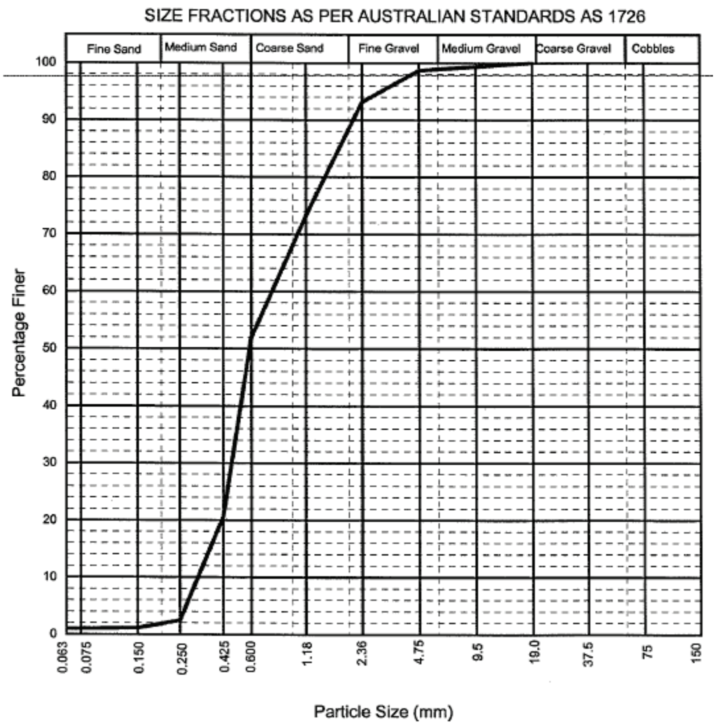

Figure 2-14 Sediment sample size distribution (Lower Beach)

2.7.2 Coffey Geotechnics (2009)

In October and November 2008, Coffey Geotechnics Pty Ltd investigated the offshore site between Boyd Point and Pera Head at the location of the proposed jetty/wharf and dredging basin. This was supplemented by onshore drilling atop the bauxite plateau.

The findings of these investigations from samples obtained within the proposed berths and departure area were as follows:

- A thin discontinuous unconsolidated marine silt and sandy layer extending seawards from the upper beach;
- A layer of hard, weathered (fissured) clay grading into the next layer; and
- Underlying low strength, highly weathered siltstone.

The bore-logs from the investigation are reproduced in Figure 2-15. More detail on the material that would be dredged is provided in Section 5.4.

It is noted that sampling undertaken to-date has not characterised materials to be dredged within the proposed departure channel. The nature of materials outside the extent of physical investigation has been inferred from available geological information when applying physical descriptors to modelled parameters.

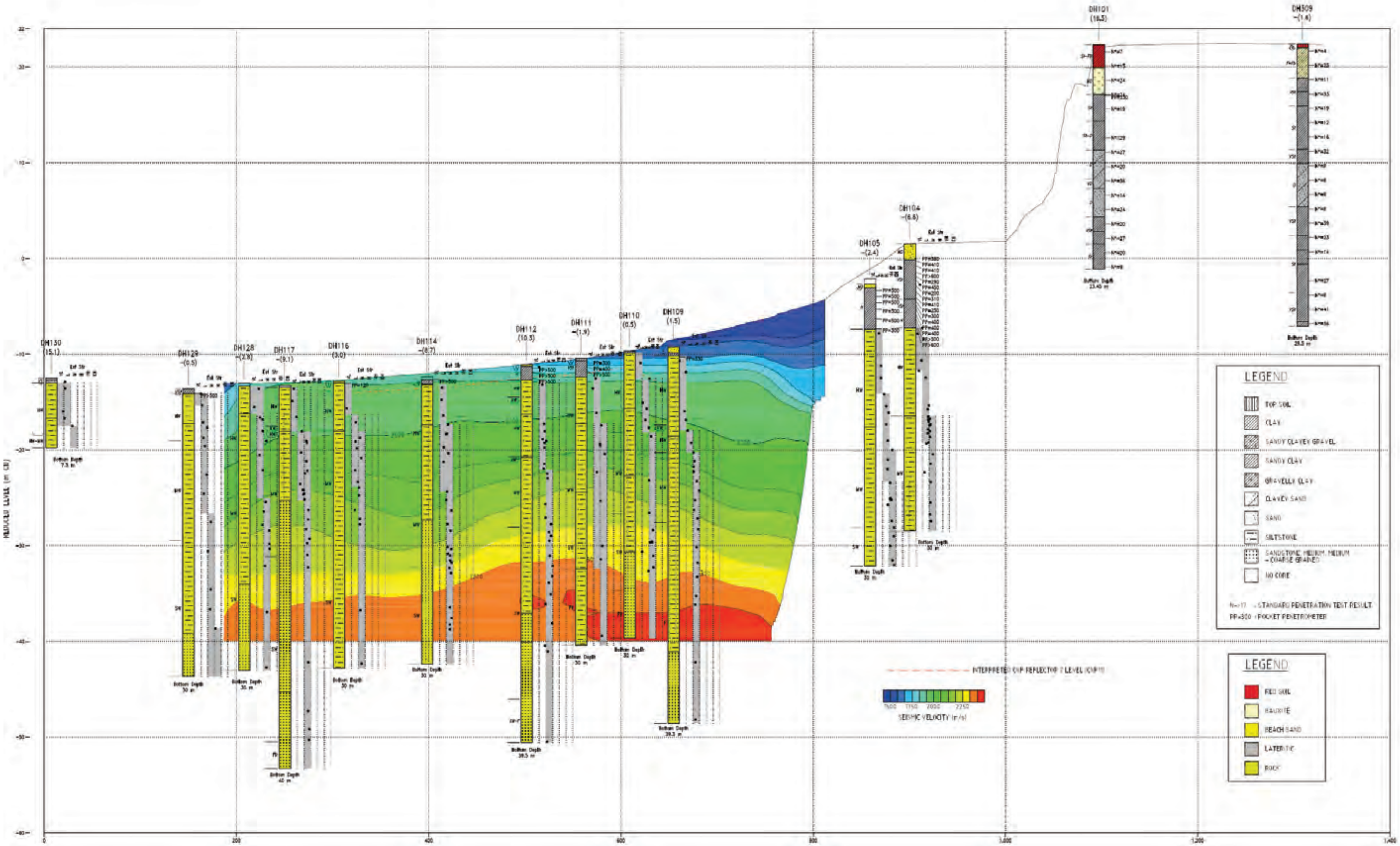

Figure 2-15 Geotech borelog profile within berth and departure area.

3 HYDRODYNAMIC MODELLING

The water velocities and levels in the area surrounding Weipa and across the entire Gulf region have been modelled using validated hydrodynamic models. A regional scale model, covering the entire Gulf Region, was developed to provide accurate boundary conditions for the finer resolution local model of the study area. This approach allowed accurate representation of the tides within the nearshore model that formed the basis of the sediment plume dispersion study whilst optimising computational time and efficiency.

Whilst the nearshore model was selected as a subset of the entire Gulf Region, the extents of this model were selected to be sufficiently large enough to properly capture wind energy transfer to the sea surface over long fetches.

3.1 Model Description

The Gulf-scale hydrodynamic model was developed using the MIKE 21-regular grid (RG) software, whilst the nearshore local hydrodynamic model employed the fully three-dimensional ocean/coastal circulation software MIKE 3 HD by DHI Software. Both platforms are widely recognised and published hydrodynamic models that have been successfully applied in many regions around the world.

MIKE 21 is a two-dimensional model that solves the unsteady incompressible flow equations using a hydrostatic pressure assumption.

MIKE 3 HD numerically solves the three-dimensional incompressible Reynolds averaged Navier-Stokes equations subject to the assumptions of Boussinesq and of hydrostatic pressure. Thus, the model consists of continuity, momentum, temperature, salinity and density equations and it is closed by a turbulent closure scheme. The free surface is taken into account using a sigma-coordinate transformation. Wetting and drying effects at intertidal areas is also accounted for in the model.

The equations in MIKE 3 HD are solved using an unstructured mesh applying a cell-centred finite volume method. A total of five different turbulent closures can be employed: constant eddy viscosity, Smagorinsky subgrid scale model, k model, k-e model, or a mixed Smagorinsky/k-e model. The equations allow wave radiation stress input to address surf area current due to wave breaking.

Full details of the model software and its governing equations can be found in DHI (2011).

3.2 Model Development

Bathymetry data from the following sources was used to develop a numerical model of the Gulf of Carpentaria and the detailed nearshore model of the study site:

- Australian Bathymetry and Topography Grid June 2005, Geoscience Australia (DVD ROM);
- Australian Hydrographic Chart 410, Booby Island to Cape Wessel including the Gulf of Carpentaria. Scale 1:1000 000 at Latitude 27°15';

- Australian Hydrographic Chart 376, Australia to Papua New Guinea. Scale 1:300 000 at Latitude 27°15'; and
- Hydrographic survey of the study site between Boyd Point and Pera Head to produce bed contours between -3 and -15m at one metre intervals to LAT datum.

The Australian Bathymetric Grid produced by Geoscience Australia (GA) is based on a collection of approximately 1400 seismic and sampling surveys conducted around the Australian margin. For ship-track data the typical spacing between data points is 25 to 200 m. Bathymetry data from the GA dataset was used as a basis for numerical model development and subsequently enhanced by the use of hydro-survey data collected along the Boyd Point coastline.

The hydrographic survey of the Boyd Point area identified an upper-beach perched below high cliffs and nearshore contours that are closely spaced indicating that the depth increases rapidly with offshore distance. Depths from -3 m to -14 m LAT are achieved over approximately 500 m. Between -14 m to -16 m LAT the seabed converts to a mild grade over a distance of approximately 2 km. Reefs and rocky outcrops are found in the vicinity of the proposed Port site.

The Gulf-scale model was created to cover the entire Gulf Region at a 1km by 1km resolution, with the extent and bathymetry of this model shown in Figure 3-1. The Outer model was rotated clockwise 19° to align the open boundaries in the Arafura Sea and the Torres Strait. Small areas to the north of the Outer model domain were filled with land to simplify the open boundaries without affecting the predicted hydrodynamics within the Gulf of Carpentaria.

As aforementioned, the extents of the nearshore model were selected to be sufficiently large enough to properly capture wind energy transfer to the sea surface over long fetches. These extents extended from 100 km south of the Project site, at Cape Keerweer, to 90 km north of the Project site at Pennefather River and to approximately 80 km offshore along this entire extent. Figure 3-2 shows the extent and bathymetry data as applied to the Inner model in greater detail. The model resolution and coverage of Albatross Bay in addition to the study site near Boyd Point is further illustrated in Figure 3-3. The Inner model spatial resolution varied to allow greater detail in areas of interest such as the proposed Port site and its surrounds.

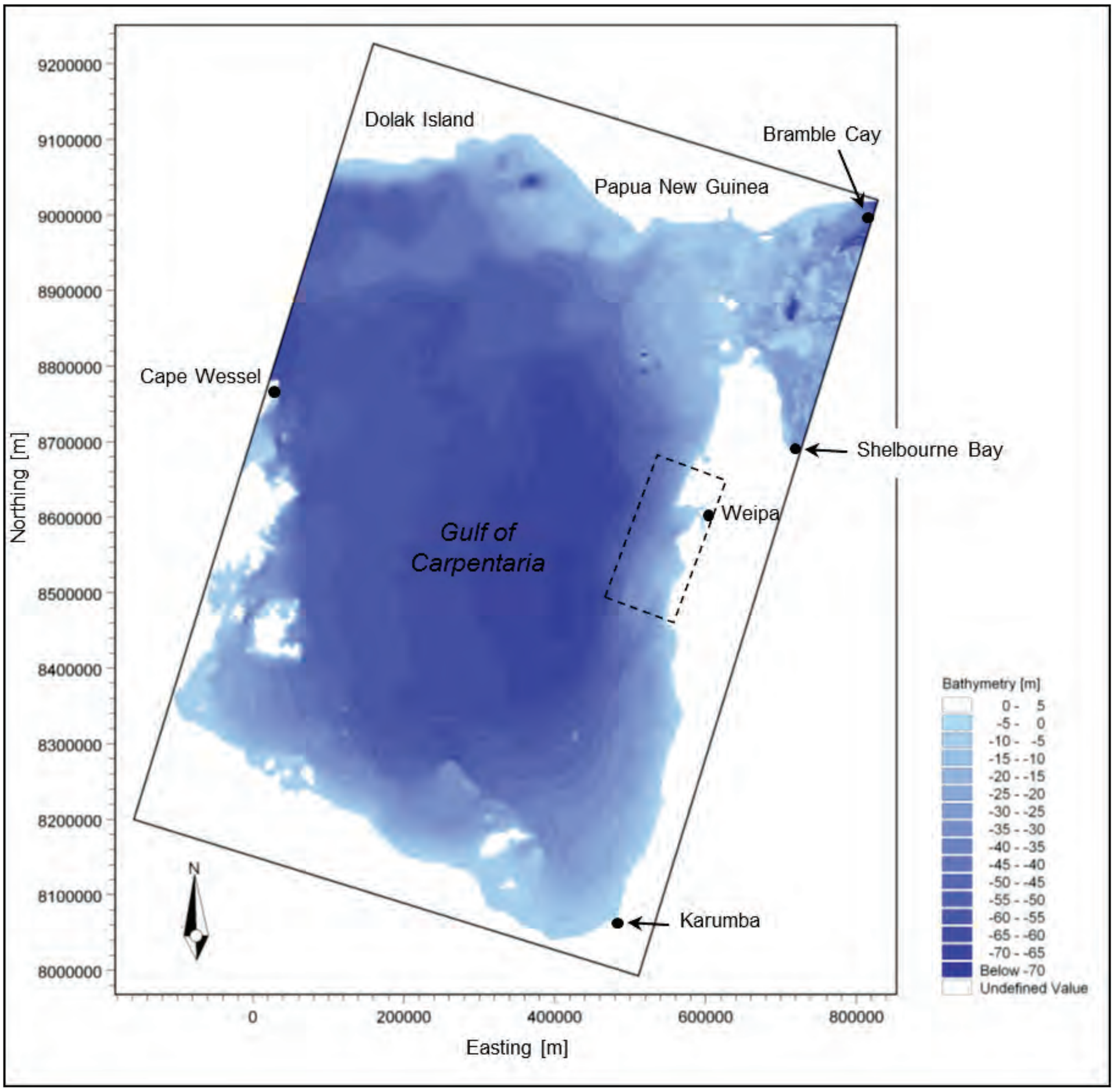

Figure 3-1 Gulf of Carpentaria regular grid bathymetry and boundary (solid line) and Inner model boundary (dash line)

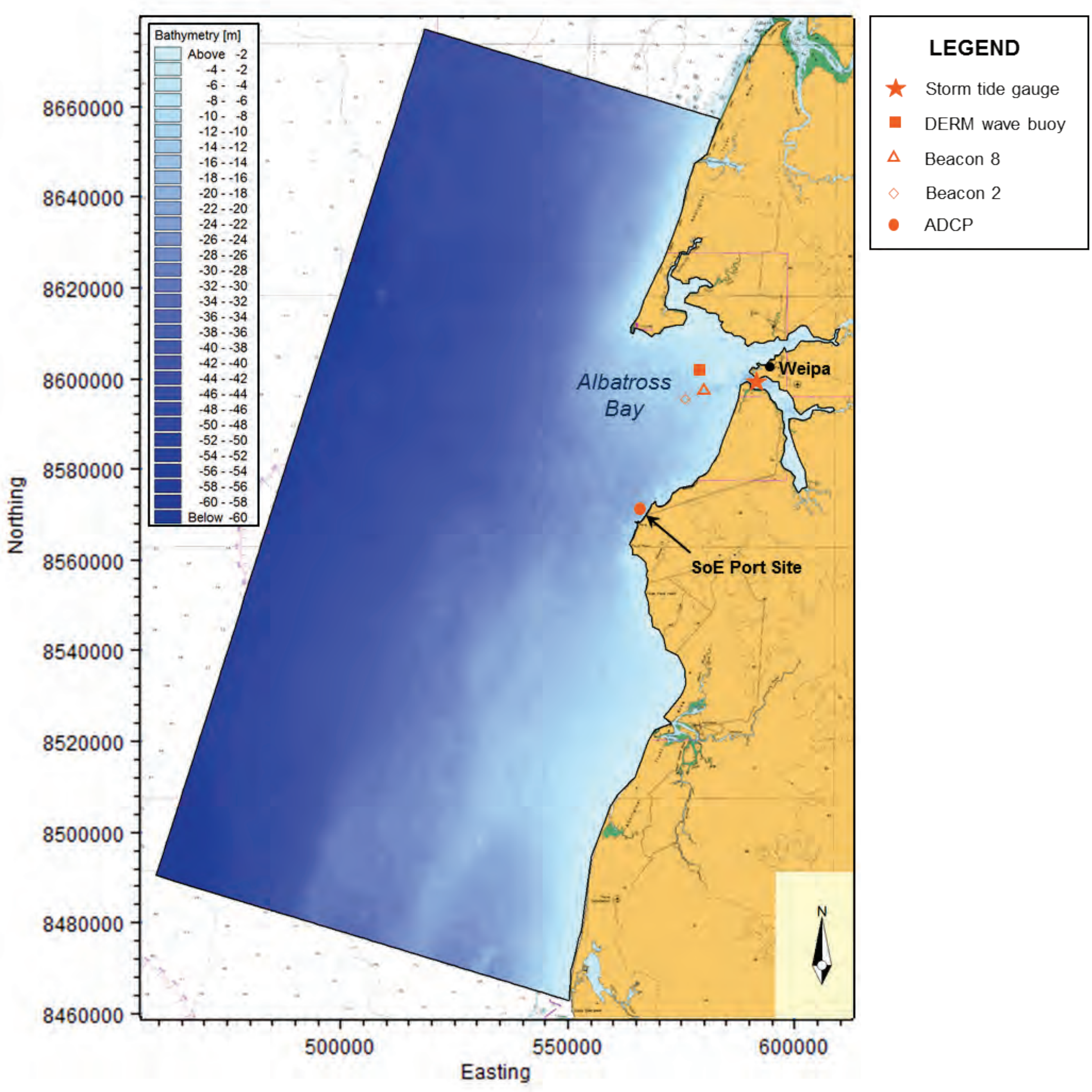

Figure 3-2 Inner model bathymetry and model boundaries with observational data locations shown

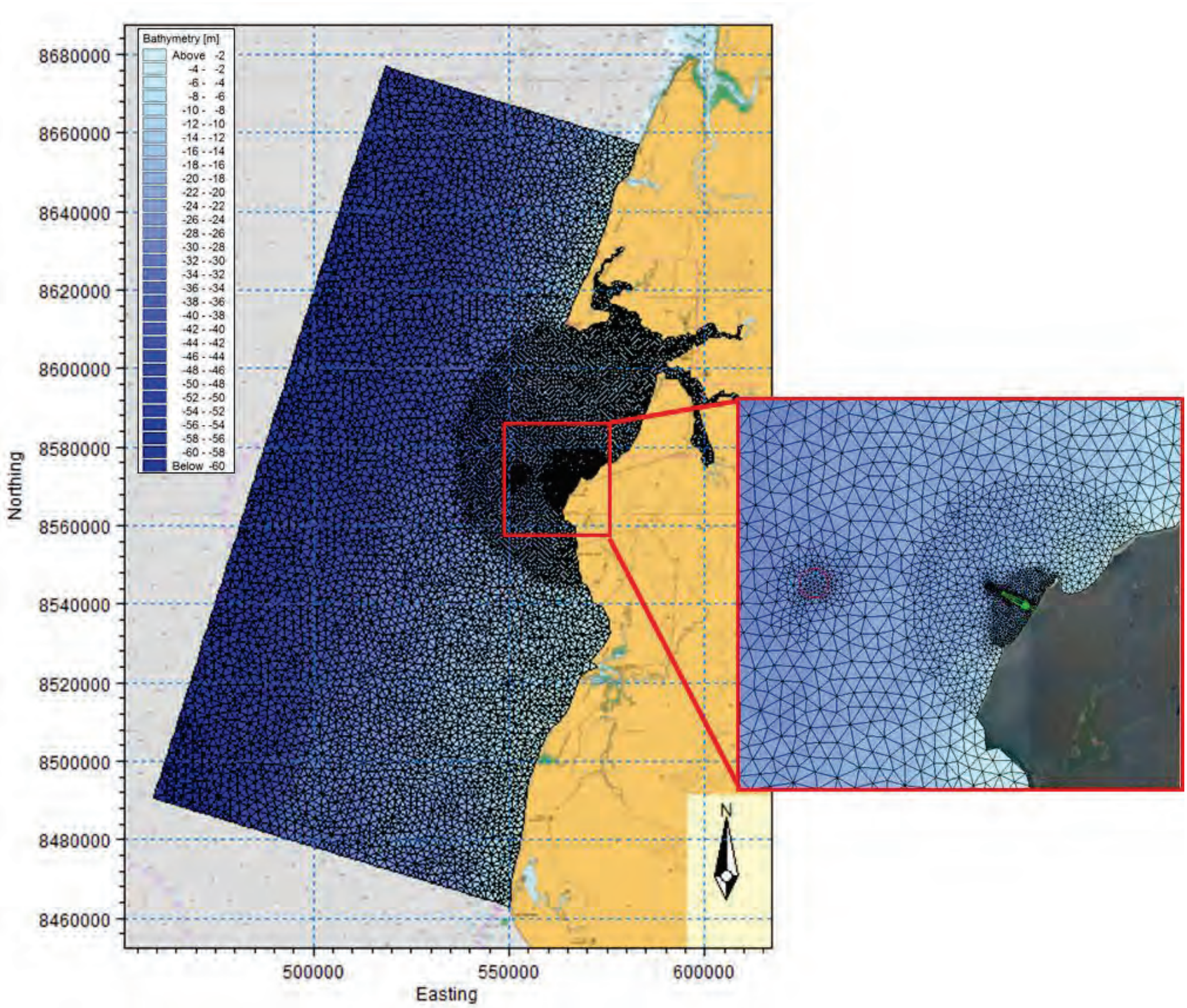

Figure 3-3 Finite element Grid of the Inner SoE Model. Inset shows proposed Port (green) and proposed new spoil ground (red circle).

3.3 Model Parameters

Model parameters employed in the MIKE 21 and MIKE 3 HD models are summarised in Table 3-1. These parameters were selected based on WorleyParsons experience with projects at locations with similar sediment characteristics and tidal forcing.

Table 3-1 Key parameters and formulations used in the MIKE3 MT and HD models

Model Parameter		
Timestep	Maximum computational timestep	60 seconds
	Minimum computational timestep	0.01 seconds
Eddy Viscosity		Smagorinsky formulation with a constant value of 0.4 m^2/s
Seabed drag coefficient		Roughness height of 0.067m

As the purpose of the model was to simulate the dispersion of sediments throughout the water column, it was necessary to determine whether the baroclinic effects, the influence of changing density as a function of salinity and temperature on flow gradients, were significant enough at the site to be incorporated into the model. An investigation into the salinity and temperature in the nearshore regions over the dry season (see Section 2.6) showed that there was negligible salinity or temperature stratification over this period, over which the dredging is proposed to occur. As a result, it can be said that density variations as a result of these two parameters would be negligible in the model. For this reason the barotropic model formulation was considered accurate for the model assessment given that the dredging and disposal sites, and ultimate plume dispersion, were maintained within the well mixed nearshore zone.

3.4 Wind Forcing

Wind forcing was applied as a time series over the whole domain using a combination of data extracted from the Weipa Aero BOM station records and data from the widely used Global Forecast System (GFS) wind database developed by the NOAAs National Centre for Environmental Prediction (NCEP). This dataset provided continuous records from January 2007 to December 2011 over a 0.5 x 0.5 degree grid and represented reliable, quality assured wind information in absence of continuous long-term ground measurements.

The closest data point from the GFS winds used in this composite wind forcing was approximately at the location of the proposed new spoil ground (at coordinates 141.5^{O}E, 13.0^{O}S). This ensured that the model forcing was representative of the offshore conditions near the Project site, whilst capturing nearshore sea-breeze effects as contained in the Weipa Aero BOM station records.

3.5 Model Boundaries

The Gulf-scale model open boundary conditions were obtained from the Danish Hydraulic Institute's Global Tide Model. The predicted tidal water levels from the Global Tide Model incorporate the major diurnal (K_1, O_1, P_1 and Q_1) and semidiurnal (M_2, S_2, N_2 and K_2) tidal constituents with a spatial resolution of 0.25° × 0.25° based on ERS 1 and TOPEX/POSEIDON altimetry data (Andersen, 1995).

The Outer (Gulf) model has two open boundaries (refer Figure 3-1):

1. The western boundary that extends from Cape Wessel to the south-western tip of Dolak Island; and

2. The eastern boundary that extends from Shelbourne Bay to Bramble Cay.

Global Tide Model predictions were used at the Outer model open boundary extents and are all shown together in Figure 3-4. A linear variation was applied to water-levels between:

1. Cape Wessel and Dolak Island for the western boundary; and

2. Shelbourne Bay and Bramble Cay for the eastern boundary.

The Inner model boundary conditions were extracted from the Outer model.

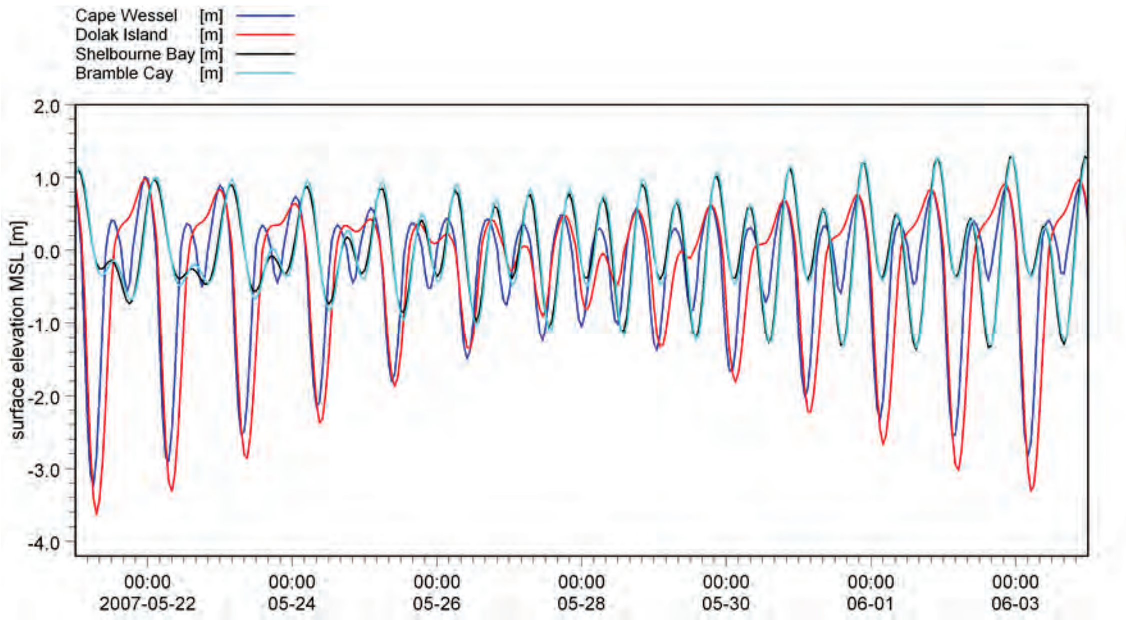

Figure 3-4 Global Tide Model prediction at Outer model open boundary extents

3.6 Validation

ADCP instrument deployment at the proposed Port site provided measurements of current speed, current direction, and water level (deployment location indicated in Figure 3-2). These were used for hydrodynamic model validation. Additional water-level data for the Weipa region collected by the Queensland EPA (now DEHP) was provided via Maritime Safety Queensland (MSQ). The data included both the Weipa storm tide gauge predictions and observations (May/June 2007) and a time-series (July/August 2003) of observational data from 'Beacon 2', located toward the western extent of the existing Weipa shipping channel.

The Gulf-scale model verification plots of observed/predicted versus simulated water levels are presented in Figure 3-5 and Figure 3-6. Model verification at the Weipa storm tide gauge and at Beacon 2 was generally good in terms of the magnitude and timing of flood and ebb tide peaks, noting some over prediction of peak water levels during neap tides. Small discrepancies between the observed and predicted water levels may be attributed to meteorological affects not included in the simulations and/or the boundary conditions not including the minor tidal constituents. These meteorological effects include atmospheric pressure variations and local wind effects. These were excluded as they significantly increase model run times and do not deliver a significantly better estimate for the offshore tide conditions forcing the nearshore model.

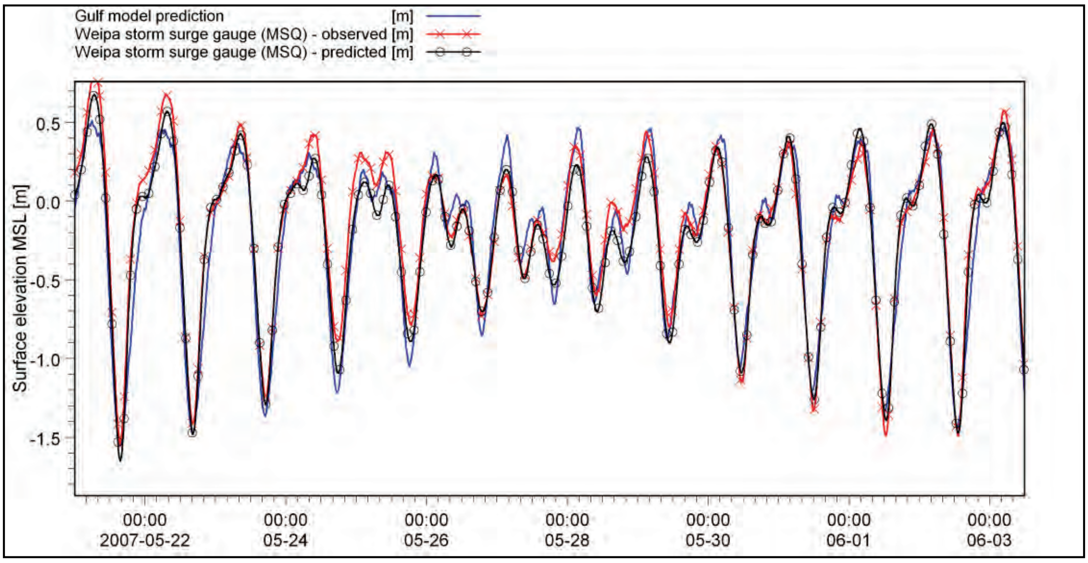

Figure 3-5 MSQ observed/predicted water level at the Weipa storm surge gauge compared to Gulf Model prediction

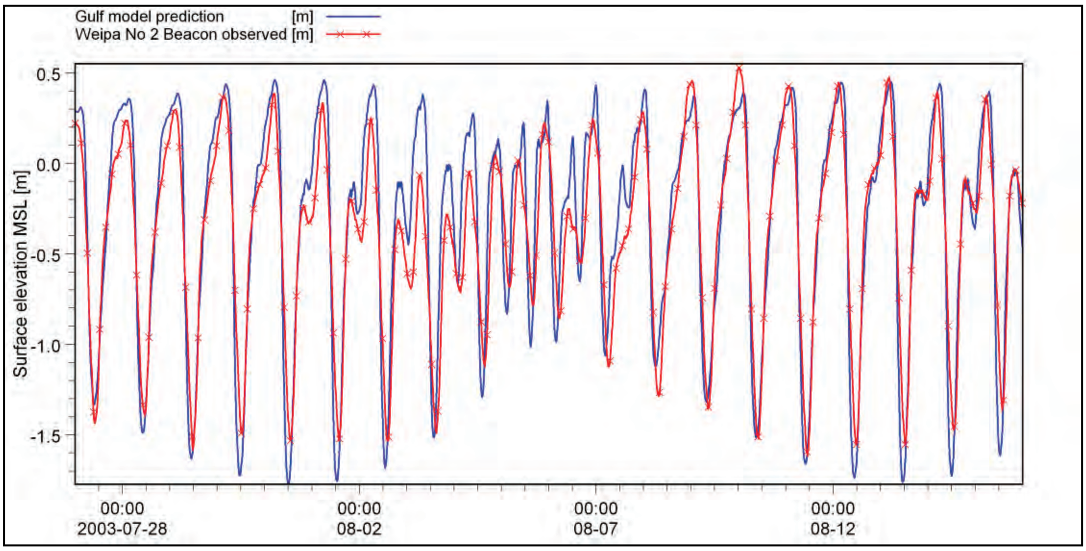

Figure 3-6 Observed water levels at Beacon 2 compared with Gulf Model prediction

The nearshore three-dimensional model was verified using the ADCP data obtained at a fixed location within the proposed Port site over the period supplied from April to May 2007. The plot of the final calibrated model against the field measurements is presented Figure 3-7 for depth averaged currents and Figure 3-8 to Figure 3-10 for seabed, mid-depth and surface currents, respectively.

The magnitude and timing of flood and ebb water levels at the study site was predicted well by the Inner model, with all peaks and tidal phasing during spring tide periods matched well over the calibration period. A small over prediction in the low water levels during neap tides was evident in Figure 3-7, however, as this is only apparent over the neap tide periods this was not expected to significantly compromise the accuracy of the model to predict plume behaviour.

The comparison of current velocities throughout the water column shows that, at all depths, the model is an accurate predictor of the hydrodynamics at the Project site. Given the complexity associated with hydrodynamics within the Gulf of Carpentaria, the magnitude and phasing of the model at all depths shows a high degree of skill at replicating the nearshore measurements. Further clarification of the models predictive capability has been provided through directional scatter plots shown in Figure 3-11. These plots show the 3D model is accurately representing the slight shift in the primary tidal axis down the water column, in addition to capturing the full current magnitude at each depth layer.

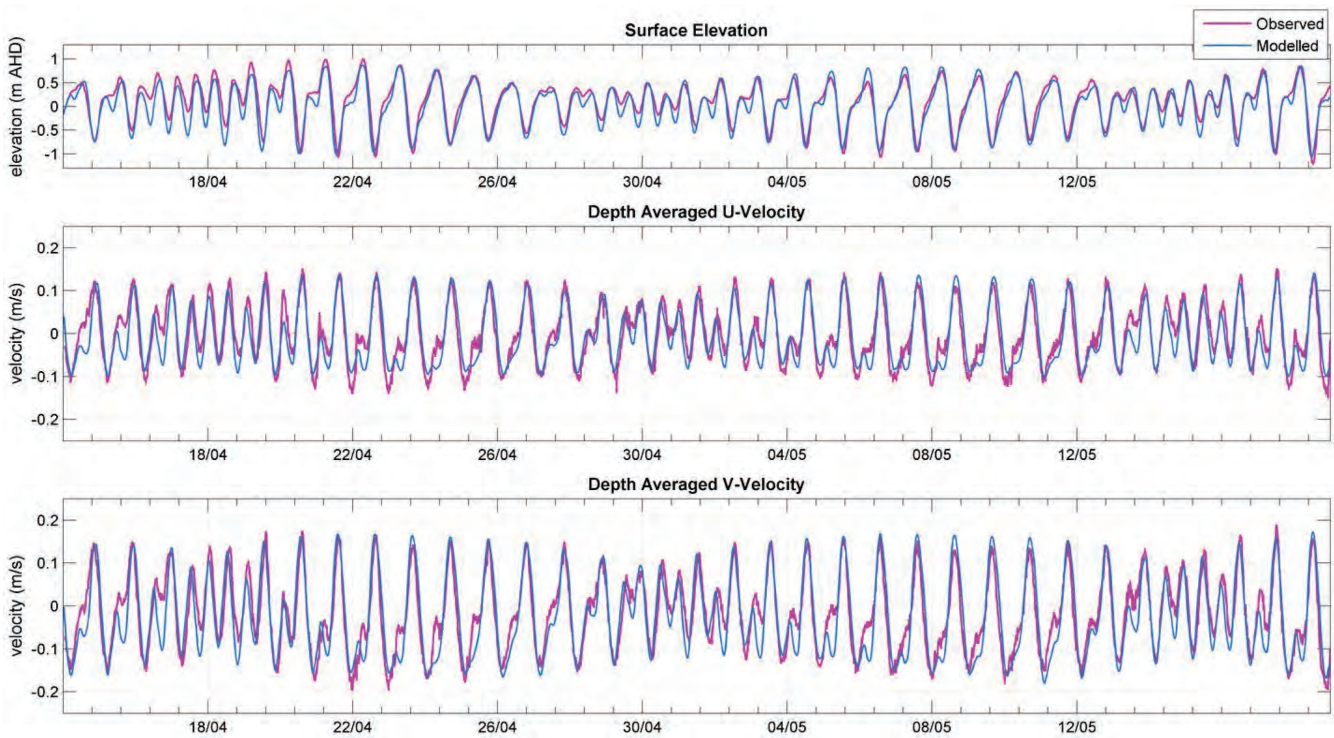

Figure 3-7 Comparison of measured and simulated water level and depth-averaged current velocity at the ADCP location over April and May 2007

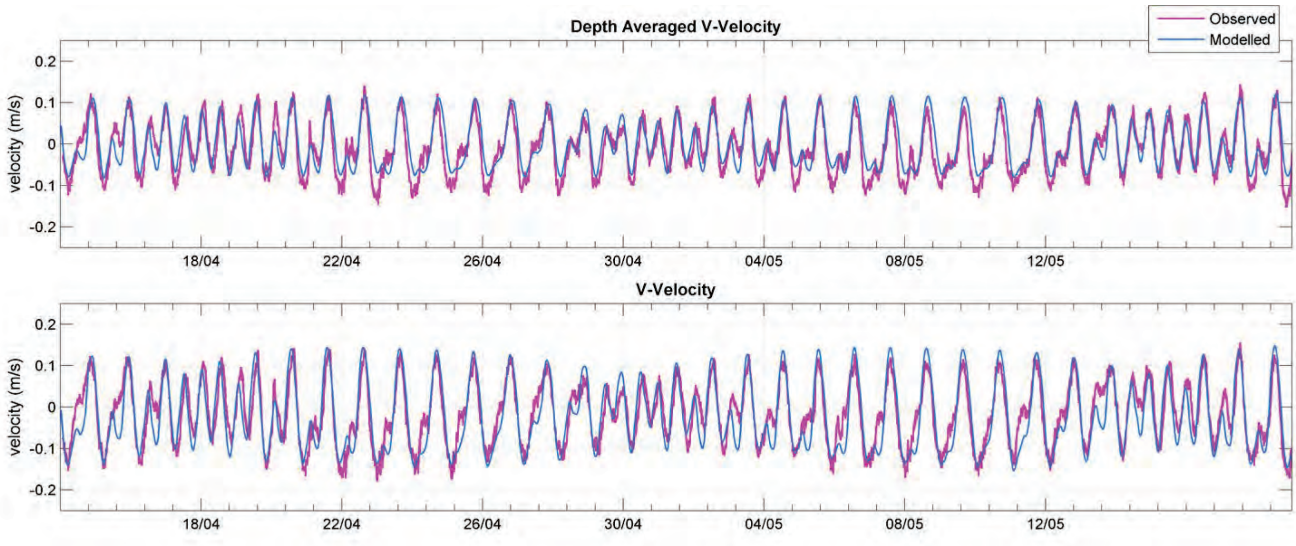

Figure 3-8 Comparison of ADCP measured and simulated current velocity at the seabed over April and May 2007

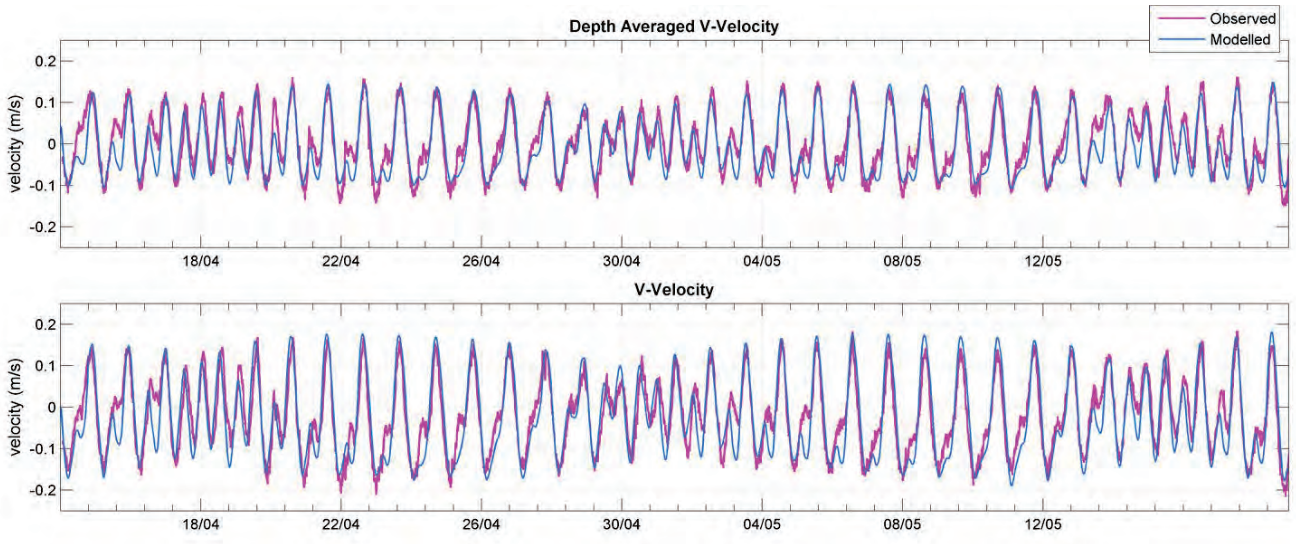

Figure 3-9 Comparison of ADCP measured and simulated current velocity at mid depth over April and May 2007

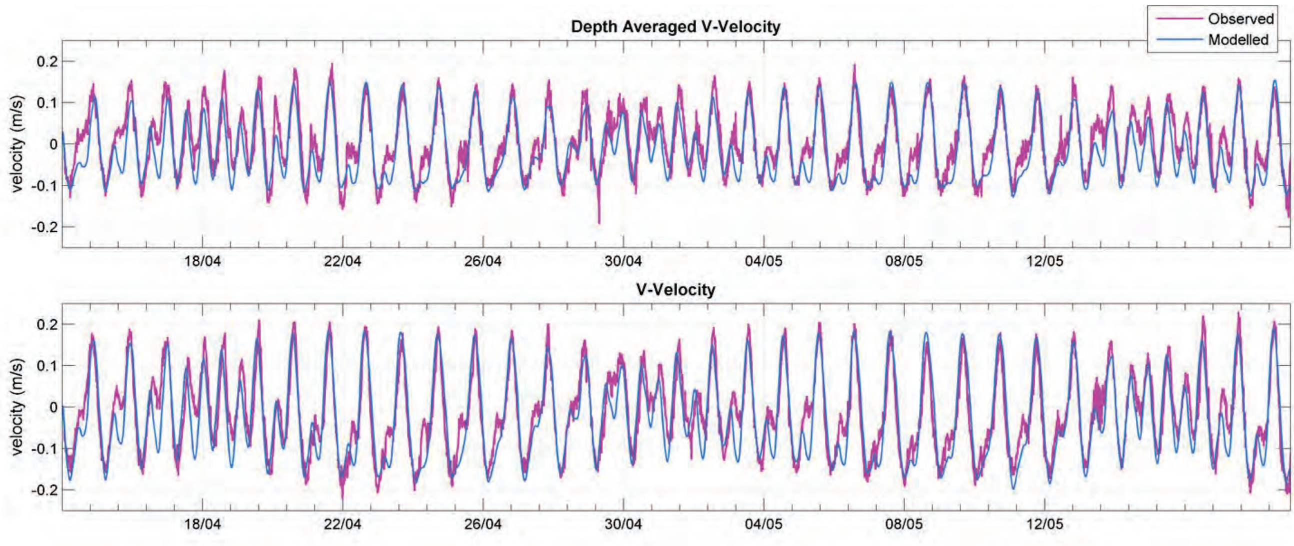

Figure 3-10 Comparison of ADCP measured and simulated current velocity at the surface over April and May 2007

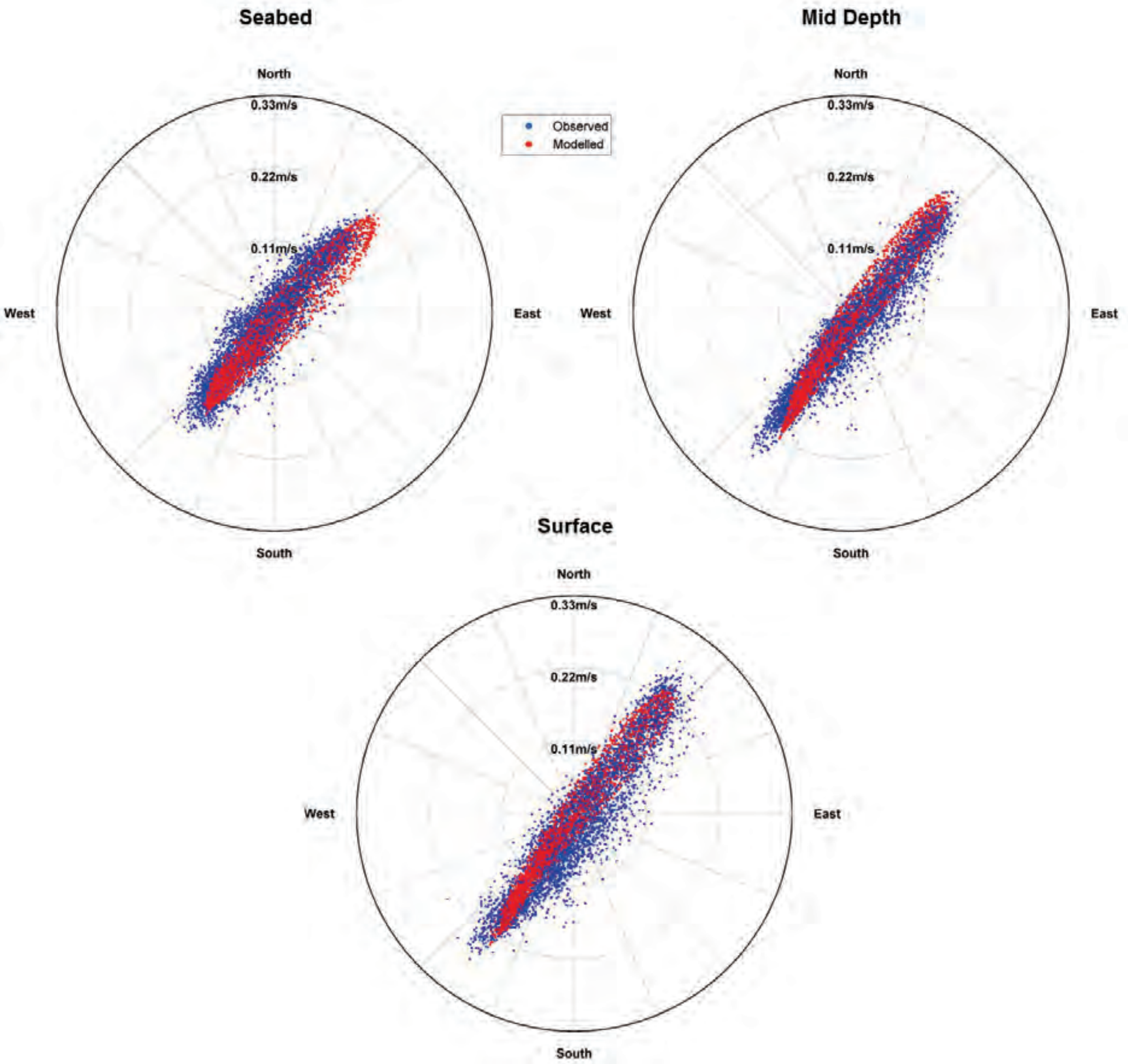

Figure 3-11 Directional scatter plots of ADCP measured and simulated current velocity at various depths (as titled) over April and May 2007

3.7 Hydrodynamic Model Results

Predicted peak flood and ebb tidal current vector plots corresponding to the proposed Port site are presented in Figure 3-12. Current vectors over the tidal cycle indicate that peak currents are typically aligned parallel to the coast in a north-east or south-west direction subject to the tidal phase. Peak, depth-averaged model currents are approximately 0.3m/s.

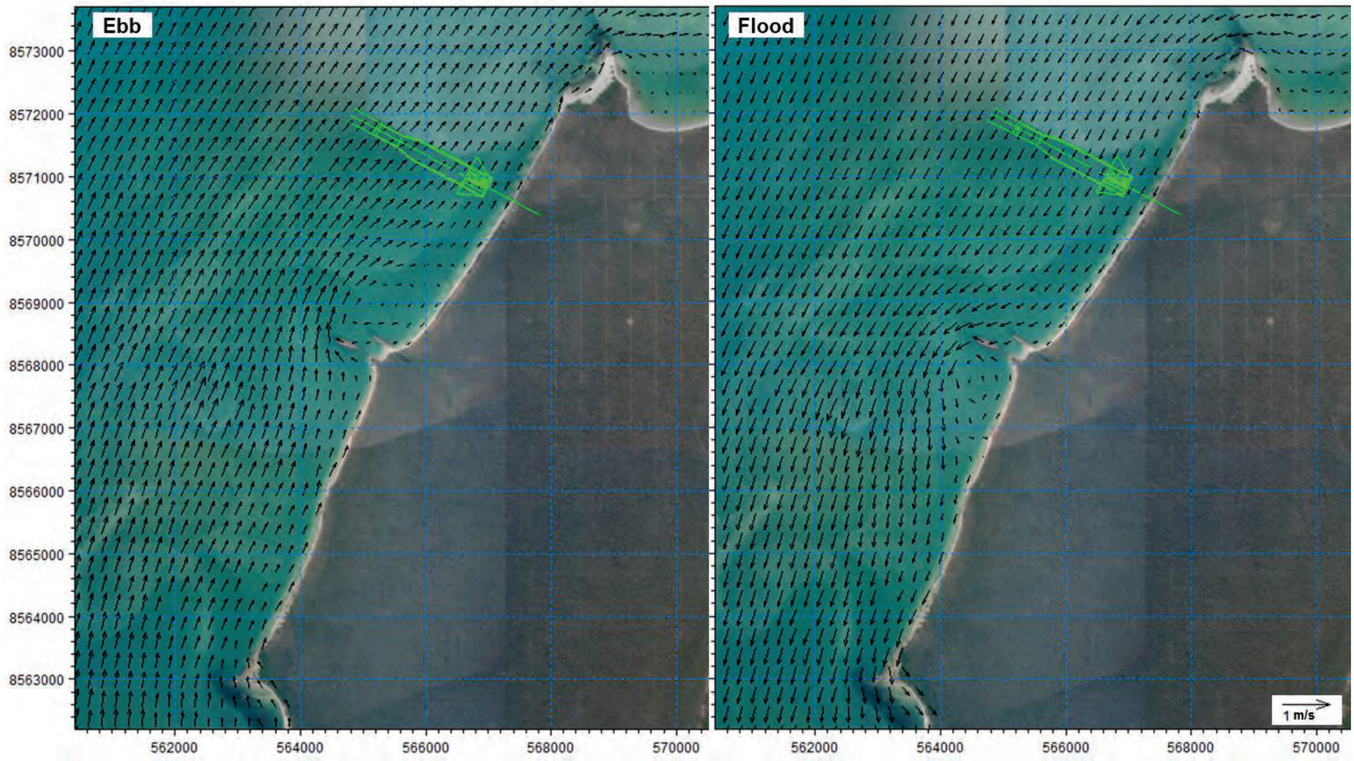

Figure 3-12 Predicted peak flood and ebb tidal surface currents (as titled) at the proposed Port site

4 WAVE MODEL

Numerical wave modelling was performed to obtain wave conditions for examination of wave-induced re-suspension and transport of sediments through coupling with the MIKE 3 MT model.

4.1 Model description

The wave model developed for this study used the MIKE21 SW software developed by the Danish Hydraulics Institute (DHI). MIKE21 SW is a third generation spectral wind-wave model based on unstructured meshes, which is particularly useful as it allows areas of interest to be refined in great detail whilst minimising computational demand. The model enables full time domain simulations, which are important for the present study area. MIKE21 SW allows for the simulation of growth, decay and transformation of wind-generated waves and swells in offshore and coastal areas.

The full spectral formulation is based on the wave action conservation equation, where the directional-frequency wave action spectrum is the dependent variable. Specifically, MIKE21 SW includes the following physical phenomena:

- Wave growth by action of wind;
- Non-linear wave-wave interaction;
- Dissipation due to white-capping;
- Dissipation due to bottom friction;
- Dissipation due to depth-induced wave breaking;
- Refraction and shoaling due to depth variations;
- Wave-current interaction; and
- Effect of time-varying water depth.

4.2 Wave Modelling Objectives

Wave input into the sediment plume dispersion model is an essential component in the calculation of particle re-suspension and transport of sediments. The DEHP wave buoy that is located inside Albatross Bay provides good long-term wave data for the Port of Weipa, but the data is *non-directional*. As such, a wave model was used in the study to meet the following objectives:

- Provide a means to predict wave height at the study site based on the DEHP wave buoy measurements in Albatross Bay;
- Determine the wave directions associated with historical wave events;
- Simulate historical events to obtain a time series of wave parameters, 'Hs', 'Tp', 'Pdir' at the study site for inclusion into coastal process models; and

- Obtain relationships for wave parameters and their corresponding bed stresses to be used in assessment of the potential for re-suspension of bed sediments associated with dredging activities.

4.3 Model Development

The MIKE21 SW model covered the same extents, and utilised the same grid and bathymetry, as that of the nearshore MIKE3 HD model (refer Figure 3-3). These wide extents of the model ensure that there is adequate wind fetch to generate the local sea-wave climate and propagate dominant offshore swell attenuation inshore.

The key parameters applied to the model are provided in Table 4-1

Table 4-1 Nearshore Wave Model key parameters

Model Parameter		
Timestep	Maximum computational timestep	600 seconds
	Minimum computational timestep	0.01 seconds
Frequency Discretisation		25 bins with logarithmic scale, frequency range 0.055 - 0.6Hz
Directional Discretisation		10° bins over 360° rose

The nearshore wave model was forced at the offshore boundary by wave input from the WaveWatch III (WW3) global wave model run by NOAA (Tolman, 2002). The wave forcing was applied as a time-series along the open boundaries. Validation of the model has indicated that occasional swells generated across the Gulf, including during cyclone events, do influence the local wave climate and hence are necessary to include in the nearshore wave model.

Wind was applied in the model using the same dataset employed in the MIKE3 HD model. As the MIKE21 SW model is also capable of including wetting and drying processes, a dynamic water level based on the Gulf-scale hydrodynamic model predictions was adopted across the entire model domain.

4.4 Wave Model Validation

To confirm that the wave model was an accurate predictor of wave conditions in the nearshore the model was compared against measurements at the Albatross Bay WaveRider® buoy (DEHP) and ADCP wave records immediately offshore from Boyd Point (GHD 2008).

4.4.1 Seasonal Comparison at Weipa Wave Buoy

A seasonal validation of the wave model was performed using measurements obtained from the Albatross Bay directional wave records (DEHP) from 2010 to 2012. Four separate 40 day simulations within each season were performed, with the year of the simulation selected based on the availability of complete measurements over the three years of data supplied.

The results of these simulations are presented in Figure 4-1 to Figure 4-4. The results indicate that the model is capturing the range of wave heights and periods, and the associated wave directions, at the Albatross Bay buoy location.

During the summer months, occasional cyclone conditions and large swell events (characterised by peak periods > 8 seconds and significant wave heights > 1.0 m) are well captured within the model, with Tropical Cyclone Olga (January 2010) fully reflected in the model in terms of the wave heights, periods and directions observed at the Albatross Bay location (Figure 4-1).

During the transition seasons, and dry season simulations, limitations in the availability of wind measurements in the region immediately offshore from Weipa meant that nearshore sea-breeze effects, both onshore and offshore as a result of thermal air-pressure changes, were not fully captured in the model. This meant that the magnitude of these events was often marginally mis-estimated within the model, however, wave heights during these seasons were relatively benign and the range of heights observed were accurately captured in the model as indicated in Figure 4-2 to Figure 4-5. During these months wave period and direction was also well represented in the model suggesting that across the Weipa nearshore region the model can be considered representative of the local wave climate.

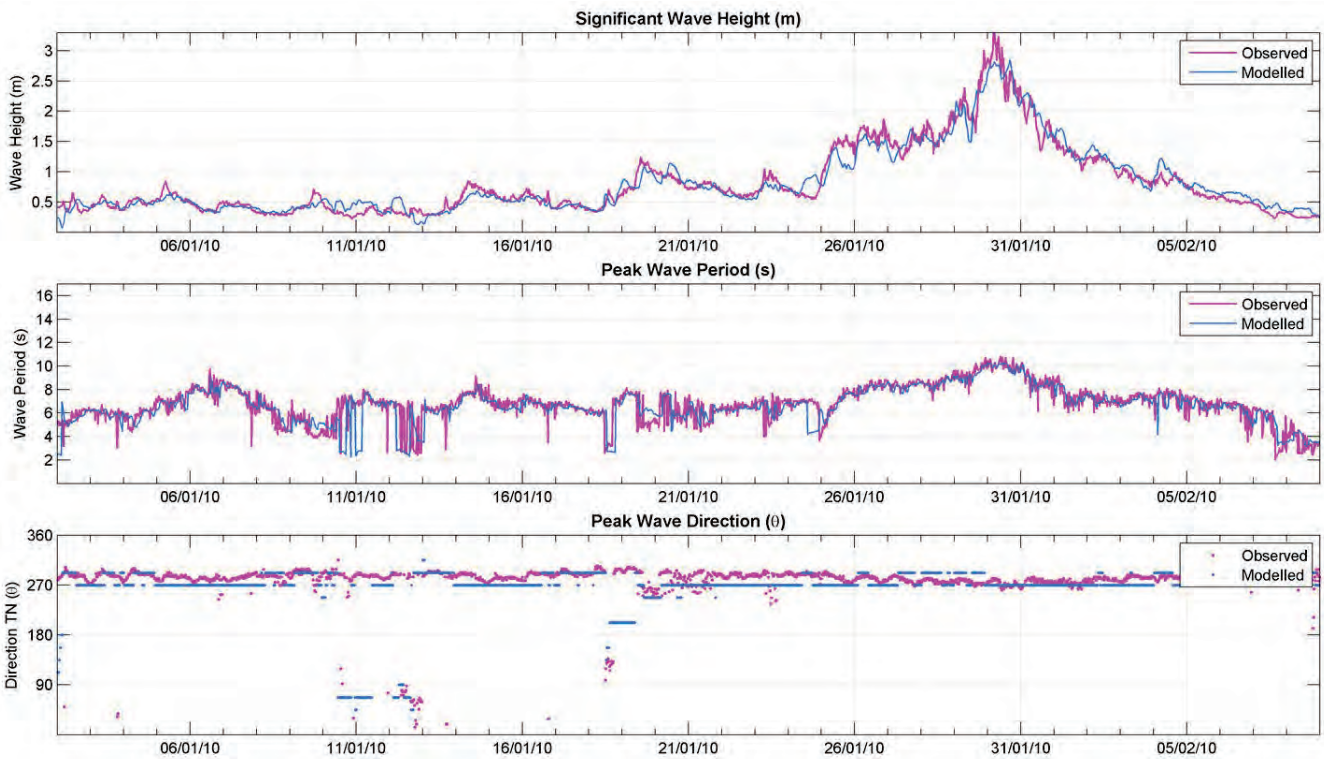

Figure 4-1 Comparison of MIKE 21 SW model results with measurements at the Weipa Offshore Wave Buoy for the representative Summer (wet season) simulation

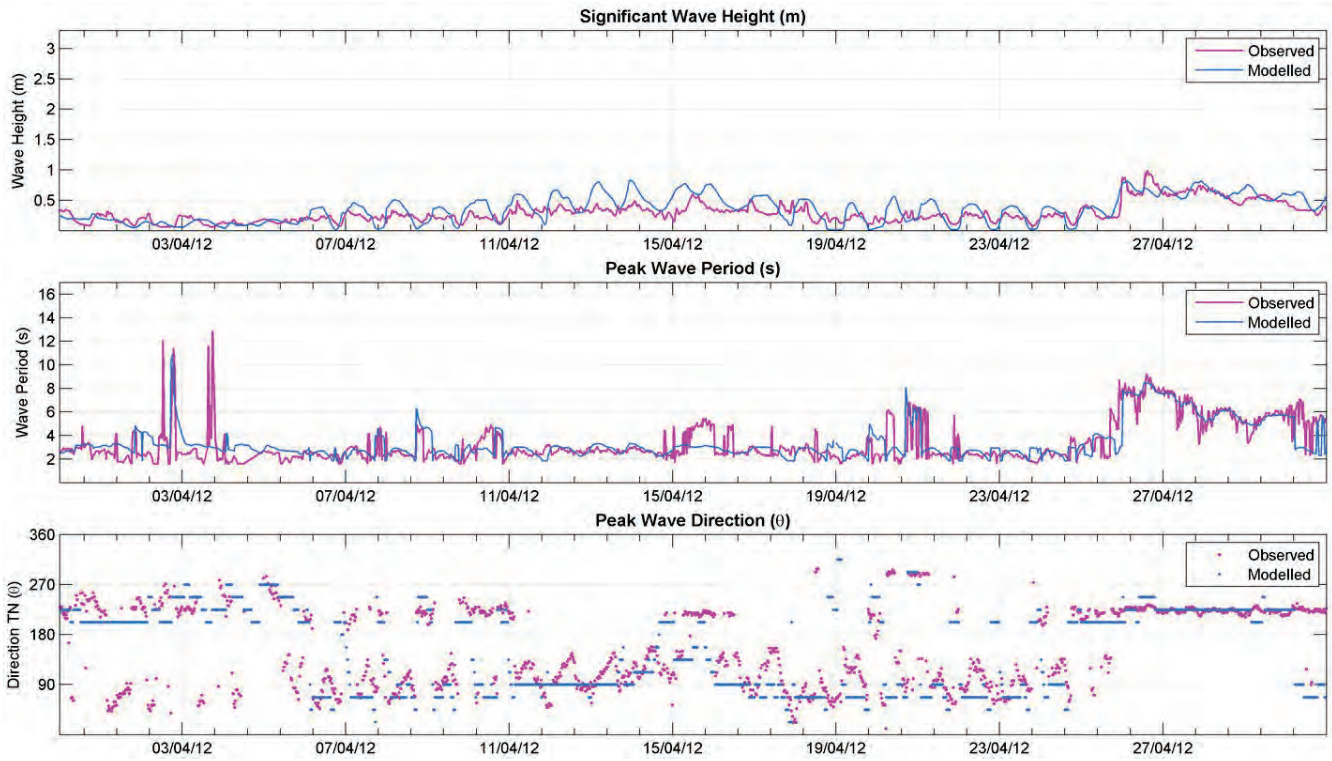

Figure 4-2 Comparison of MIKE 21 SW model results with measurements at the Weipa Offshore Wave Buoy for the representative Autumn (transition season) simulation

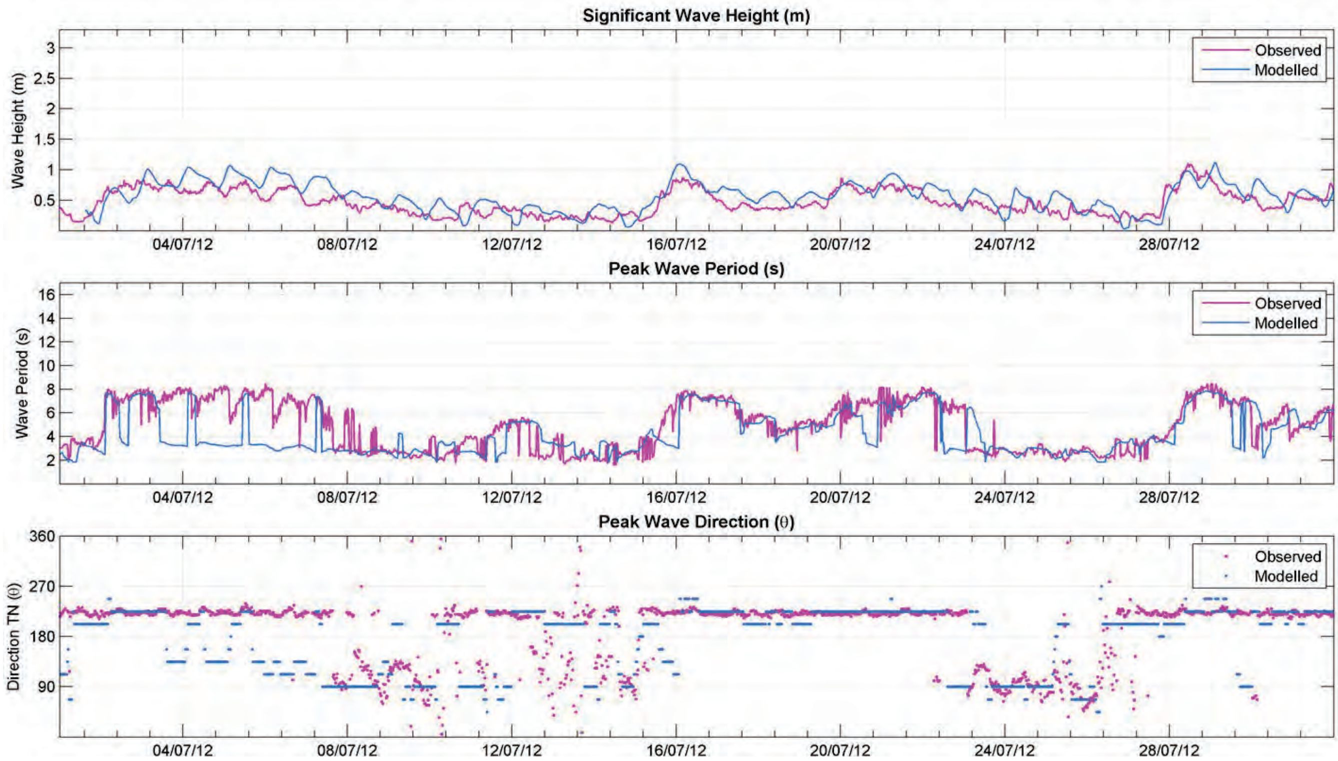

Figure 4-3 Comparison of MIKE 21 SW model results with measurements at the Weipa Offshore Wave Buoy for the representative Winter (dry season) simulation

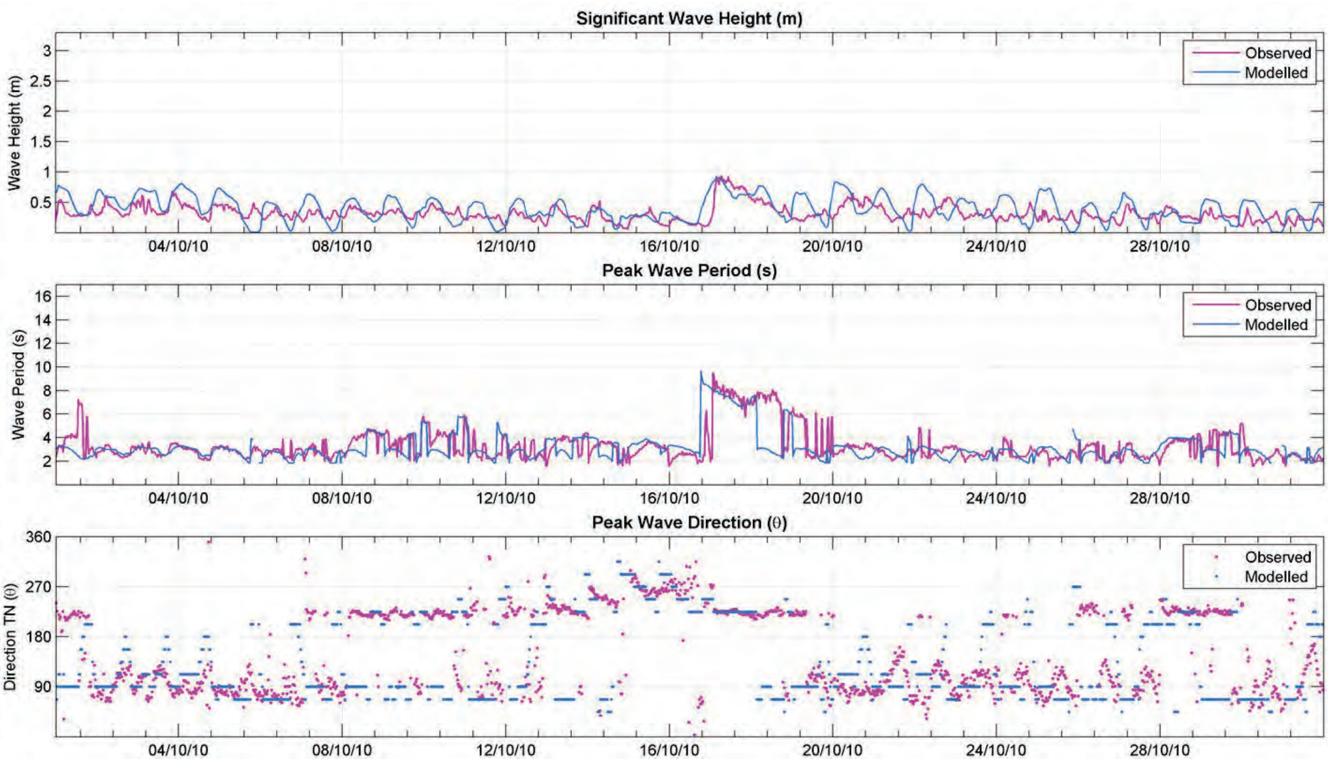

Figure 4-4 Comparison of MIKE 21 SW model results with measurements at the Weipa Offshore Wave Buoy for the representative Spring (transition season) simulation

4.4.2 Site Comparison with ADCP Observations

A comparison of the model with the Boyd Point ADCP measurements was performed over the period from January to February 2007, selected for the completeness of the dataset and presence of another cyclone event in which to validate the model performance. The results of this comparison are presented in Figure 4-5, with the model again reproducing the measured wave heights, periods and directions observed at the nearshore measurement site.

Tropical cyclone Nelson, captured during this validation period, is again well represented in the model in terms of its influence on the extreme wave heights and peak wave periods observed at the nearshore Boyd Point site.

Given the similarity between the modelled and measured data, at both the Boyd Point ADCP and Albatross Bay WaveRider® buoy, it can be concluded that the model is representative of the normal annual wave climate of the nearshore region.

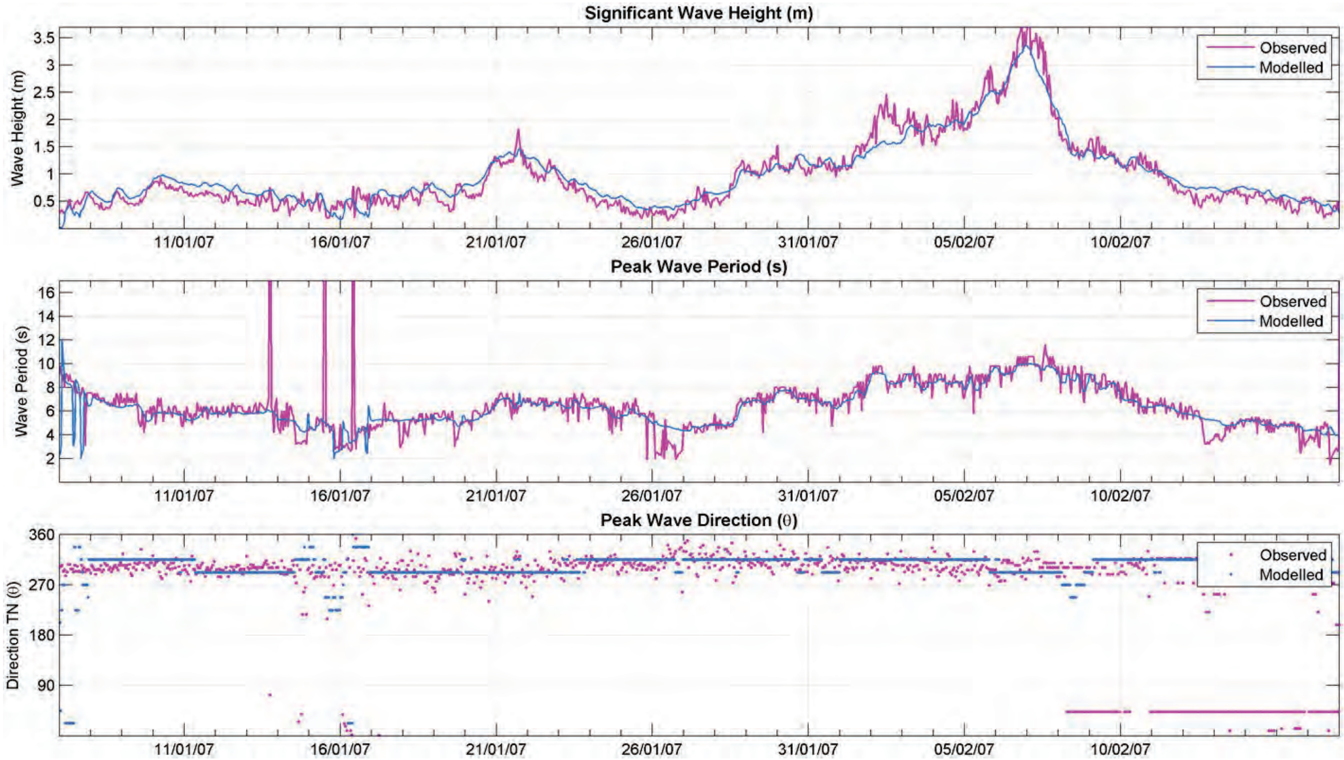

Figure 4-5 Comparison of MIKE 21 SW model results with measurements at the Boyd ADCP location over the January – February 2007 deployment period

4.5 Model Results at Project Site

A brief summary of the results at the Project site for the representative seasonal runs performed are shown in Figure 4-6 and Figure 4-7 for wave height and period, respectively. The results suggest that waves at the Project site are expected to be dominant from the west during the summer (wet season) period, with occasional cyclones bringing large swell events (peak periods > 8 seconds, significant wave heights > 1.0 m). During the transitional months north-easterly waves dominate, with fetch limitations resulting in waves typically less than 0.5 m. The dry season has a higher occurrence of waves from the southwest, with the larger fetch allowing longer period swells to occur yet with smaller waves (typically < 0.75 m) than during the wet season.

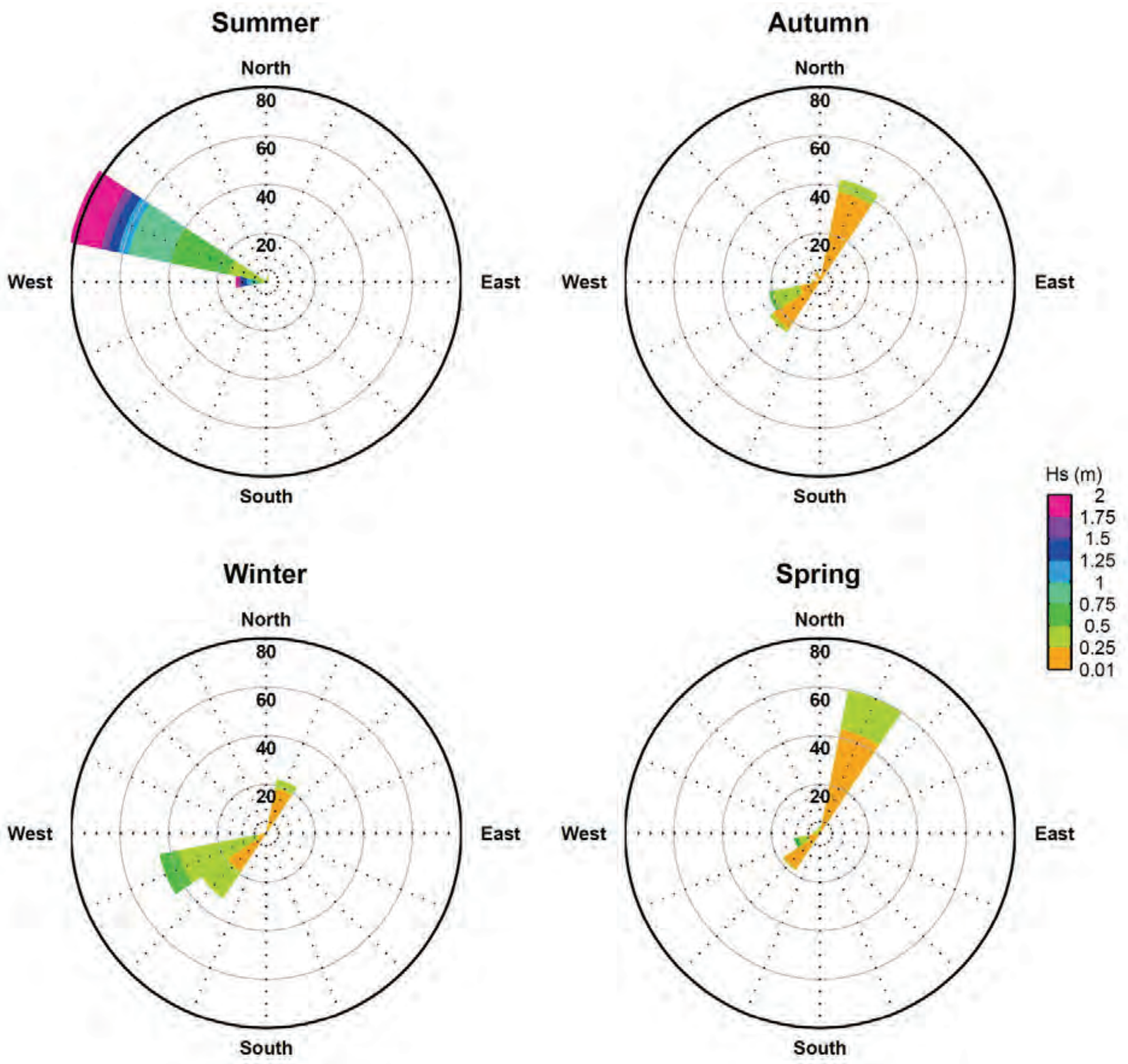

Figure 4-6 Modelled Wave Height and Direction Roses at the Boyd Point ADCP Location

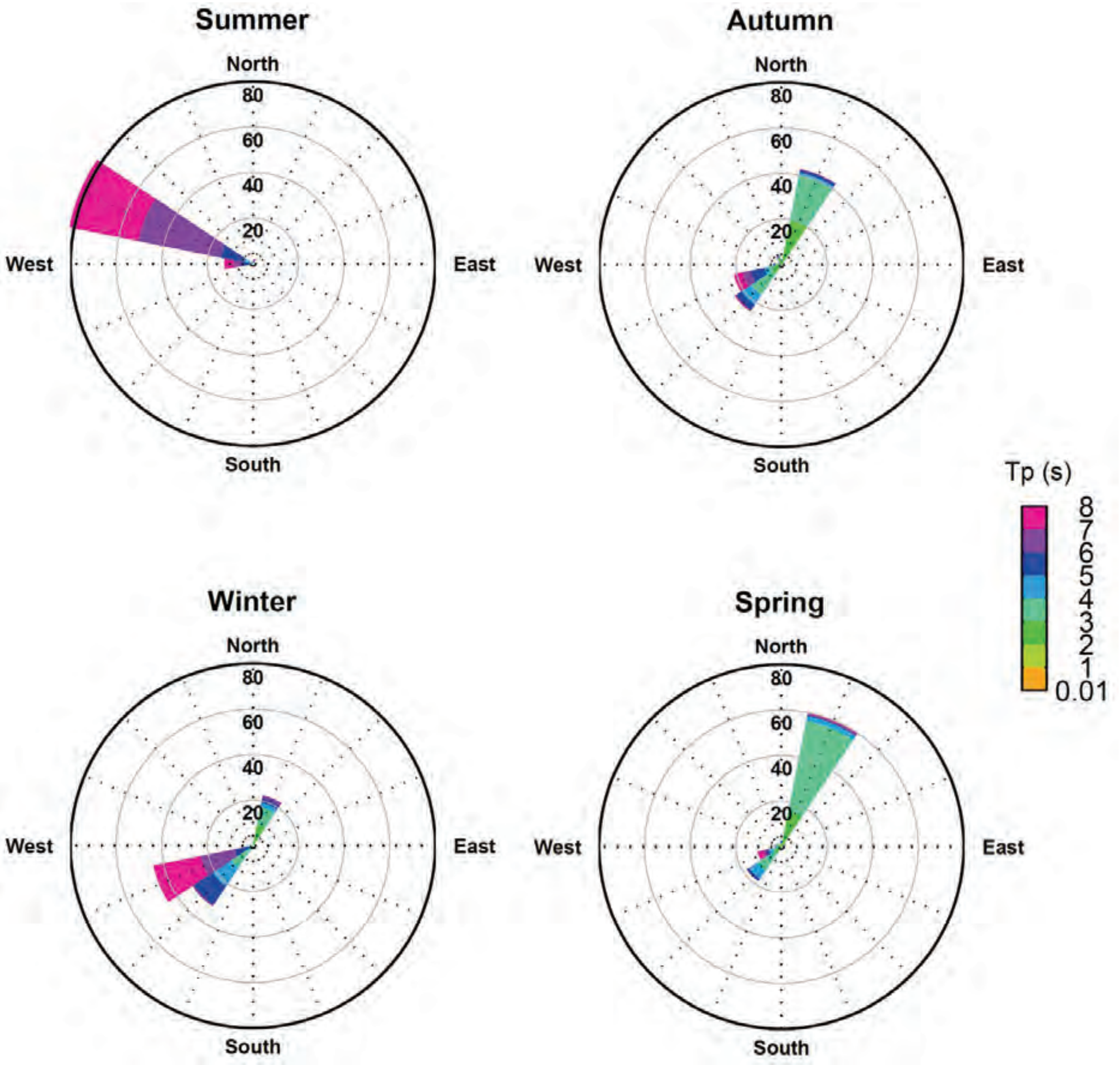

Figure 4-7 Modelled Wave Period and Direction Roses at the Boyd Point ADCP Location

5 PROJECT SITE AND DREDGING DESCRIPTION

5.1 Proposed Dredging Works

Based on the dredging and disposal works shown on Drawing No. 25403-501-S0-1721-00100-RevC, Stage 1 dredging works associated with the proposed Port are described as:

- a straight 1,000 m long, 182 m wide departure channel starting offshore at the 17.3 m depth contour;
- the departure channel widens to accommodate a 302 m departure area that extends 1,550 m before terminating at the existing -11.0 m Chart Datum (CD) depth contour, approximately 570m from shore;
- berth pockets are provided either side (north and south) of the proposed wharf facility.
- the departure channel and northern section of the departure area would be dredged to a design level of -17.30 m CD;
- the northern berth pocket would be dredged to a design level of -19.7 m CD, while the southern DPPV berth pocket would be dredged to a design level of -14.4 m CD;
- the southern section of the departure area, immediately adjacent to the DPPV berth pocket, would be dredged to a design level of -13.30 m CD;
- two turning basins are provided north and south of the departure area, turning basins would be dredge to a design level of -11.60 m CD;
- batter slopes are typically 1:3;
- an overdredge allowance for siltation and survey averaging 0.55 m and 0.9 m has been allowed for the departure channel and departure area and the berth pockets, respectively; and
- dredge spoil is proposed to be disposed offshore at the proposed new spoil ground located 17 km offshore of the berth near the 25 m depth contour. The proposed new spoil ground is circular with a 2,000 m diameter.

The current proposal supersedes a number of iterations of the proposed plan. For the initial campaign dredging, including overdredging, the estimated in-situ dredge volume is approximately 2.6 million cubic metres.

5.2 Cross-Shore Profile at Port Site

The cross-shore profile used in the computations derived from the hydrographic survey contour information, and its location in relation to the coastline between Boyd Point and Pera Head, is shown in Figure 5-1 and Figure 5-2, respectively.

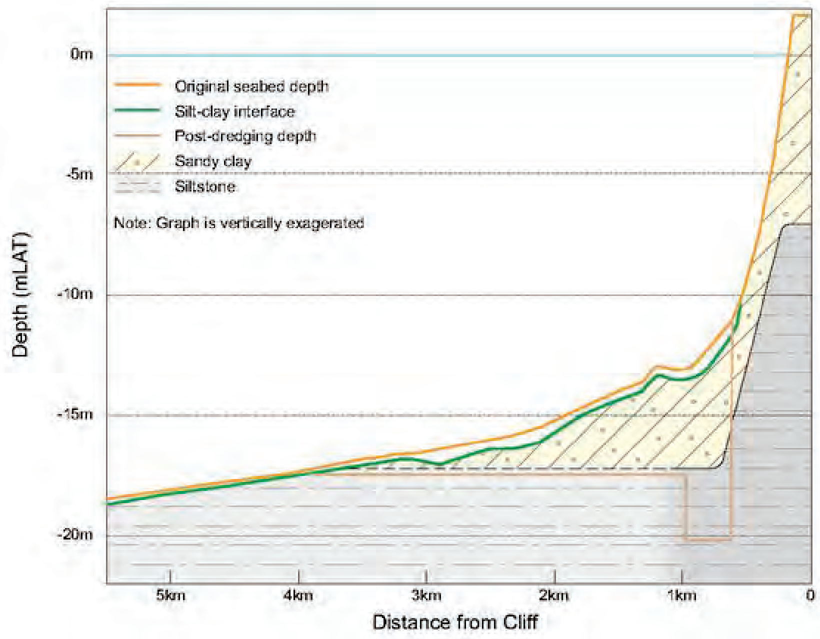

Figure 5-1 Cross-shore profile along central wharf axis at SoE Port site

Figure 5-2 Nearshore bathymetry and location of cross-shore profile

5.3 Proposed New Spoil Ground

The location of the proposed new spoil ground and its proximity to the proposed Port development site is illustrated in Figure 5-3. The proposed new spoil ground would provide a highly accessible location for the deposition of material removed from the proposed Port site. The proposed new spoil ground would have the following characteristics:

- 23 m water depth (LAT).
- Approximately 17 km from the proposed Port site;
- Coordinates: Longitude 141º 28' 52.7", Latitude 12º 54' 43.6".
- Composition of in-situ bed is 20% gravel, 50% sand, 30% mud.

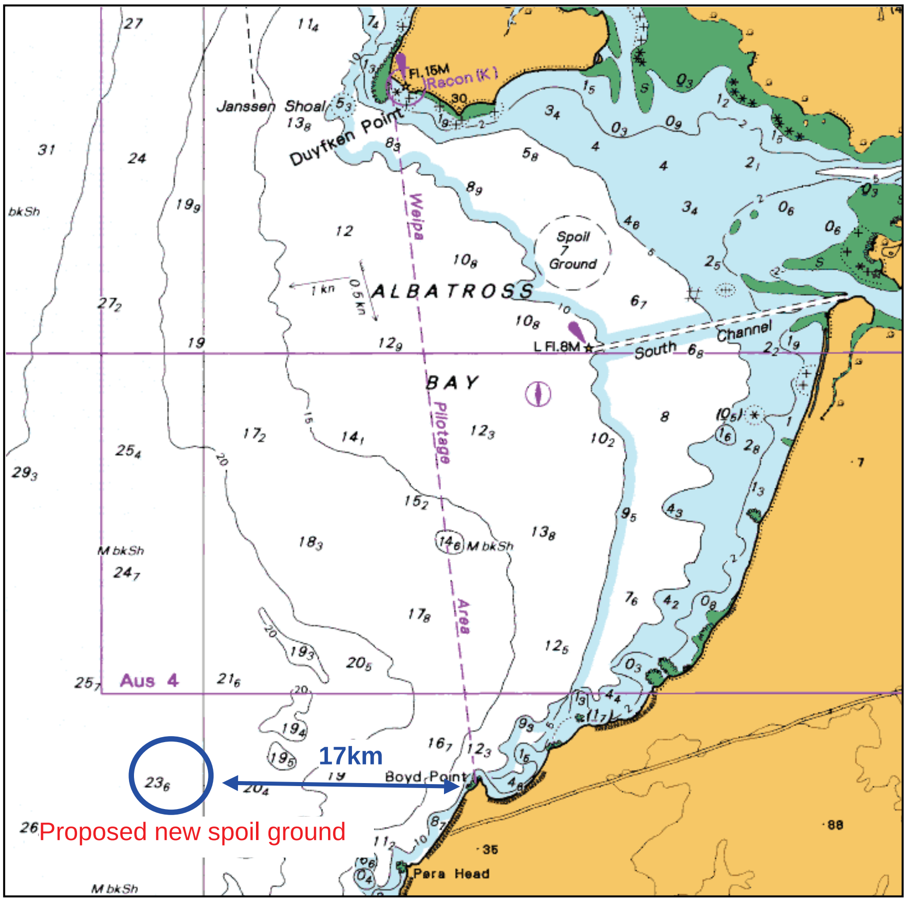

Figure 5-3 Location of the proposed new spoil ground

5.4 Materials to be dredged

The fate of a dredge plume will depend on the duration it remains in suspension and its dispersion through hydrodynamic and wave forcing. The mobility of non-cohesive sandy material is controlled by the particle size whereas the transport of cohesive materials in suspension is influenced by the concentration and the attractive forces between flocs. Knowledge of the material settling velocity is essential for modelling dredge plumes and required testing and analysis of the site samples.

Five geotechnical core samples were obtained at the proposed Port site (refer Sediment Characteristics Report – samples obtained by Coffey Geotechnics). These provided material for Particle Size Distribution (PSD) and settling tube analyses. Sediment particle size distribution and settling velocities have been established for the three sediment types representing the vertical sediment profile that would be dredged and incorporated within the model (see Table 5-1).

Table 5-1 Dredge material characteristics used in plume modelling

Fraction	Material	size (mm)	Particle Size Distribution (%)			Settling velocity (mm/s)
			Layer 1 (unconsolidated marine sediments and sandy clay)	Layer 2 (stiff sandy clay)	Layer 3 / 4 (siltstone)	
1	Clay	<0.002	44	11	13	0.03
2	Silt	0.06 - 0.002	35	50	10	1
3	Fine Sand	0.2 – 0.06	10	20	47	15

The methods adopted for PSD analysis incorporated the use of saline water in determining distributions of the fine fraction to best reflect the dredging process and release of fine sediments. Comparative testing using a freshwater matrix concluded that the use of saline water resulted in an altered clay and silt distribution, where some decreases in clay and fine silt fractions were reported. The term 'effective particle size' was applied to describe the PSD distribution obtained under this method.

Cohesive sediments flocculate (attract) as they are brought into contact with each other. The size and settling velocity of flocculated particles is larger than that of the constituent particle and the median settling velocity is strongly dependant on the suspended sediment concentration (Whitehouse et al., 2000). Flocculation calculations for the cohesive sediment fractions (Fraction 1 and Fraction 2) have been included in all dredge plume modelling scenarios.

For the purpose of this modelling exercise, and based on information contained in the geotechnical reports, the material that would be dredged can in general be described as occurring in three layers. These layers are described as:

- Layer 1: a thin (approximately 1 m thick) surface layer of unconsolidated sandy mud with a composition of 44% clay, 35% silt 18% sand and 3% gravel. This composition is based on the mean of the nine samples collected from WorleyParsons (2008).
- Layer 2: Stiff sandy clay (unit 6). A layer of hard sandy (lateritic) clay of medium to high plasticity, which is typically less than one metre thick in the area that would be dredged (Coffey Geotechnics, 2009) is found below the mobile layer. The lateritic clay is generally not found level below -14m CD.

- Layer 3 / 4: Siltstone (unit 7). A bottom layer of low to medium strength, highly weathered siltstone extends well below the design dredge depths (Coffey Geotechnics, 2009).

The extents of previous geotechnical investigations are limited to the nearshore area. For areas to be dredged seaward of the extent, the main assumption has been that the siltstone unit continues seaward at a similar level as identified by the nearshore boreholes. This is a reasonable assumption based on the geology of the region (pers. comm, Iain Turner, Coffey Geotechnics).

5.5 Dredging Methodology

5.5.1 Options Considered

The plant considered for this dredging campaign includes a self-propelled Cutter-Suction Dredger (CSD), Trailing Suction Hopper Dredger (TSHD) and Split Hopper Barges (SHBs). The potential combinations that these separate vessels would operate in are described below, with details of how each of these methods have been included in the environmental modelling summarised in Sections 5.5.2 to 5.5.4.

CSD and TSHD

SKM and Pro Dredging & Marine Consultants (2010) completed a *Review of Options for Dredging and Disposal of Dredging Materials* (RODDM). This review resulted in a recommended proposed dredging method that consists of the following:

- A large self-propelled CSD required to dredge the hard clays and siltstones. The CSD would be solely used to break up the hard substrate, with the dredged material re-deposited directly on the sea bed behind the submerged pump of the cutter dredge (a minimum of 3,000 kW at the cutter head); and
- A TSHD used to pick up the crushed material deposited by the CSD and load the material into its hopper. The loaded TSHD would transport dredged material offshore to the proposed new spoil ground for marine dumping. The hopper capacity was assumed to be 11,500 m^3, with a “green valve” allowing overflow discharge during loading to occur at the keel level of the vessel.

Under this arrangement, the TSHD is assumed to commence dredging three weeks after the CSD in order for sufficient dredging to have been undertaken by the CSD for all the cuts to allow the TSHD to work continuously until the end of the dredge campaign.

CSD and SHB

An alternative dredging method with the use of the CSD loading directly into four self-propelled SHBs is also being considered. This CSD would be of similar size to that used in the CSD and TSHD combination, however, material would be loaded directly into the SHB’s during dredging.

The nominal capacity of the four separate SHBs used in this arrangement would be 3,700 m^3, with these vessels capable of overflowing at the keel level due to the presence of the same “green valve” system present on the TSHD.

Details of each of these methods are summarised in Sections 5.5.2 to 5.5.4.

5.5.2 Sources of turbidity/suspended sediments

There would be a number of sources of turbidity associated with the activities of the CSD, including:

- action of the cutter head and movement of suction pipes and suction heads through the water at a velocity in the order of 1-2 m/s, suspending sediments near the bed;
- propeller wash during manoeuvring of the dredger;
- re-deposition of material from suction pipes, suspending sediments near the bed; and
- return flow under and along the dredger, especially with low keel clearance;

The stages of dredging with a TSHD that would generate suspended sediment include (Pennekamp and Quaak, 1990):

- movement of suction pipes and suction heads through the water at a velocity in the order of 1-2 m/s, suspending sediments near the bed;
- return flow under and along the dredger, especially with low keel clearance;
- propeller wash during manoeuvring of the dredger;
- hopper overflows during the loading process, particularly towards the end of a dredging session when this overflowing mixture would be closer to the concentration of the pumped slurry;
- release of any gas from the bed due to disturbance of the sediments; and,
- dumping of hoppers offshore at the proposed new spoil ground.

For the SHB, the relevant sources of suspended sediments would include:

- propeller wash during manoeuvring of the dredger (far more sediment is suspended in this operation compared to trailing);
- hopper overflows during the loading process, particularly towards the end of a dredging session when this overflowing mixture would be closer to the concentration of the pumped slurry; and
- dumping of hoppers offshore at the proposed new spoil ground.

For the proposed dredging activities, the largest contribution to the suspended sediments would be associated with the overflow of the TSHD and SHBs. In this study the material that is released into suspension as a result of dredging activities will be termed the spill. The rate of release is termed the ‘spill rate’ (this is equivalent to ‘release rate’).

5.5.3 Dredge spill rates and cycle times

The spill rates from the dredging activities vary and are dependent on the sediment layer, as a result of the variable sediment composition and density of the layers (Table 5-1), with four layers identified across the proposed dredge site. The adopted spill rates decrease with layer depth because material strength, and associated released particle size from the dredging activities, increases with depth resulting in a larger portion of heavier material that is expected to settle immediately after being mobilised by the cutterhead. Given the physical differences in material within the vertical sediment profile, as documented by Particle Size Distributions (PSD) and core inspections, these reductions in fine material release have been extended to apply to spill rates for the CSD, TSHD drag head and propeller disturbance.

The spill rates, cycle times, and production rates for the CSD and barge overflow activities have been provided by RTA, through an assessment made by a potential dredge contractor, and are shown in Table 5-2 and Table 5-3 for the two proposed dredging options. These rates and times were reviewed by WorleyParsons dredging specialists and considered appropriate based on experience with similar dredging operations. To ensure consistency with the previous modelling, spill rate reduction for layers 2, 3, and 4 are assumed to reduce by the same factors used in the previous study.

Table 5-2 Adopted spill rates (kg/s) and cycle times for CSD and TSHD option

	Dredge Parameters		Spill rates (kg/s)			
Activity	**Production rate**	**Activity time per cycle**	**Layer 1**	**Layer 2**	**Layer 3**	**Layer 4**
CSD draghead	1,300 m^3/h (berths & departure areas) 1,400 m^3/h (departure channel)	2 – 2.5 hrs. operation (over 4 hr cycle)	3	1.4	1	0.6
CSD : diffuser at 1/2 water depth			6	3	1.9	1
TSHD draghead and propeller disturbance	2,750 m^3/cycle (11,500 m^3 hopper capacity)	Hopper loading 30 mins till overflow and thereafter 60 mins with overflow (total 90 min loading) over cycle times 188 - 215 mins	5.5	3	2	1.5
TSHD overflow (at 9 m depth due to “Green Valve”)			17	12	8	5
TSHD disposal (at keel level of 9 m)		20 min	70	65	65	65

Table 5-3 Adopted spill rates (kg/s) and cycle times for CSD and SHB option

	Dredge Parameters		Spill rates (kg/s)			
Activity	**Production rate**	**Activity time per cycle**	**Layer 1**	**Layer 2**	**Layer 3**	**Layer 4**
CSD draghead	1,400 m^3/h (berths & departure areas) 1,500 m^3/h (departure channel)		3	1.4	1	0.6
SHB (four barges) overflow (at 5.5 m depth due to “Green Valve”)	1,220 m^3 per cycle (3,700 m^3 hopper capacity)	20 mins to overflow, thereafter 30 mins with overflow (total 50 min loading) over cycle times of 166-203 min	17	12	8	6
SHB disposal (at keel level of 5.5 m)		10 min	70	65	65	65

Based on the cycle times and volumes shown in the tables, the following number of offshore disposals under the two dredging options are assumed:

- TSHD Inshore = six full cycles and disposals per day;
- TSHD Offshore = seven full cycles and disposals per day; and
- SHB Inshore and Offshore = 14 full cycles and disposals per day in total (approximately three per dredger per day)

Based on these assumptions the total overflow time, a significant contribution to the total spilt material from dredging, is approximately 390 minutes per day under the CSD and TSHD option and 420 minutes under the CSD and SHB option. Given that these numbers are comparable, the additional spilt material from the diffuser and TSHD draghead are expected to result in a larger plume under the two dredger option.

5.5.4 Dredging Schedules

The overall duration of dredging for each of the investigated methods is shown in Figure 5-4. The operational hours of each vessel was based on estimates of effective production hours based on the material to be dredged, sailing distances, vessel production rates and anticipated downtime. These operational hours were consistent for each vessel type and as follows:

- CSD: in channel area 100 operational hours per week and 80 operational hours per week in the departure area and berth pocket.
- TSHD: 140 operational hours per week in all areas.

As indicated in the Gantt chart, the CSD and SHB case is expected to complete dredging 40 days ahead of the CSD and TSHD methodology.

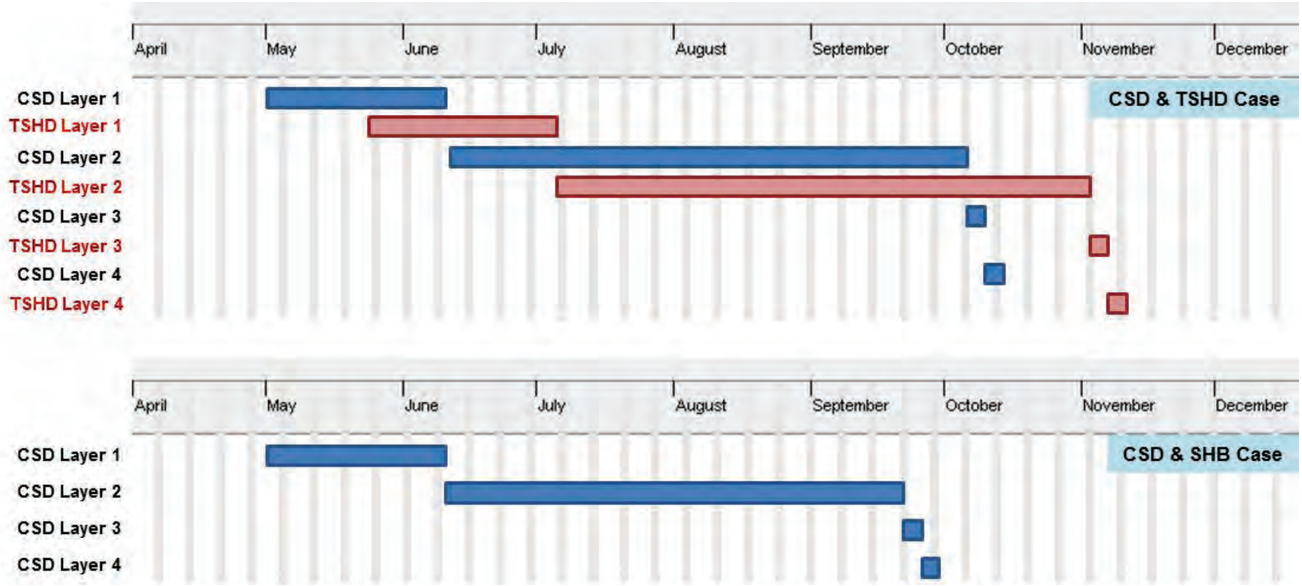

Figure 5-4 Gantt chart of dredger operation times for the two methodologies investigated

6 SEDIMENT DISPERSION MODEL

The dispersion and deposition of sediment from the proposed dredging activities was simulated with the MIKE 3 MT sediment dispersion model, coupled with the validated MIKE3 HD and MIKE21 SW models (described in Sections 3 and 4, respectively). The MIKE3 MT module was considered the most suitable given its accurate representation of wetting and drying effects and its ability to dynamically change the flow regime as sedimentation and erosion changes the seabed during the dredging program. The finite element mesh utilised in the model also enabled a large area, spanning approximately 190 km from Cape Keerweerin in the south to the Pennefather River in the north (Figure 3-3), to be included in the model which was important in this study given that both the offshore dumping and nearshore dredging were to be included in the same model.

The model was run under typical tide, wind and wave conditions, all of which was realistically varied in time and space, to coincide with those most likely to be experienced during the dry and transition (spring) seasons predicted to be encompassed during the dredging operation. Dredge plume modelling during extreme weather conditions, monsoonal activity and cyclones, was not considered necessary as dredging would not be undertaken under such conditions due to safety issues.

6.1 Model Description

The sediment plume modelling is based upon DHI's MIKE3 MT multi fraction cohesive sediment transport model. The MIKE3 MT Module describes erosion, transport and deposition of mud or sand/mud mixtures under the action of currents, wind and waves. The bed is described as layered and characterised by the density and critical shear strength for erosion. For the sediment plume study, a single seabed layer has been assumed.

The MIKE3 MT module, which calculates the combined transport of cohesive sediments (silt/clay; with grain size Diameter ≤ 75µm) and non-cohesive sediments (sand; Diameter > 75µm), is basically a solution of the advection dispersion equation. For a selected water layer, the equation can be expressed as:

$$\frac{\partial c}{\partial t} + v_x \frac{\partial c}{\partial x} + v_y \frac{\partial c}{\partial y} = \frac{1}{h}\frac{\partial}{\partial x}\left(hD_x \frac{\partial c}{\partial x}\right) + \frac{1}{h}\frac{\partial}{\partial y}\left(hD_y \frac{\partial c}{\partial y}\right) + Q_L C_L \frac{1}{h} - S$$

where:

c= suspended sediment concentration;

$v_x, v_y =$ current speed in the x and y directions;

$h =$ water layer thickness;

$D_x, D_y =$ dispersion coefficients in x and y directions;

Q_L =source discharge rate

C_L =source discharge sediment concentration

S = deposition / erosion rates.

Re-suspension of material from dredging is included within the model predictions, with all fines released from dredging available for later re-suspension as based on a critical shear-stress formulation.

6.2 Source Inputs

The MIKE 3 MT module allows for the input of time-varying point-source suspended sediment inputs. These point sources are fully defined in their magnitude, spatial location, duration and discharge depth within the water column.

For the proposed initial capital dredging for the Port, the fine material generated from the dredging activities were released at 58 positions within the proposed dredged area and 10 positions within the proposed new spoil ground offshore in order to provide realistic spatial variability into the discharge from the dredger across the Project site. These spill locations, along with the assumed dredge cut path, are shown graphically in Figure 6-1.

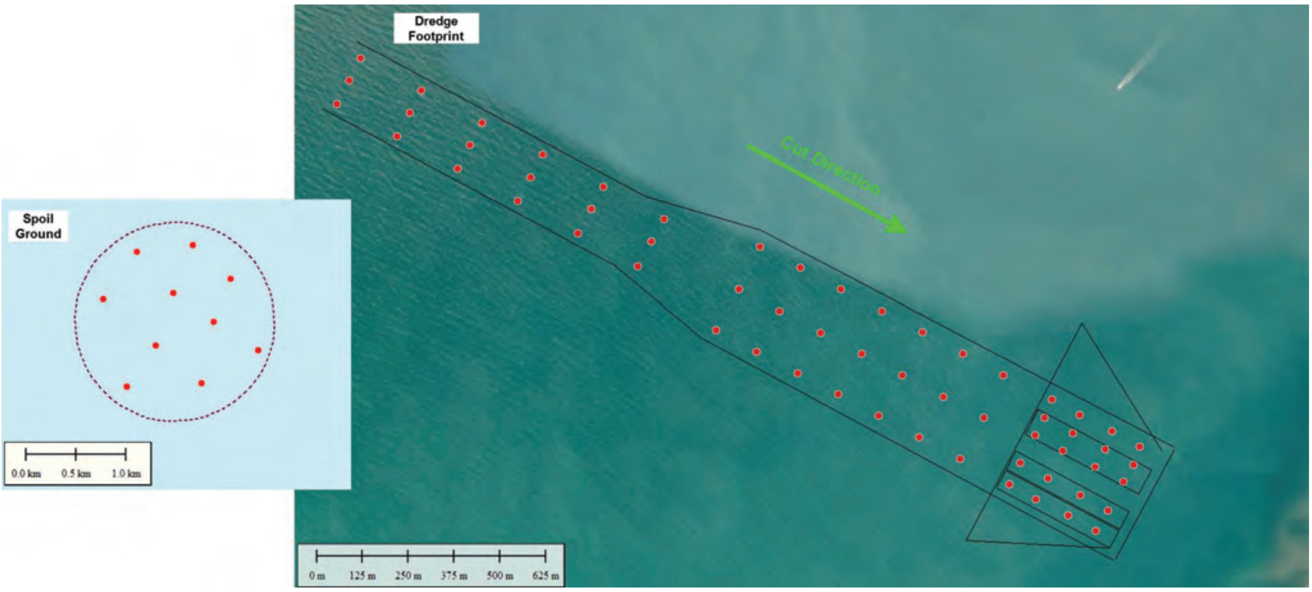

Figure 6-1 Location of modelled spill locations within the dredge footprint and spoil ground sites. Dredge cut-direction shown in Green.

It was assumed that the dredge vessel would cut in the shoreward direction, starting in the offshore extent of the departure channel and heading towards the berth pockets and would do this across four separate layers as follows:

- Layer 1 – dredge nearshore region to -14.4 m CD (design depth of DPPV Berth pockets)
- Layer 2 – dredge offshore and nearshore sections of the departure channel and Capesize berth pockets to -17.3 m CD (design depth of departure channel)
- Layer 3 – dredge Capesize berth pockets to -18.5 m CD
- Layer 4 – dredge Capesize berth pockets to -19.7 m CD (final design depth)

6.3 Domain and Bathymetry

As the MIKE3 MT model is dynamically coupled with the hydrodynamic model (MIKE3 HD) the sediment plume model adopted the same model domain as that used in the hydrodynamic model.

To correctly characterise the dispersion pattern over the course of the dredging operation it was necessary to conduct the dredging operation over two stages. This was done to ensure that the hydrodynamic forcing in the model provided an accurate representation of the dynamic seabed change as the dredge vessel progressed across the dredge footprint. The MIKE3 MT and HD model domain over these two stages is shown in Figure 6-2.

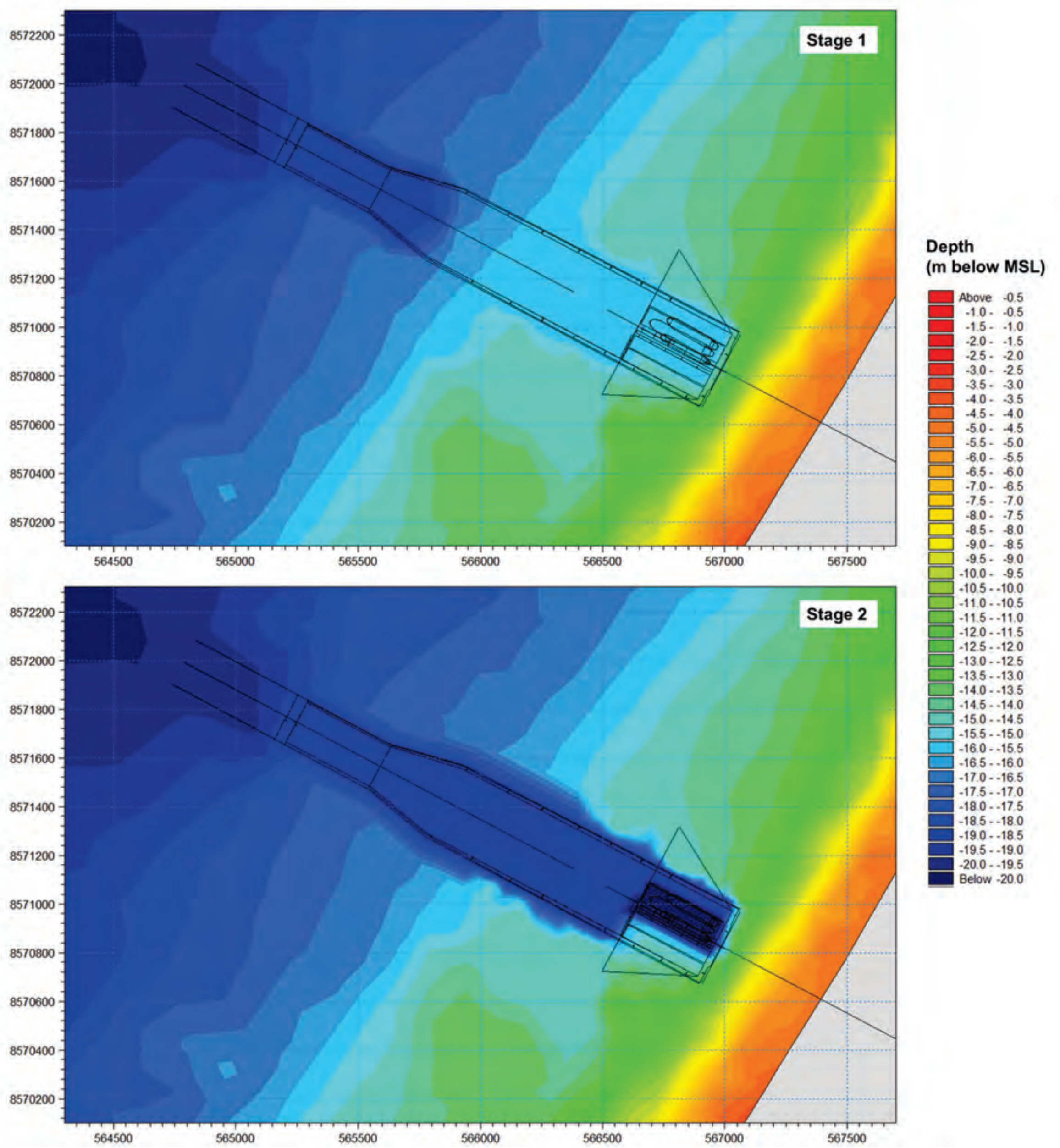

Figure 6-2 MIKE 3 MT Model bathymetry for the two dredging stages modelled (as titled). Please note depths here are shown with respect to mean sea-level (MSL).

6.4 Hydrodynamic Forcing

As the MIKE3 MT model was dynamically coupled to the hydrodynamic model (MIKE3 HD), changes to the flow regime as a result of sedimentation and erosion patterns during the simulation were incorporated in the model results. The hydrodynamic forcing covered the full period of the dredging operation, inclusive of a one month buffer on either side of the designated dredging dates illustrated in Figure 5-4.

6.5 Wave Forcing

Wave forcing was taken directly from the MIKE21 SW model described in Section 4. Spatially and temporally varying wave height (H_S), period (T_P) and direction (θ_P) information was included in the model at half-hourly intervals over the entire simulation period. The model then internally calculates the associated level of seabed shear stress and orbital velocity that relates directly to the level of particle re-suspension and transport in the model associated with wave action.

To coincide with the hydrodynamic forcing, the wave input covered the full period of the dredging operation for the two dredge cases modelled over the dry and transition (spring) seasons, inclusive of a one month buffer on either side of the designated dredging dates illustrated in Figure 5-4.

6.6 Model parameters

6.6.1 Deposition

In the model, the deposition rate is formulated as a function of the settling velocity, the near-bed concentration and the actual critical bed shear stress for deposition. The settling velocity in this formulation depends on two key parameters, namely the grain size and an estimation of the level of flocculation, with larger grain sizes (i.e. those associated with sands) containing much higher settling velocities than finer materials. As such, sands are more readily deposited in the model than the fine silt and clay materials, which tend to remain suspended and transported greater distances in the model.

For the current study, a critical bed shear stress for deposition of 0.1 N/m^2 was employed, consistent with recommendations for dredge dispersion studies in areas of similar seabed characteristics (Doorn-Groen & Foster 2007).

6.6.2 Erosion

The erosion rate depends on the seabed properties, whether the seabed is dense and consolidated or soft and only partly consolidated. In the present model, the bed is described as one layer with the material deposited and resuspended solely that resulting from the dredging works at the project site. This enabled the impact of the proposed dredging works to be isolated in the analysis. The layer contains the material which is re-suspended and subsequently settled during each tidal cycle. A threshold criteria shear stress is usually set to determine whether the deposition material is re-suspended or not. The criterion for erosion is exceeded corresponding to the driving forces exceeding the sediment stabilising forces.

Partheniades, (1965) and Parchure & Mehta, (1985) investigated the critical shear stress listed in Table 6-1. For the present modelling study, however, in the absence of site measurements, the critical shear stress parameter in the model was set to the value of 0.3 N/m^2 for the whole area given that partly consolidated mud covers most of the surface in the immediate surrounds to the Project site. This value is also consistent with critical shear stress values recommended in recent dredge dispersion studies near environmentally sensitive areas, where mud-type substrates dominated (Doorn-Groen & Foster 2007).

Table 6-1 Criteria Shear Stress for Sedimentation Erosion. (Partheniades, (1965) and Parchure & Mehta, (1985))

Mud Type	Density (kg/m3)	Typical critical shear stress (N/m2)
Mobile fluid mud	180	0.05 – 0.1
Partly consolidated mud	450	0.2 – 0.4
Hard mud	600+	0.6 – 2.0

6.7 Results

It was expected that a turbid plume would eventuate as material was released to the water column during the operation of the CSD and TSHD dredgers. The fine clay and silt fractions, with their lower settling velocity, may remain in the water column for long periods (days) and a low concentration plume may disperse for several kilometres in the direction of the tide. Given that the plumes are predominantly advected by currents at this site (and to a lesser extent waves), the individual flood and ebb tide phases influence their shape and trajectory, as do spring and neap tide phases. To confirm this, the model results for the entire dredging operation were examined for both cases.

Predictions of the sediment plume dispersion and deposition patterns have been extracted from the sediment dispersion model. Percentiles of total suspended sediments (TSS) and sedimentation have been calculated over the entire simulation. The results are presented in Sections 6.7.1 and 6.7.2, respectively. The spatial images of percentiles were selected as the most appropriate means of presenting the results as they provide a clear indication of the scale and magnitude of the environmental footprint of the dredging operation.

All values presented here for TSS and sedimentation rates are based on simulation of the initial capital dredging operation for the proposed Port and offshore disposal at the proposed new spoil ground. The results are representative of concentrations above background levels, with background TSS and sedimentation rates not included in the analysis.

6.7.1 Suspended Sediments

Percentile and Timeseries Analysis

The median and 80th percentile of the TSS concentrations from the dredge plume dispersion model have been extracted and plotted for the two separate dredging methodologies considered, with the results presented in Figure 6-4 to Figure 6-7. To aid in the analysis of the plumes, time series of TSS were extracted from the model at specified locations near sites of interest. The locations of modelled time series extracts are shown in Figure 6-3.

Figure 6-3 Location of modelled time series extracts

The results agree with the aforementioned expectation that the plume would migrate along the main tidal axis near the Port site and proposed new spoil ground. Model outputs identify that during flood tides the turbid plume generated by the Port area initial capital dredging extends generally parallel to the coast, from the dredge location to beyond Pera Head, with Boyd Point experiencing a relief from the increased TSS concentration during this tide. In contrast, during the ebb tide the dredge plume extends along the coast extending from Pera Head to Boyd Point. Pera Head does not experience this full relief of the elevated TSS levels due to the net south-west tidal current direction causing suspended material to accumulate between the proposed Port and Pera Head. This results in the plume extending up to 27 km south of the proposed Port development, under both dredging options, as depicted in the 80^{th} percentile maps (Figure 6-5 and Figure 6-7).

Modelled TSS time series data from Boyd 1 (Boyd Point) and Pera 1 (Pera Head) are illustrated in Figure 6-9 and Figure 6-11, respectively, for the two dredging options. Periods of high TSS concentration generally coincide with the TSHD and CSD operating in the inshore area (i.e. in the berths and departure area) over the first layer of sediments (Layer 1 in the plots) as a result of the higher fine content in this layer. The results show that whilst the Boyd Point locations experience higher instantaneous TSS levels (primarily due to their closer proximity to the dredging operations as shown in Figure 6-3), the Pera Head sites show more consistently maintained TSS levels, particularly during the first three months of the dredging.

Comparatively, the CSD and TSHD combination is shown to produce a significantly larger plume in the nearshore than the CSD and SHB option. Higher TSS levels in the nearshore are due to the action of the two dredge vessels in the CSD and TSHD case, which do not necessarily have synchronised downtimes, resulting in a more consistently present plume as the operations of the vessels are more-or-less continuous. The discharge from the CSD diffuser also contributes to the larger plume present under this dredging methodology.

For the sites closer to the dredge footprint (i.e. Pera, Beach and Boyd sites) the TSS values are visibly higher under the two dredger case, with the CSD and TSHD option not only producing higher instantaneous and daily average concentrations but also a more prolonged plume in this vicinity due to the longer dredging operations. It should be noted, however, that the daily-averaged TSS is generally considerably lower than 20 mg/L at all of these nearshore sites.

Sites around Thud Point experience low TSS concentrations, with daily average TSS levels less than 5 mg/L under the CSD and SHB case and 7 mg/L under the CSD and TSHD case. As shown by the 80^{th} percentile plot for the two dredger case (Figure 6-5) in the Thud Point vicinity, TSS levels are considerably higher than that of the CSD and SHB case (Figure 6-7).

Offshore at the Nine Mile Reef receptor sites (Figure 6-10), concentrations are shown to be consistently low under both dredging operations, with the instantaneous depth-averaged TSS less than 5 mg/L, and daily average less than 3 mg/L, under both dredging methodologies. In contrast, the proposed new spoil ground sites, given their proximity to the offshore dumping, observe the highest instantaneous TSS levels of all the sites analysed across both dredging cases. Due to the larger volume of material being dumped by the TSHD the instantaneous TSS concentrations are higher under this case, however, the daily-averaged TSS is comparable amongst both cases due to the more frequent SHB dumping. Furthermore, the median and 80^{th} percentile plots for the CSD and SHB case (Figure 6-6 and Figure 6-7) shows that the more frequent dumping of the SHB results in a more consistently elevated TSS concentration (5 to 10 %) in the vicinity of the proposed new spoil ground.

It should also be noted that the modelled TSS concentrations, under both dredge cases modelled, are within the range of the relatively high and variable background concentrations at the proposed Port and new spoil disposal sites. Measurements at Pera Head suggest that the 80th percentile background concentrations are of the order of 9 mg/L in the dry and 22 mg/L in the wet seasons, with background concentrations in the proposed new spoil ground approximately 4 mg/L in the dry and 40 mg/L in the wet season (Section 6.4.4 in RTA, 2011).

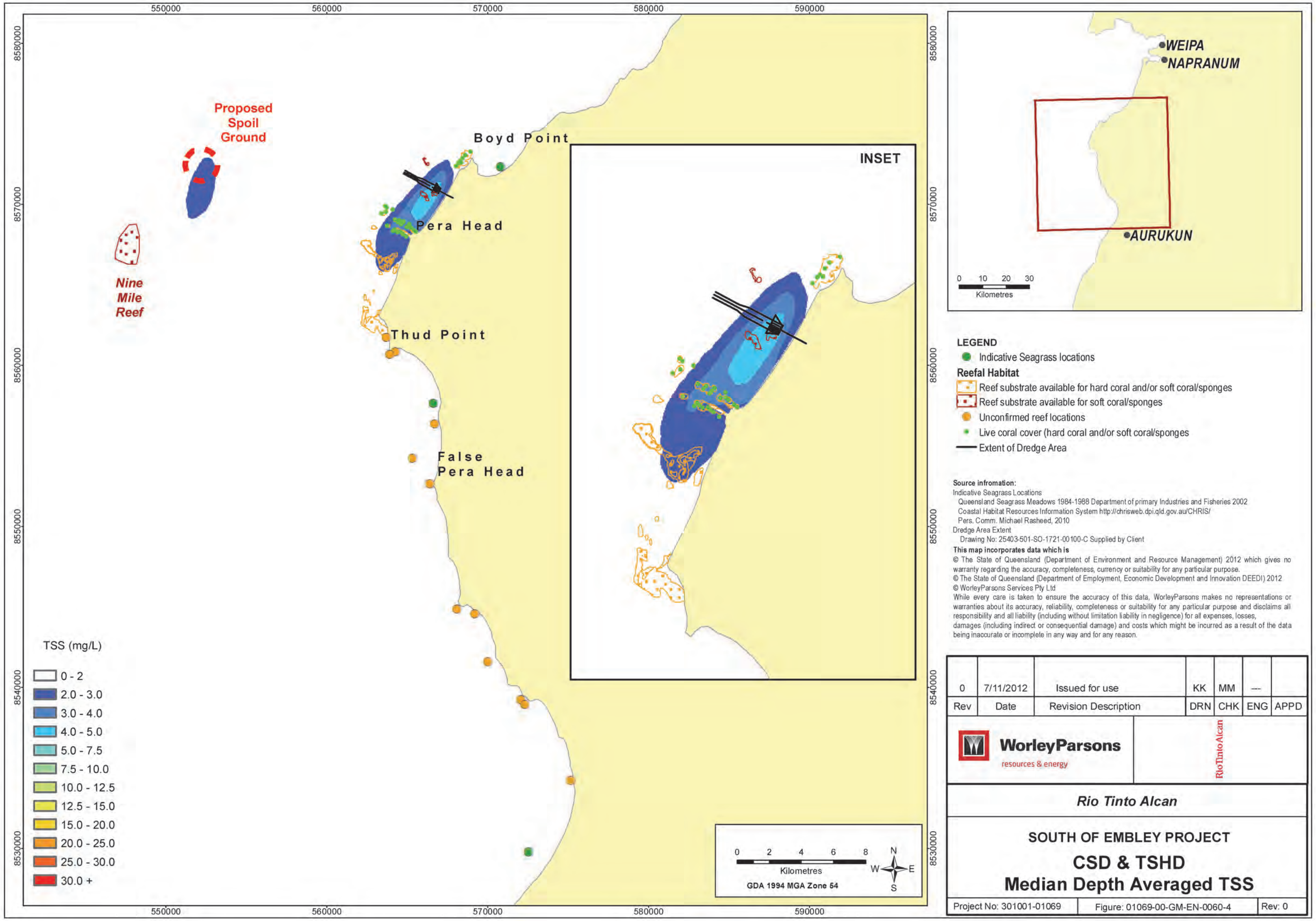

Figure 6-4 Median TSS (above background) for CSD and TSHD case over the entire simulation period.

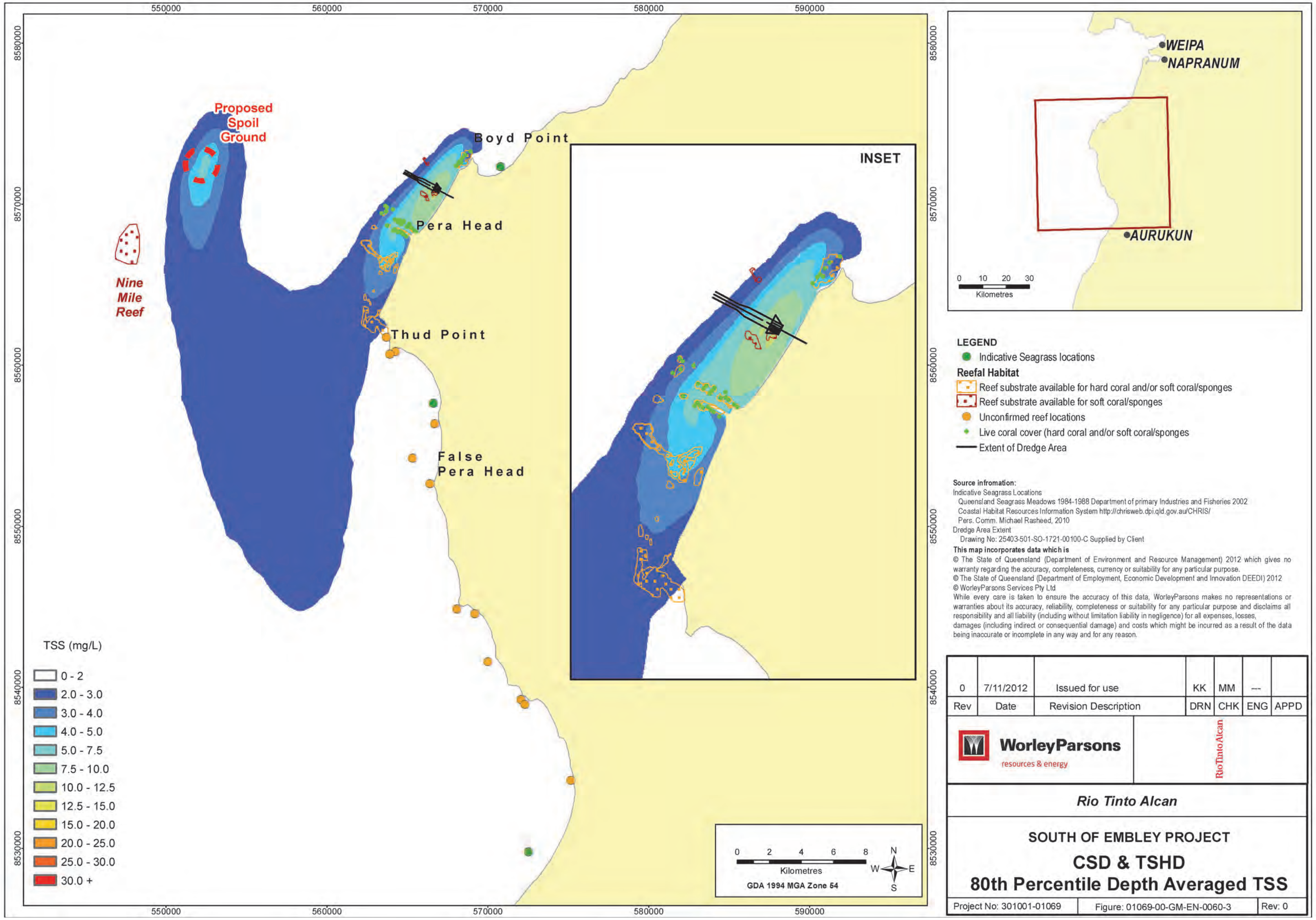

Figure 6-5 80th Percentile TSS (above background) for CSD and TSHD case over the entire simulation period.

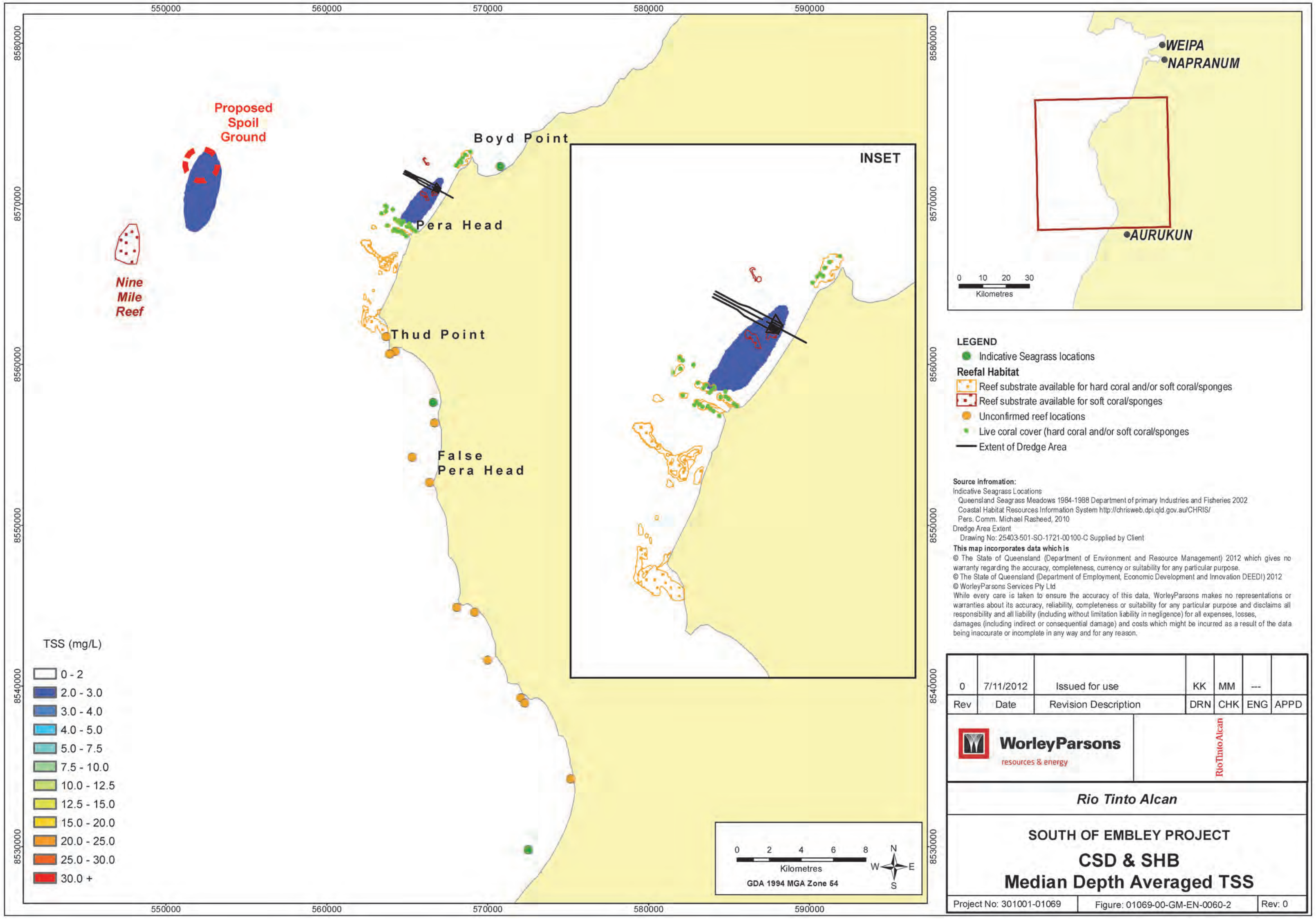

Figure 6-6 Median TSS (above background) for CSD and SHB case over the entire simulation period.

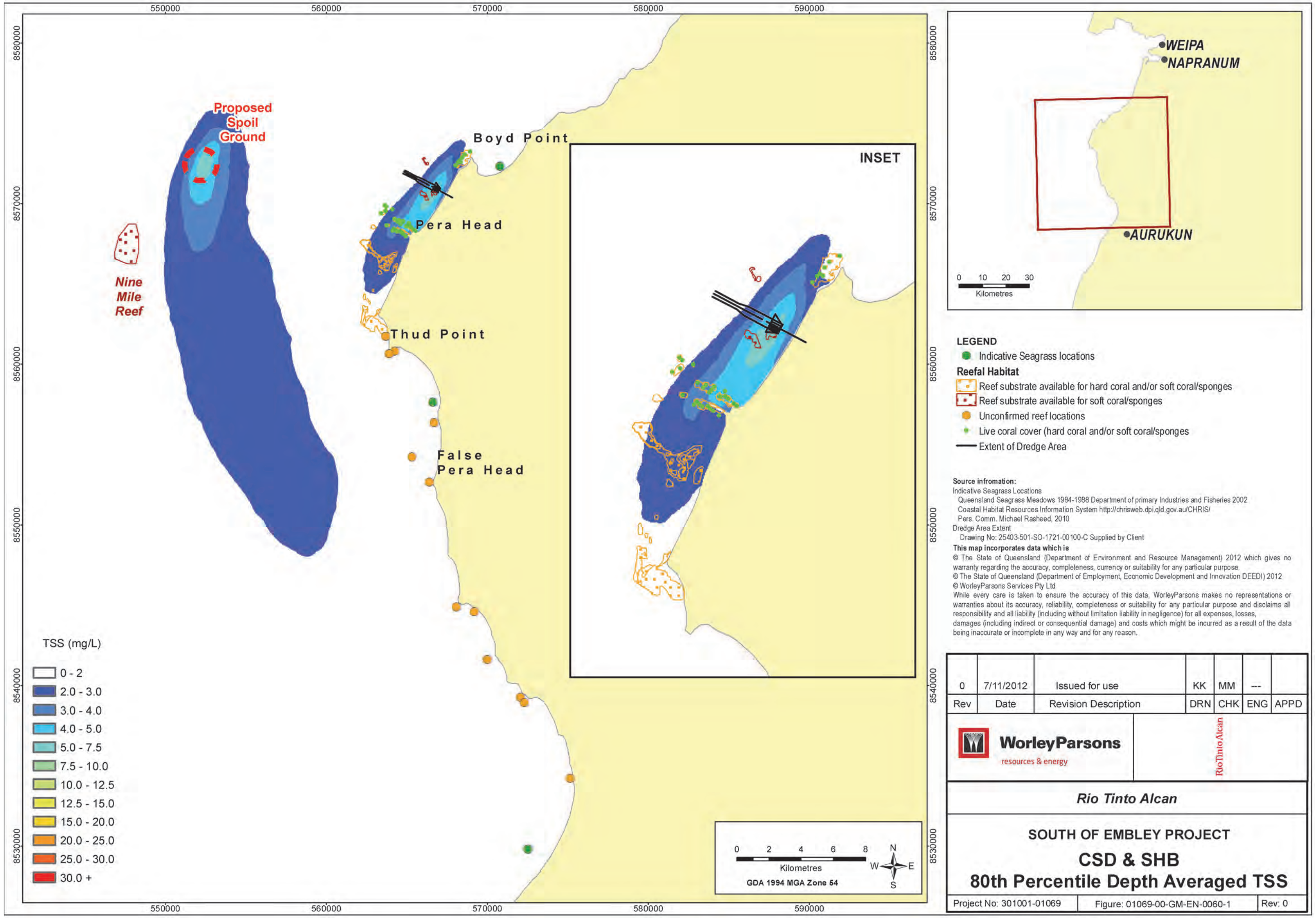

Figure 6-7 80th Percentile TSS (above background) for CSD and SHB case over the entire simulation period.

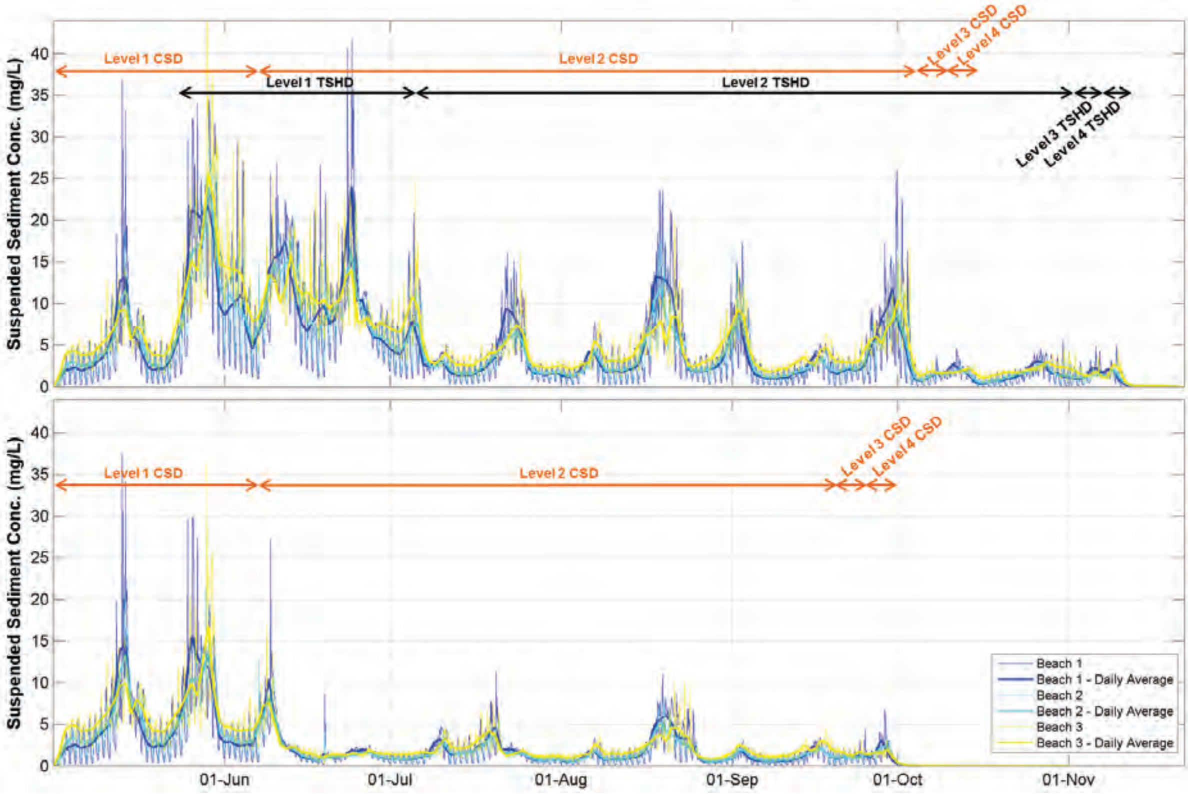

Figure 6-8 Time series of predicted TSS (above background) at the *Beach* sites for CSD and TSHD case (top) and CSD and SHB case (bottom) over the respective dredging periods.

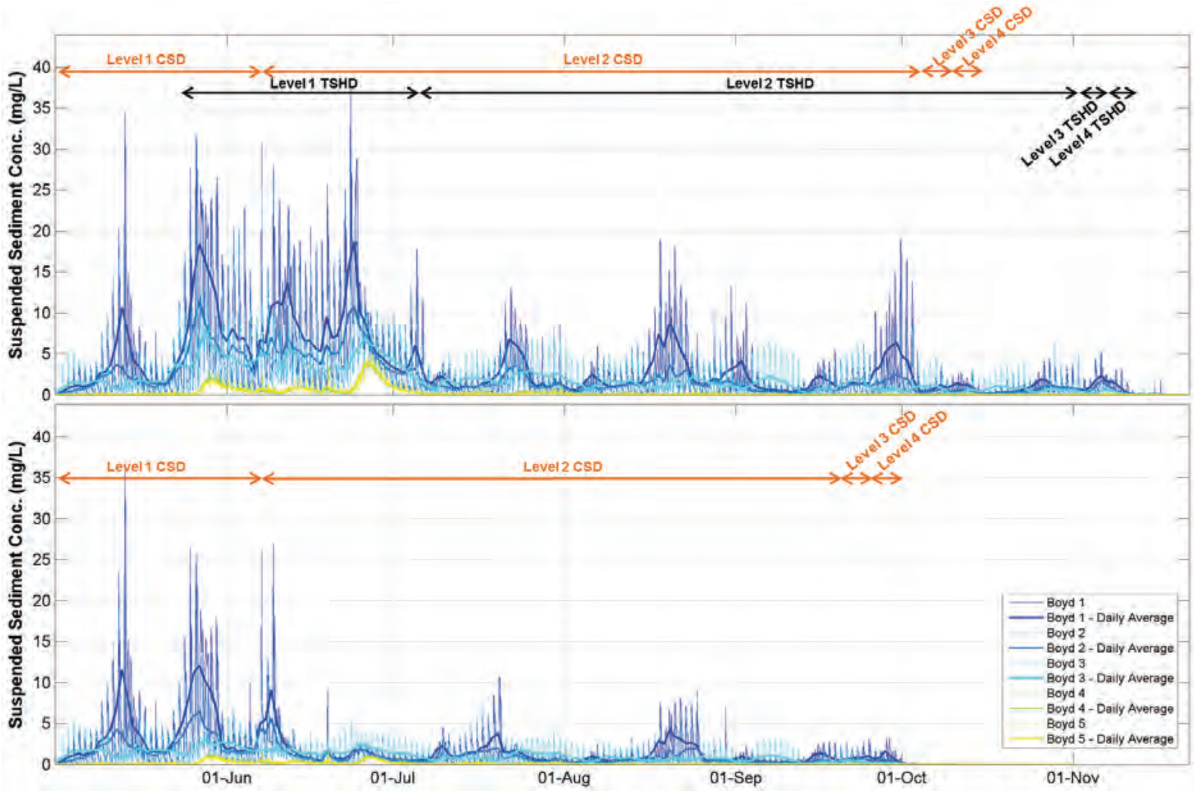

Figure 6-9 Time series of predicted TSS (above background) at the *Boyd Point* sites for CSD and TSHD case (top) and CSD and SHB case (bottom) over the respective dredging periods.

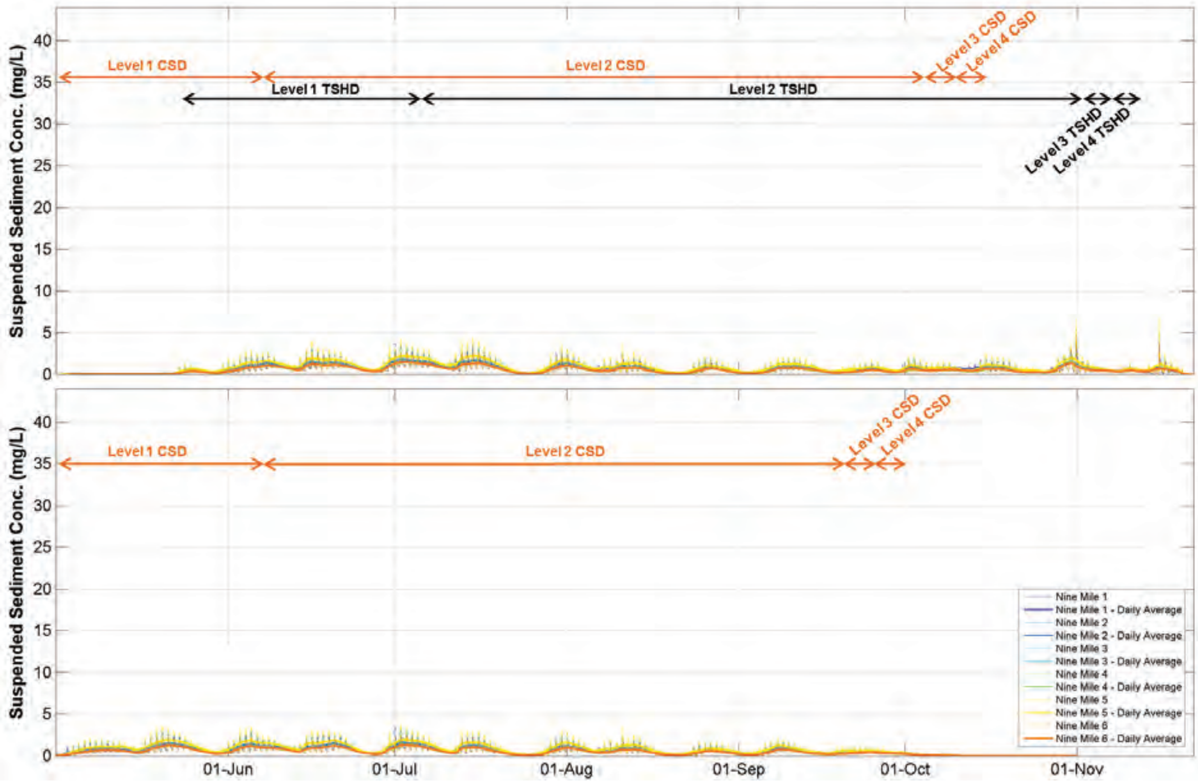

Figure 6-10 Time series of predicted TSS (above background) at the *Nine Mile Reef* sites for CSD and TSHD case (top) and CSD and SHB case (bottom) over the respective dredging periods.

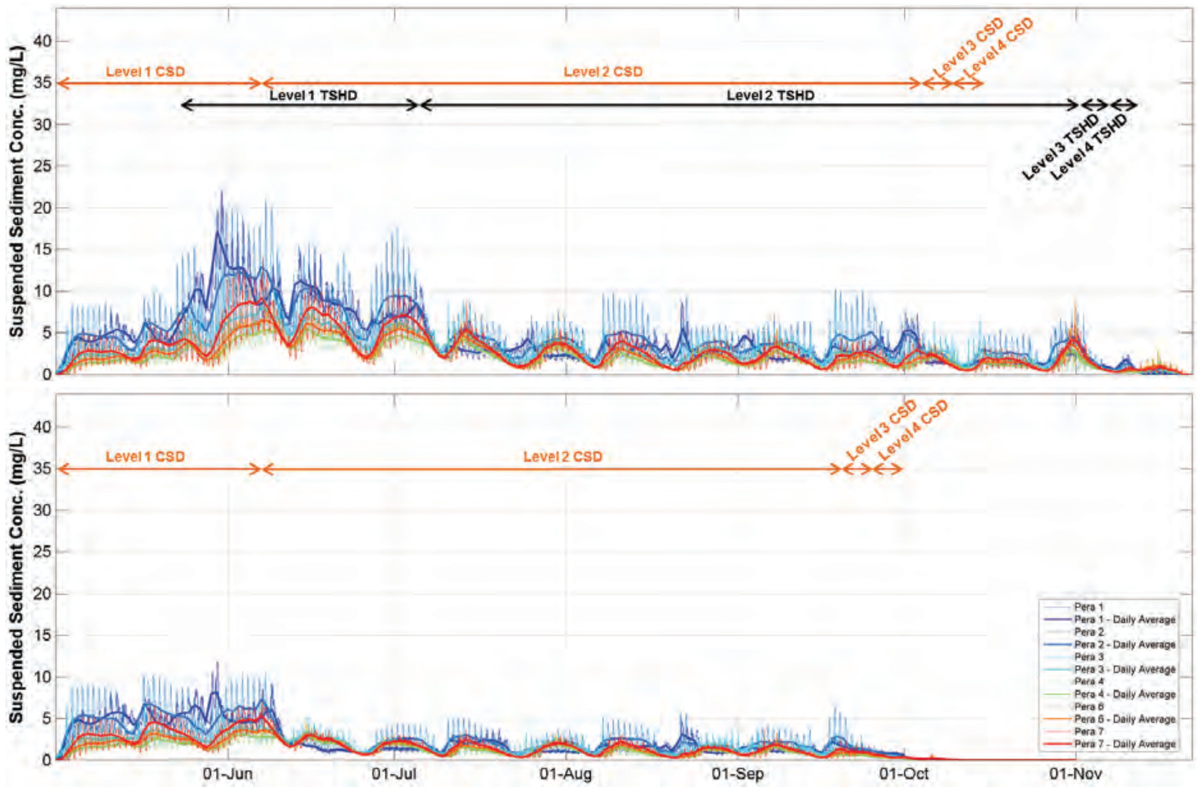

Figure 6-11 Time series of predicted TSS (above background) at the *Pera Head* sites for CSD and TSHD case (top) and CSD and SHB case (bottom) over the respective dredging periods.

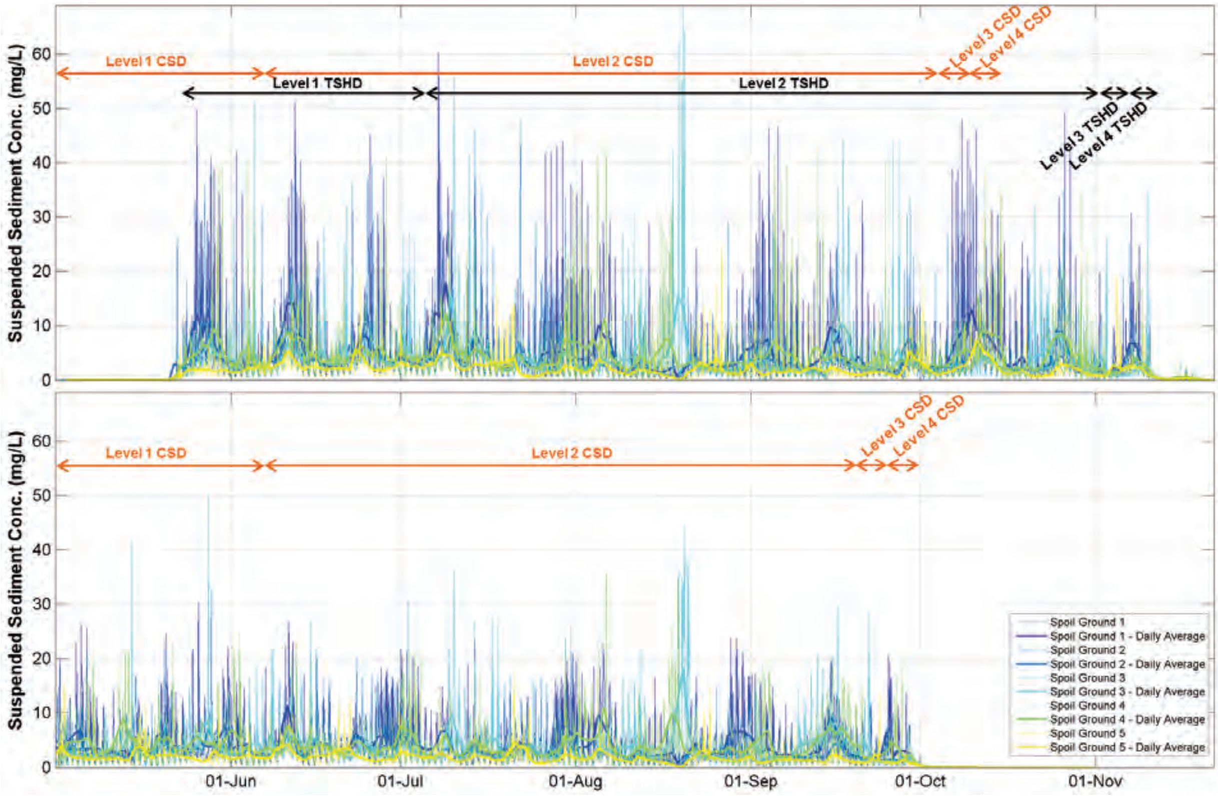

Figure 6-12 Time series of predicted TSS (above background) at the *Spoil Ground* sites for CSD and TSHD case (top) and CSD and SHB case (bottom) over the respective dredging periods.

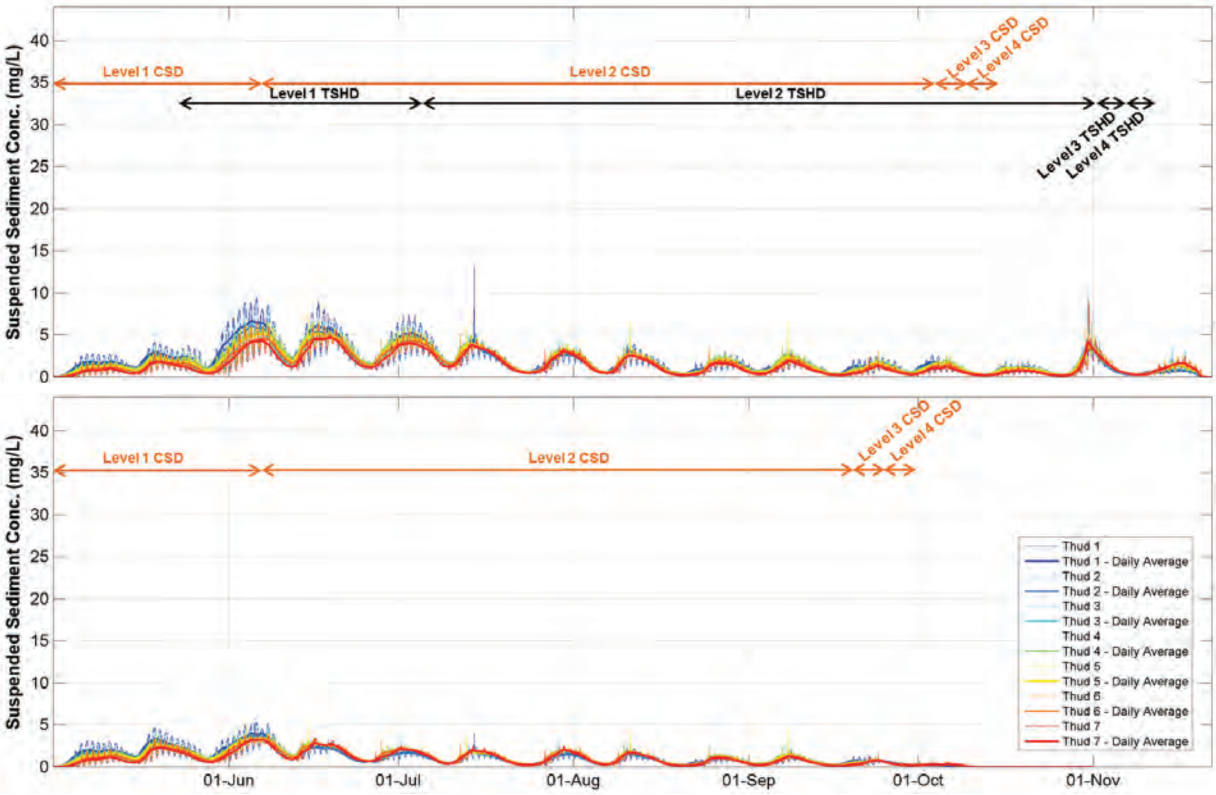

Figure 6-13 Time series of predicted TSS (above background) at the *Thud Point* sites for CSD and TSHD case (top) and CSD and SHB case (bottom) over the respective dredging periods.

Depth Variation of Suspended Sediments

The three-dimensional computation of the MIKE 3 MT model meant that the location of the plume in the vertical space was fully captured in the model. With the variety of the spill locations, and discharge depths of each of the sources, it was important to investigate the plume behaviour in the vertical water column at the receptor sites.

This investigation is illustrated in Figure 6-14 to Figure 6-18 for selected nearshore sites (Boyd 3 and 4 and Pera 3 and 6) and an offshore site (Nile Mile 5) over two full tidal cycles during the surface (Layer 1 and 2) dredging period. The plots indicate that during periods of low TSS, for which a diurnal signal of TSS exists corresponding to the stronger diurnal tidal signal at Weipa (Figure 2-1), the Boyd and Nine Mile Reef sites show consistently low concentrations throughout the water column. During elevated TSS periods, however, the depth variation in TSS is more significant and apparent at all sites.

For the Boyd locations, variations in the vertical distribution of TSS are more significant at the Boyd 3 site, with seabed TSS values often double those at the surface during the peak daily TSS periods. Further afield at the Boyd 4 site this variance is less apparent, however, surface values are still typically 20 to 40% less than those at the seabed.

The general migration of the plume to the south (as aforementioned) results in a consistently elevated TSS concentration at the Pera sites investigated. These sites again both show seabed TSS levels of nearly double those at the surface, with a relatively consistent declination in concentrations from the seabed to the surface layers.

Instantaneous peaks in the seabed TSS concentrations are evident in nearly all plots, however, these peaks are generally restricted to the seabed layer and associated with either disposal or dredging related discharge and instantaneous re-suspension of recently settled material near the seabed.

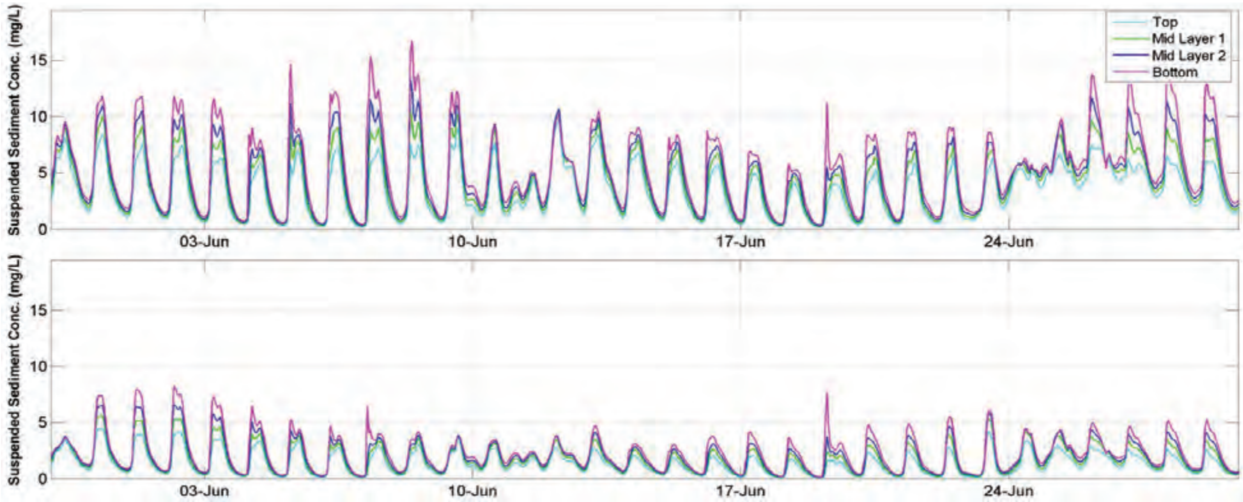

Figure 6-14 Time series of depth-variation in predicted TSS (above background) at *Boyd_3* for CSD and TSHD case (top) and CSD and SHB case (bottom) over the respective dredging periods.

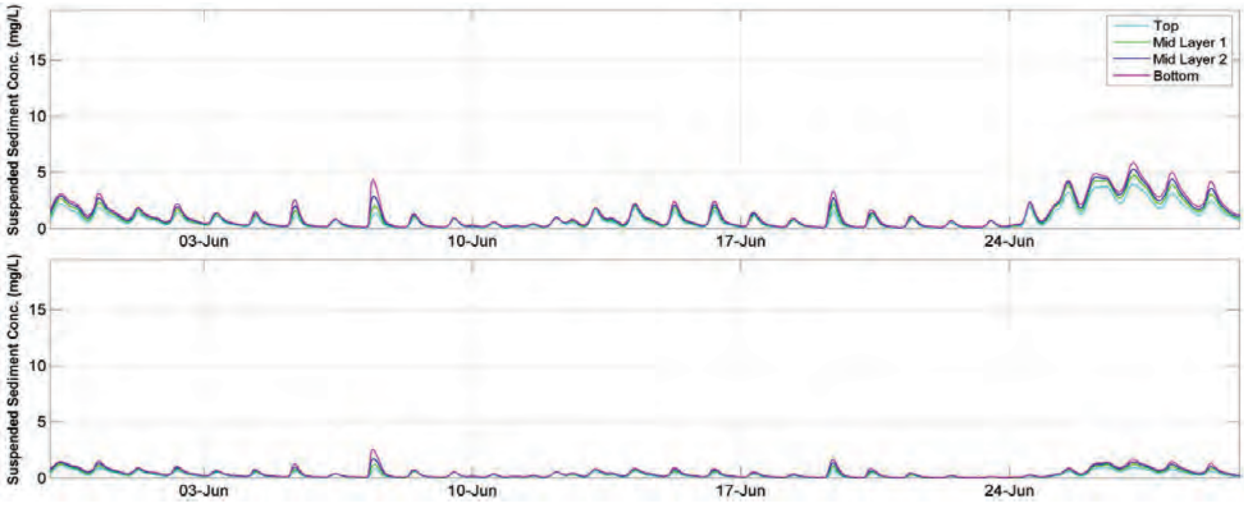

Figure 6-15 Time series of depth-variation in predicted TSS (above background) at *Boyd_4* for CSD and TSHD case (top) and CSD and SHB case (bottom) over the respective dredging periods.

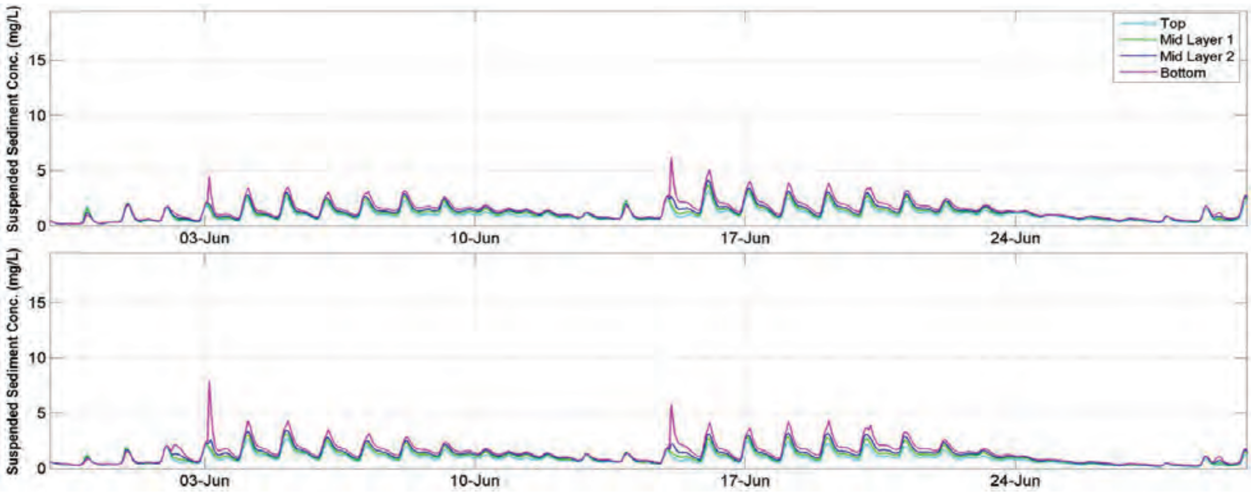

Figure 6-16 Time series of depth variation in predicted TSS (above background) at *Nine_Mile_5* for CSDandTSHD case (top) and CSDandSHB case (bottom) over the respective dredging periods.

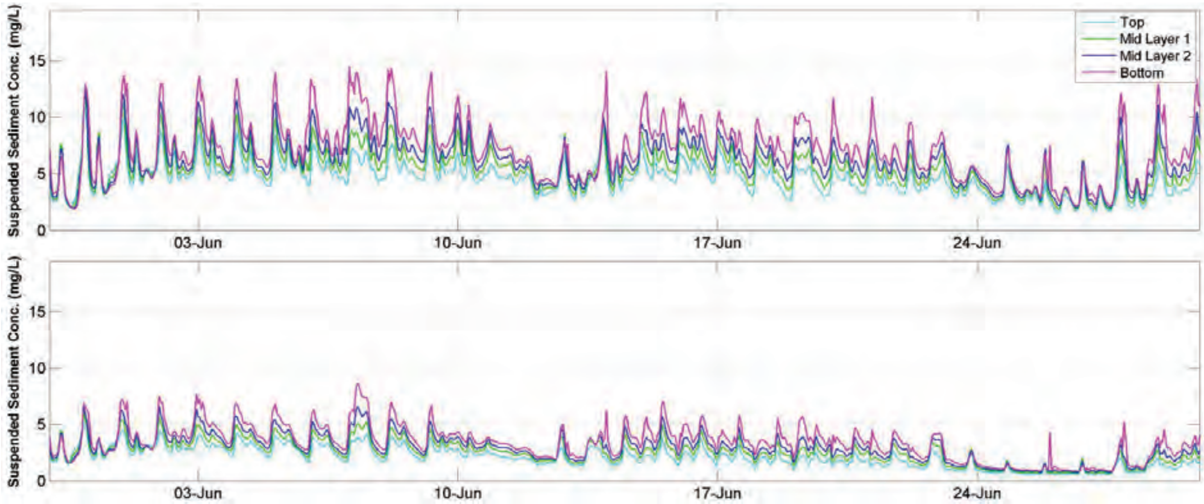

Figure 6-17 Time series of depth-variation in predicted TSS (above background) at *Pera_3* for CSD and TSHD case (top) and CSD and SHB case (bottom) over the respective dredging periods.

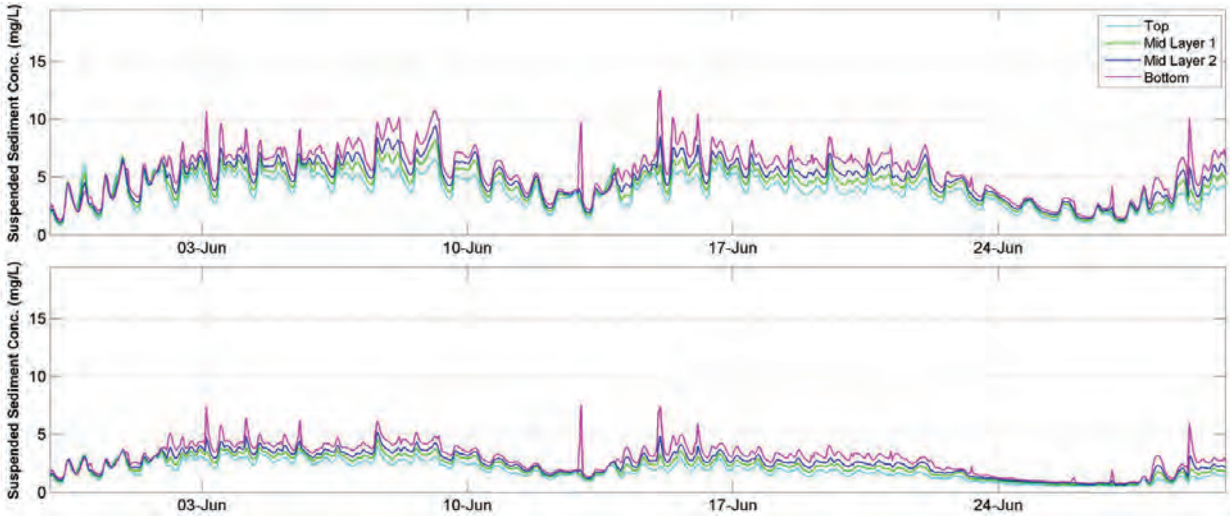

Figure 6-18 Time series of depth-variation in predicted TSS (above background) at *Pera_6* for CSD and TSHD case (top) and CSD and SHB case (bottom) over the respective dredging periods.

Set Limit Exceedance

Further analysis of the predicted plume behaviour was performed through analysis of TSS exceedance of set threshold limits over the model simulation. The durations of TSS plume concentrations at or above 5, 10 and 15 mg/L above background were extracted from the model and plotted as a percentage of the entire dredging period. The results of this, for the respective threshold TSS limits, are presented in Figure 6-19 to Figure 6-24.

Consistent with the findings in the percentile analysis, the two dredger case (CSD and TSHD) results in a more significant exceedance, in terms of both duration and scale, across all threshold limits analysed. The nearshore area receiving greater than 3 % exceedance of 5 mg/L extends from immediately adjacent to Thud Point in the south to 2 km north of Boyd Point in the north and offshore approximately 2.5 km under this case. Areas receiving 5 mg/L for greater than 30 % of the time over the CSD and TSHD dredging operation are restricted to between 1 km north of the dredge footprint and Pera Head. For the CSD and SHB case this exceedance is considerably lower in the nearshore area, with less than 8 % exceedance on the far side Boyd Point or Pera Head and the 5 mg/L limit above background exceeded less than 25 % of the time near the dredging area.

The 10 mg/L limit for the CSD and TSHD case sees the impact area (characterised as >3 % of the time over the dredging period) extend from Boyd Point to Pera Head, with this reduced to only 2 km either side of the dredge footprint for the CSD and SHB case. Under the CSD and TSHD case, exceedance of10 mg/L is expected to occur less than 20 % of the time in the immediate vicinity of the dredge footprint, reduced to less than 12 % of the time for the CSD and SHB case.

Results show that concentrations in excess of 15 mg/L are not predicted to occur beyond Pera Head or Boyd Point for any of the dredging options for over 3 % of the time.

Offshore near the disposal ground, the exceedance of all the limits investigated is relatively similar amongst both dredging options. The more frequent disposal of the SHBs results in a marginally higher exceedance of 5 mg/L of up to 25 % of the time compared with 20% of the time for the CSD and TSHD case.

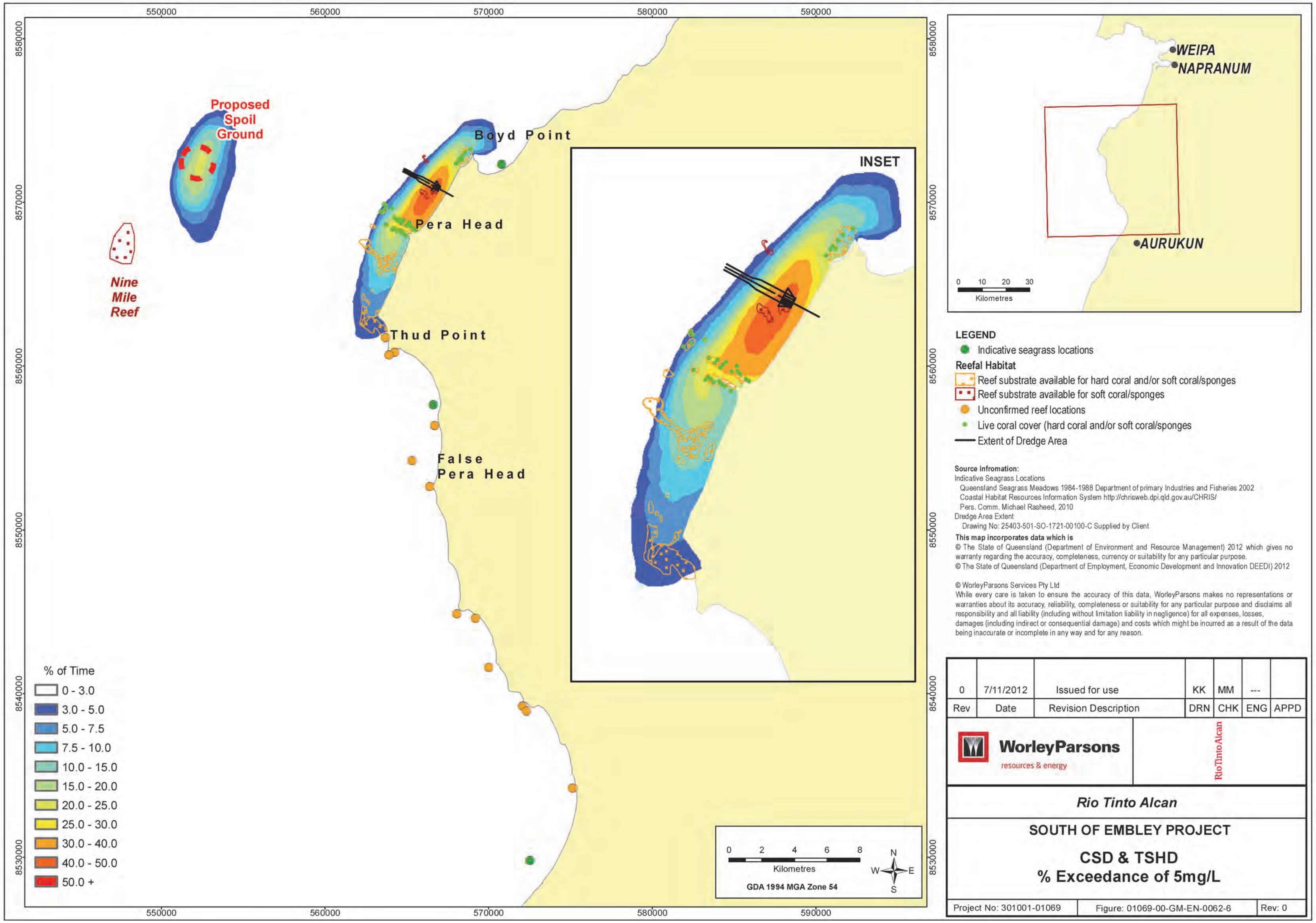

Figure 6-19 Percentage exceedance of 5 mg/L for CSD and TSHD case over the entire simulation period.

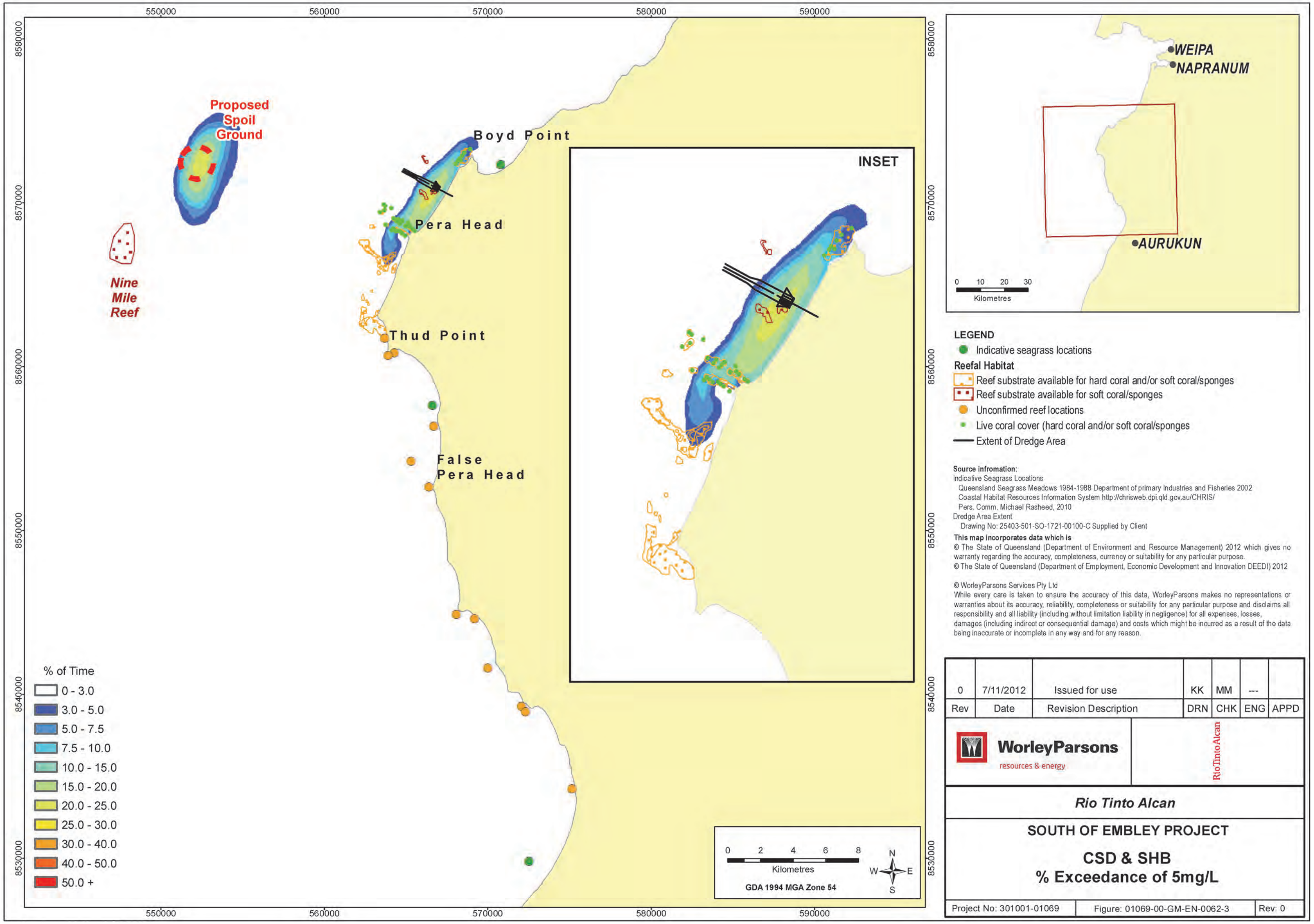

Figure 6-20 Percentage exceedance of 5 mg/L for CSD and SHB case over the entire simulation period.

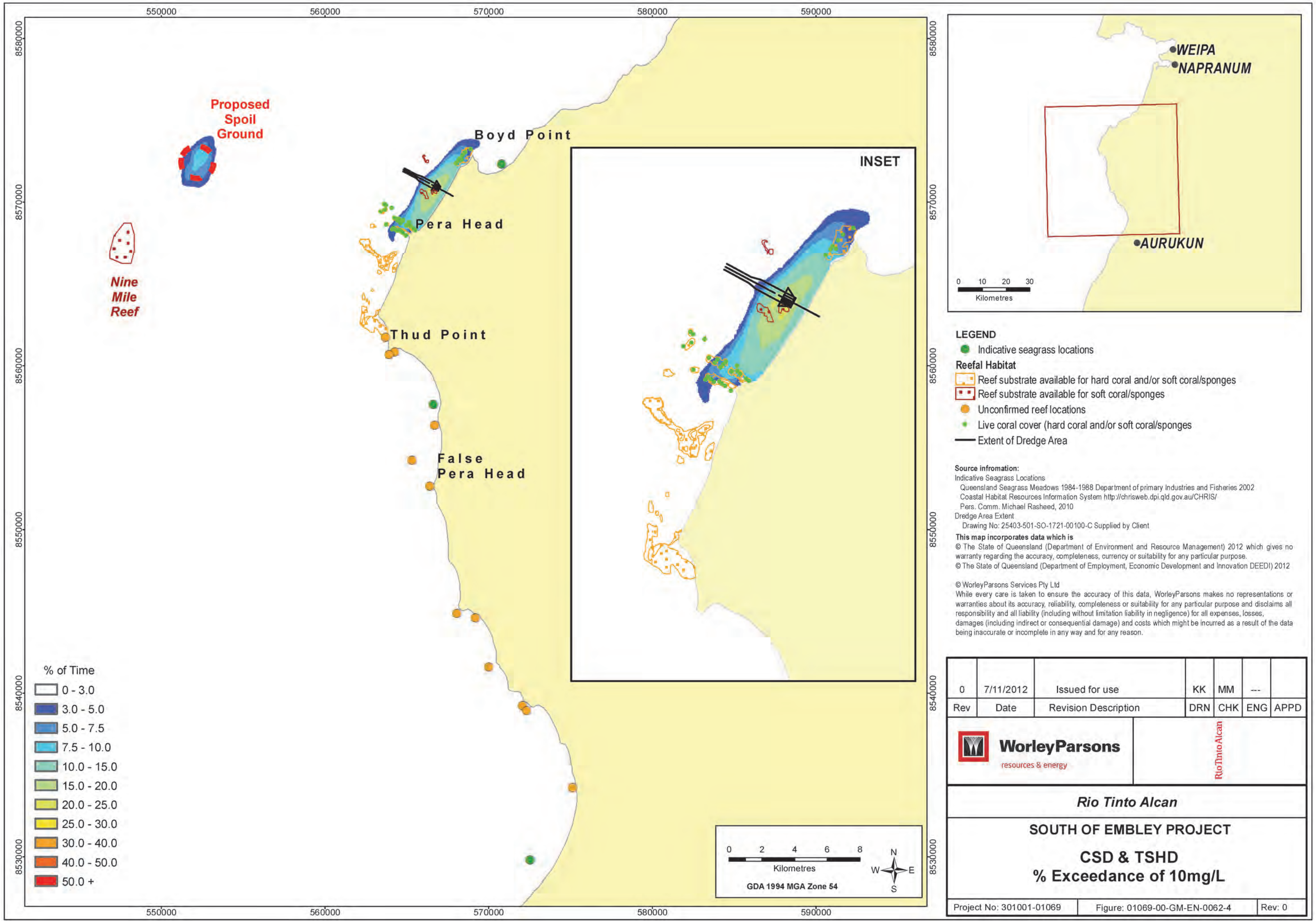

Figure 6-21 Percentage exceedance of 10 mg/L for CSD and TSHD case over the entire simulation period.

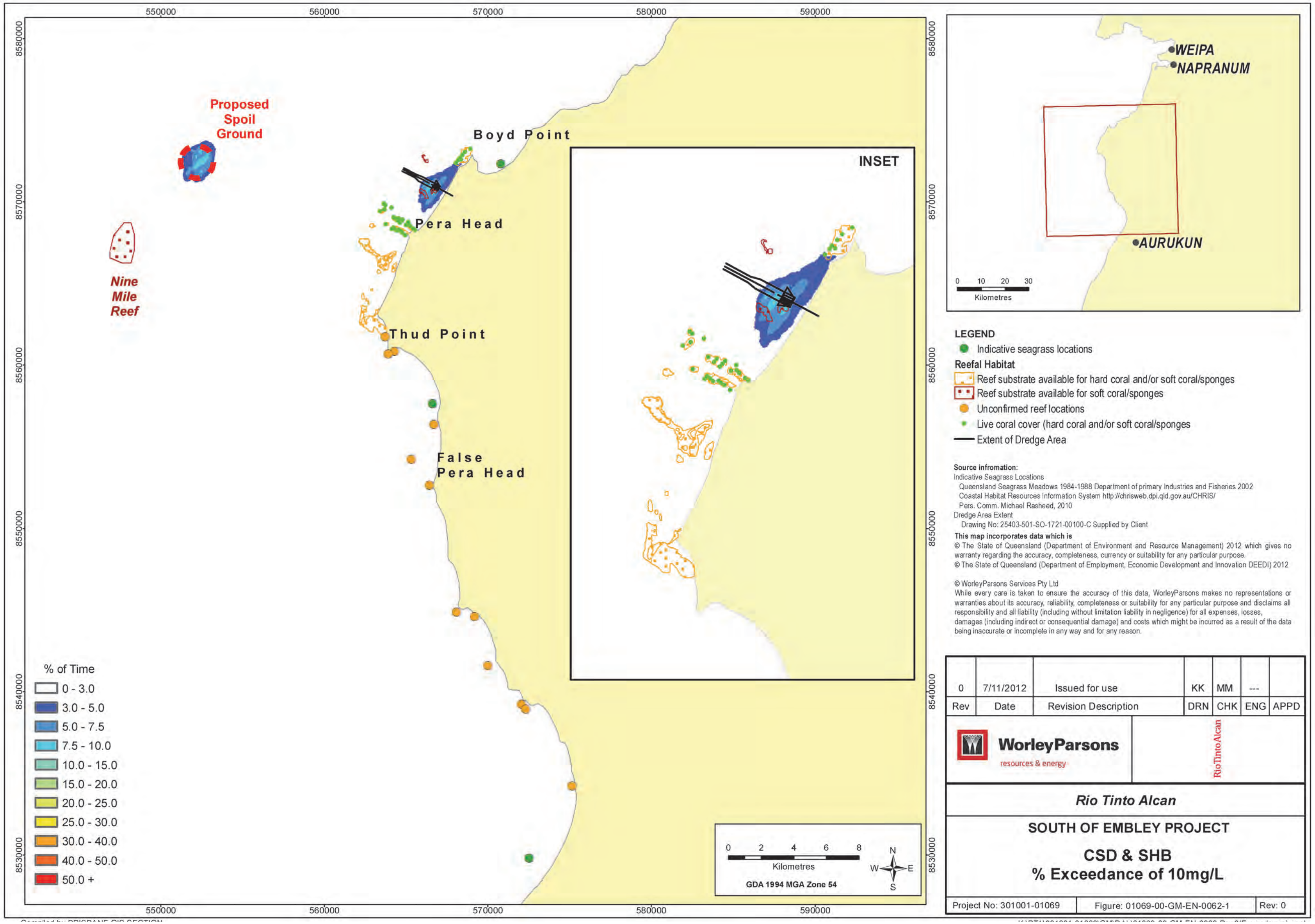

Figure 6-22 Percentage exceedance of 10 mg/L for CSD and SHB case over the entire simulation period.

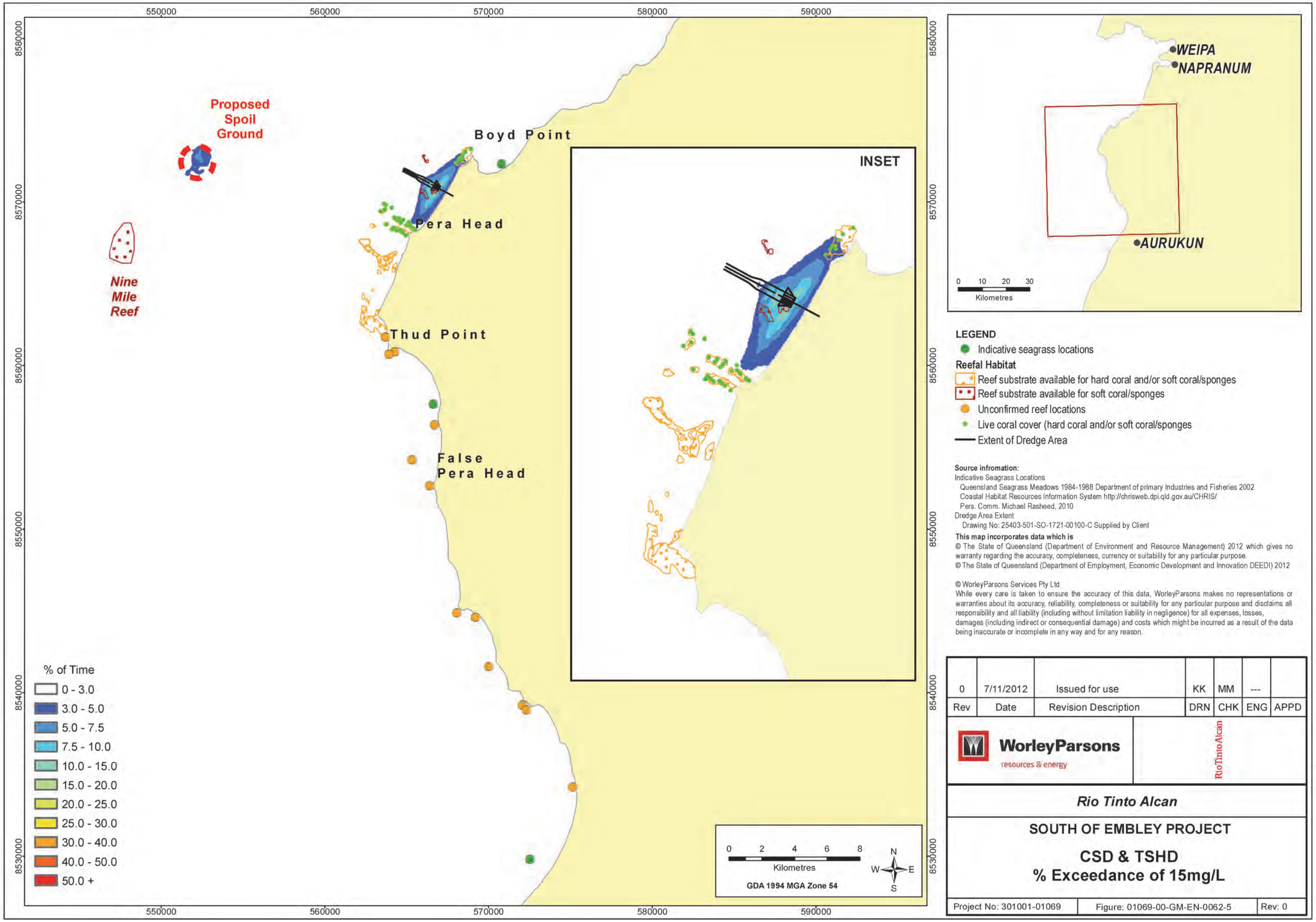

Figure 6-23 Percentage exceedance of 15 mg/L for CSD and TSHD case over the entire simulation period.

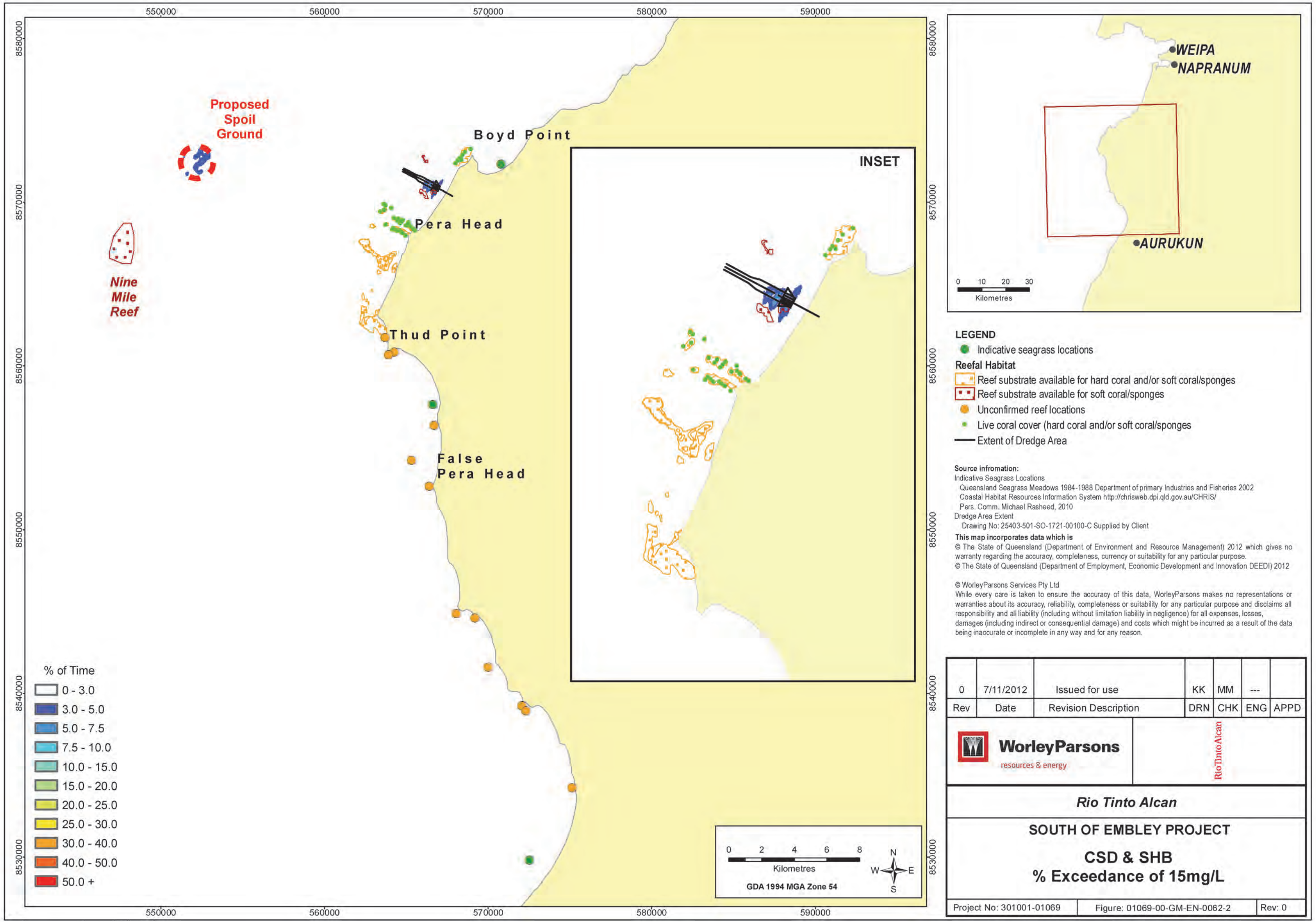

Figure 6-24 Percentage exceedance of 15 mg/L for CSD and SHB case over the entire simulation period.

6.7.2 Sediment Deposition

Outputs from sediment deposition modelling for the 2.6 million m^3 case have been plotted over the study area. The results have been presented as a daily averaged rate of sedimentation in $mg/cm^2/day$. The resulting deposition, as depicted by the median and 80th percentile daily averaged sedimentation rate, is presented in Figure 6-25 to Figure 6-28.

The sedimentation maps show that areas between Pera Head and Boyd Point are expected to experience the highest deposition rates under both dredging options. Deposition rates outside of this area, and at distances greater than 5 km from the proposed new spoil ground offshore, are expected to be negligible compared to the mean ambient conditions. Model predictions in the area immediately offshore from Pera Head, show the median above-ambient deposition as less than 2.0 $mg/cm^2/day$ for the CSD and TSHD case and for the CSD and SHB case it is only 0.8 $mg/cm^2/day$ above background.

The highest sedimentation rates are immediately within and adjacent (within 500 m) of the dredge footprint. This is the only region where the sedimentation rates are expected to exceed 7.5 $mg/cm^2/day$ under the CSD and TSHD case, with the reef colonies immediately south of the dredge area (approximately 1 km to the southwest) the only sites expected to receive a daily sedimentation rate in excess of 5.0 $mg/cm^2/day$ for more than 80 % of the dredging operation. For the CSD and SHB option this is significantly lower at below 3.0 $mg/cm^2/day$ in the same reef colonies.

Variable conditions at the proposed new spoil ground offshore during the separate SHB disposals result in a low occurence of continual depositon at any one location. As such, the TSHD disposal, given its larger load and disposal over a short timeframe, results in a larger level of sedimentation, of up to 3 $mg/cm^2/day$, under both the median and 80th percentile.

It is true that the supply of additional fine sediment loads via the dredging process also has the capacity to induce chronic changes to those areas susceptible to the accumulation of fine sediments. The remobilisation of dredge derived sediments following the completion of dredging, particularly from shallow waters, is likely to persist for several years. The active nature of the coastline, however, and frequent passage of cyclones and tropical storms, is likely to limit such effects and favour a rapid rehabilitation phase following completion of the dredging as sediments are restored to appropriate depositional environments.

It should also be noted that the sedimentation rates shown in the model, under both dredge cases modelled, are considerably lower than the relatively high and variable background sedimentation rates at the proposed Port and new spoil disposal sites. Measured background rates at Pera Head are of the order of 17 $mg/cm^2/day$ in the dry and 63 $mg/cm^2/day$ in the wet seasons, with background rates in the proposed new spoil ground approximately 47 $mg/cm^2/day$ in the dry season and 31 $mg/cm^2/day$ in the wet season (Section 6.4.4 in RTA, 2011).

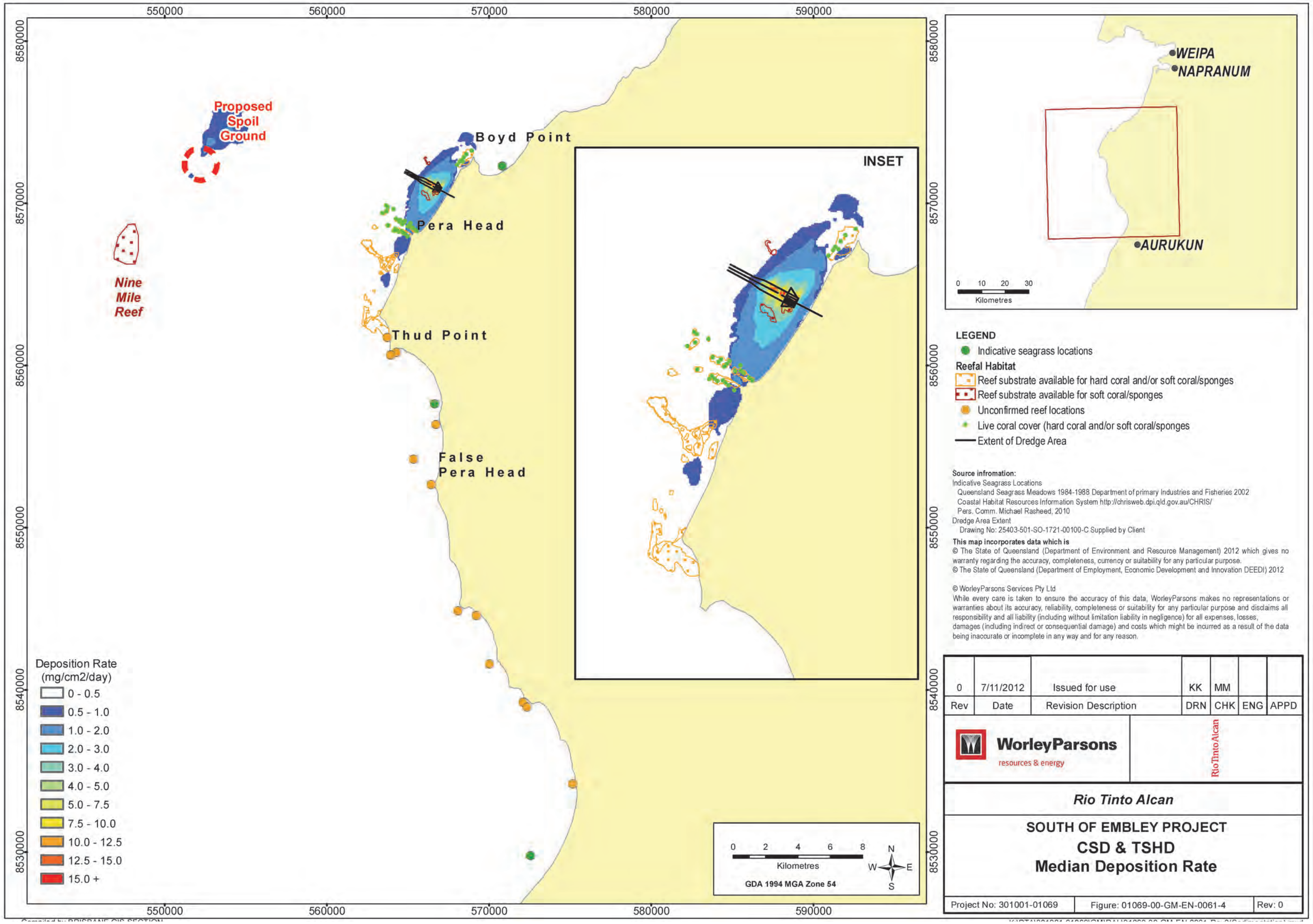

Figure 6-25 Median daily deposition rate (above background) for CSD and TSHD case over the entire simulation period.

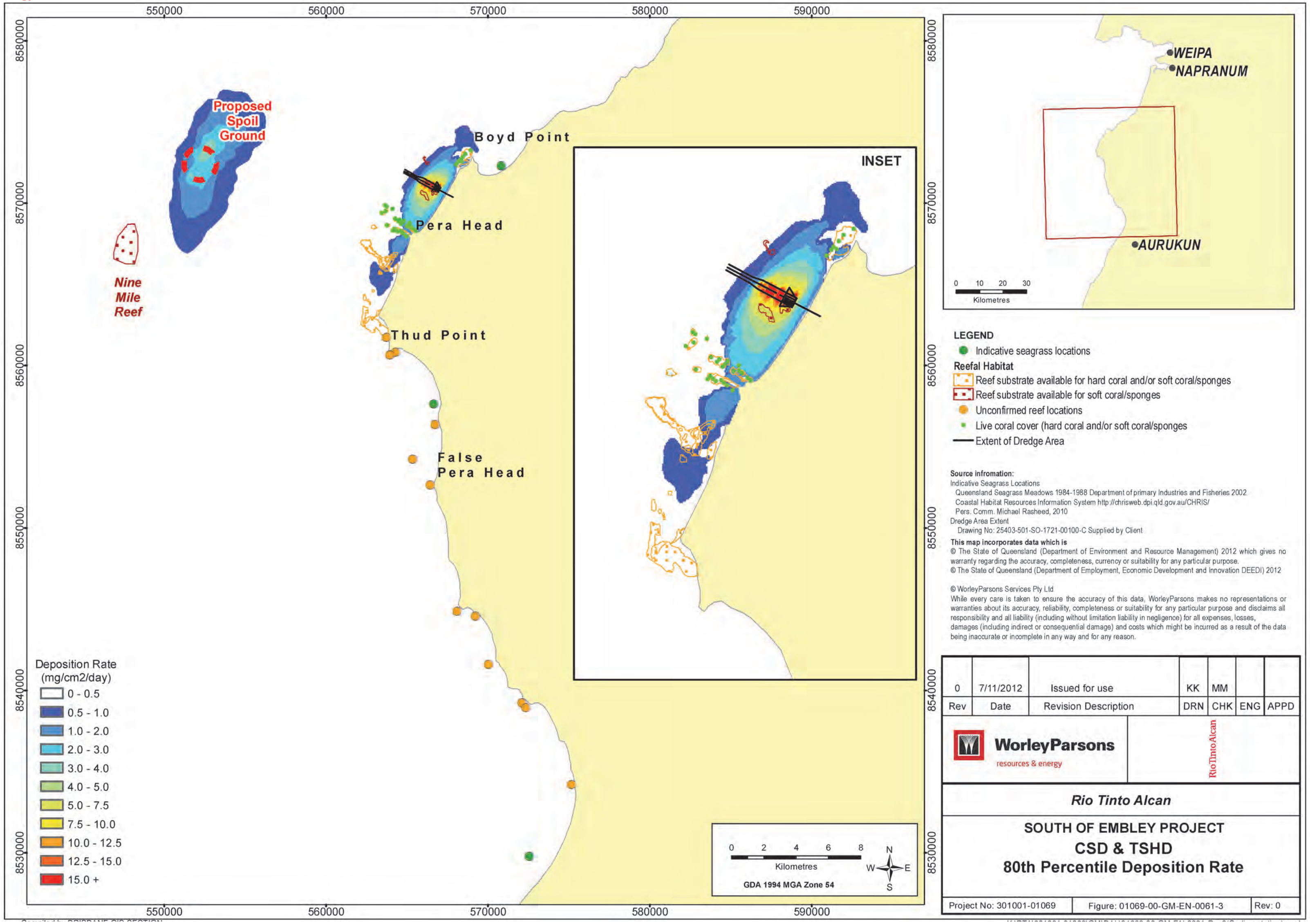

Figure 6-26 80th Percentile daily deposition rate (above background) for CSD and TSHD case over the entire simulation period.

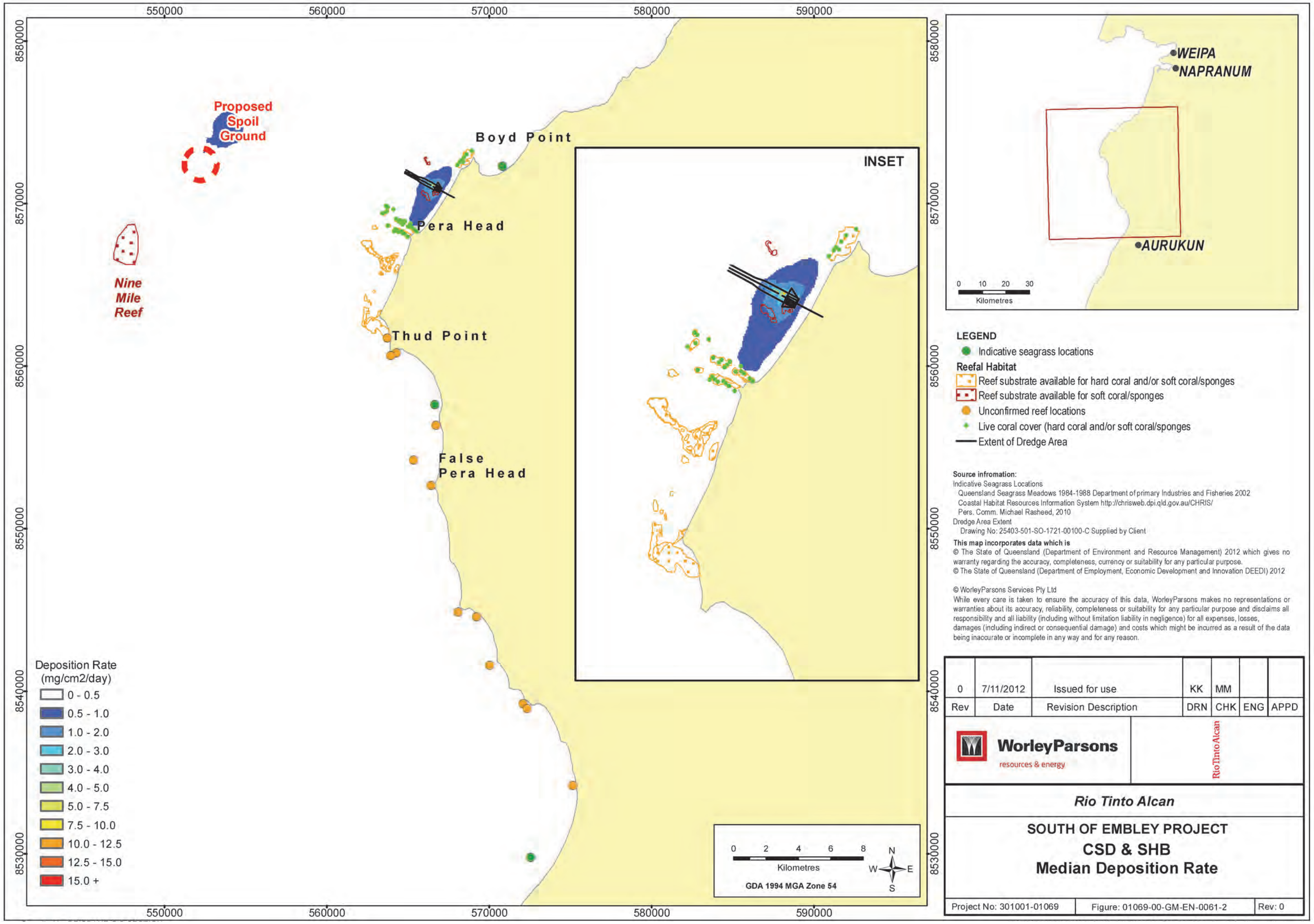

Figure 6-27 Median daily deposition rate (above background) for CSD and SHB case over the entire simulation period.

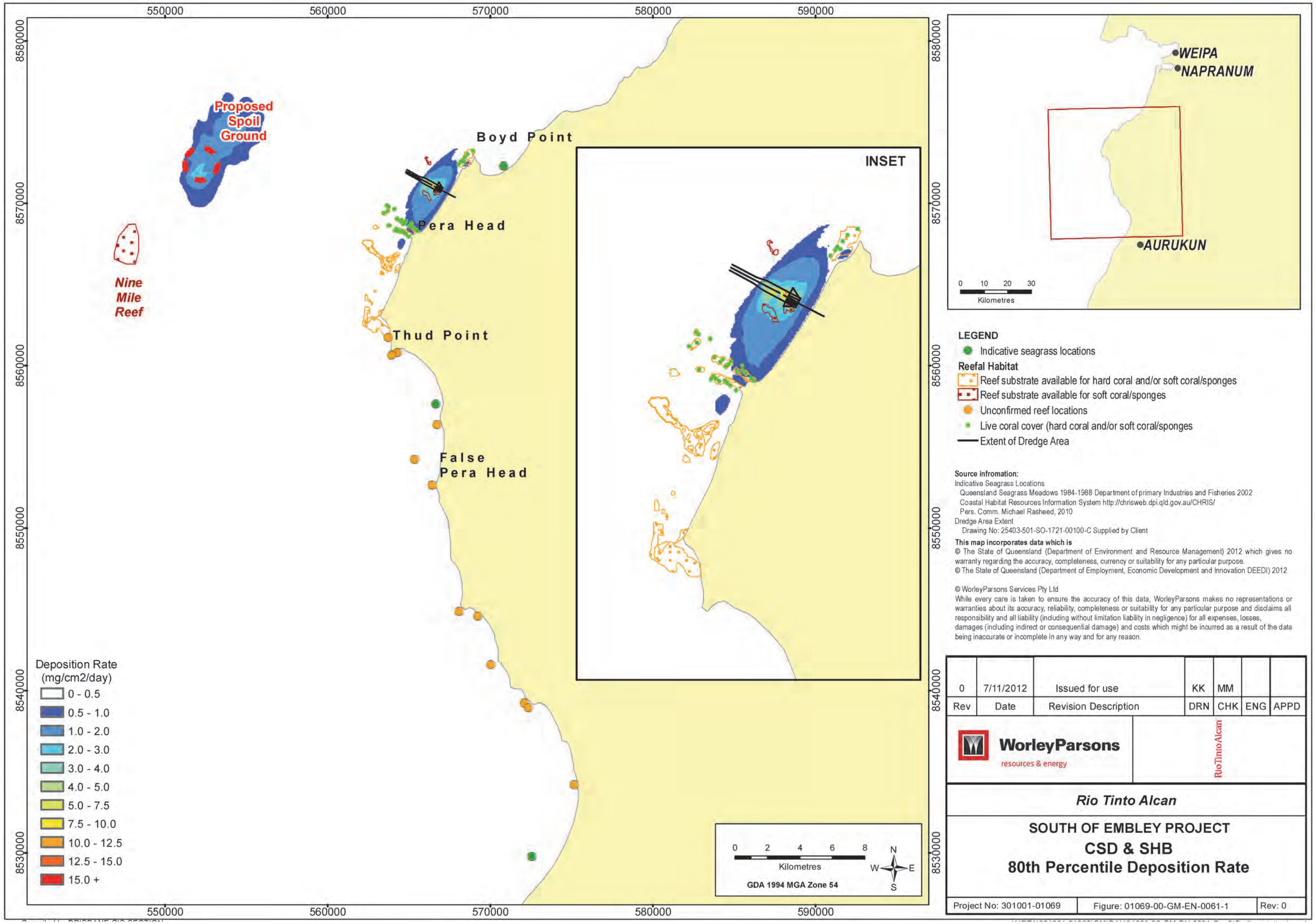

Figure 6-28 80th Percentile daily deposition rate (above background) for CSD and SHB case over the entire simulation period.

7 ASSESSMENT OF MAINTENANCE DREDGING REQUIREMENTS

7.1 Sediment Characteristics

Mobilisation of sediments surrounding the proposed dredged berth pocket is a function of the cohesive or non-cohesive nature of the material and the bed stresses that are able to be developed under prevailing current and wave conditions.

The bed material is a mixture of clays, silts, and sand, with the mean proportion for each sediment fraction shown in Table 2-4 for surface sediments. A sand-mud mixture behaves with cohesive properties when the mud fraction (sediment < 0.06 mm) is dominant and this occurs when there is more than 30% mud, and importantly when the clay fraction is greater than 5 to 10%. Clearly, from the percentage of mud in the samples, the offshore bed material at Boyd Point would behave with cohesive properties. Once the current and wave conditions are able to overcome the critical bed-shear stress, initiation of sediment motion would take place.

The cohesive strength of the seabed increases with increasing clay content and the amount of consolidation that has taken place. Van Rijn (2005) has posed the following relationship for the critical bed-shear stress:

$$\tau_{b,cr} = (1+p_{mud})^3 \, \tau_{b,cr(\text{pure sand})}$$

where:

$\tau_{b,cr}$ is the critical bed-shear stress for erosion of the sand-mud mixture

$\tau_{b,cr(\text{pure sand})}$ is the critical bed-shear stress of a pure sand bed

p_{mud} is the percentage of mud (clay + silt)

Using this relationship for the cohesive material at the proposed Port site the critical bed-shear stress is calculated to be $\tau_{b,cr}$ = 1.2 N/m^2, which is five to six times more than for a non-cohesive fine sand material. However, the critical bed-shear stress can be much lower, 0.15 N/m^2, for fresh deposits of mud (similar to pure fine sand d_{50}=0.2 mm). It is assumed here that the critical bed-shear stress is not greater than 0.3 N/m^2 for a weakly consolidated mud and greater than 1.2 N/m^2 for a moderately consolidated mud.

The conditions under which the sediment motion will occur have been calculated using hydrodynamic data and sediment characteristics from bed sampling. Assumptions for the calculations are:

- Water depth is associated with mean sea level (1.76 m LAT);
- Sand fraction 22%, mud fraction 78%;
- 10% particle size in bed d_{10} = 0.0001 m;
- 50% particle size in bed d_{50} = 0.00015 m; and
- 90% particle size in bed d_{90} = 0.0002 m.

Cases 1 to 8 are as follows:

- Case 1 – Neap tides, no waves;
- Case 2 – Neap tides, H_s=0.5m, T=5s, Θ=120 º;
- Case 3 – Neap tides, H_s =1 m, T=7s, Θ=90 º;
- Case 4 – Spring tides, no waves;
- Case 5 – Spring tides, H_s =0.5 m, T=5s, Θ=120 º;
- Case 6 – Spring tides, H_s =1 m, T=7s, Θ=90 º;
- Case 7 – Spring tides, H_s =1.5 m, T=8s, Θ=90 º; and
- Case 8 – Storm currents, H_s =4.5 m, T=10s, Θ=120 º.

Where H_s is the significant wave height, T is the peak period and Θ is the peak wave direction.

Cases 7 and 8 have assumed a moderately consolidated mud bed.

Table 7-1 shows that critical bed-shear stresses are exceeded in the situation where significant wave heights are larger than 1 metre in neap tides, assuming that the bed is not consolidated. No turbid conditions will appear in neap tide conditions without wave action as shown in Case 1, and when significant wave heights reach 0.5 m an unconsolidated bed will still not be in motion. Along the shoreline there will be some turbidity due to the shallow depths and wave breaking. Only when significant wave heights reach 1 m at times of neap tides will turbid conditions be expected to persist. In winter, 1 m waves are exceeded about 0.1% of the time, and in summer 8% of the time.

Table 7-1 Bed-shear stress at times of neap tide and varying wave conditions

Neap tide cases	Abbrev.	Case 1	Case 2	Case 3
Water depth adjacent to berth (MSL)	HD (m)	14.51	14.51	14.51
Mean vel. In current dir	VR (m/s)	0.15	0.15	0.15
Significant wave height	H_s (m)	0	0.5	1
Peak wave period	T_p (s)	0	5	7
Angle current and waves	PHI (deg)	0	120	90
Water temperature	TE (ºC)	25	25	25
Salinity of fluid (promille)	SA (promille)	35	35	35
Results				
Critical Bed-Shear Stress	Tau_cr (N/m^2)	**0.27**	**0.27**	**0.27**
Wave-related bed-shear stress	Tau_W (N/m^2)	0.00	0.19	0.92
Current-related bed-shear stress	Tau_C (N/m^2)	0.05	0.05	0.07
Total bed-shear stress	Tau_b (N/m^2)	**0.05**	**0.24**	**0.99**

Table 7-2 shows that at times of spring tides, the peak flood and ebb current forces alone are large enough to initiate sediment motion in Cases 4 to 6, and additional wave action is required to exceed the critical bed-shear stress associated with a moderately consolidated bed for Case 7 and 8. Case 7 indicates that a moderately consolidated bed will resist motion until significant wave heights have exceeded 1.5 m. Case 8 shows that the storm event captured in Figure 7-1 (b) produces much larger bed-shear stresses (5.86 N/m^2) than the critical value (1.52 N/m^2). These will result in high concentrations of the bed material in suspension and therefore available for deposition in the proposed dredge berth area.

As shown in the next section, however, it is the infrequent, short duration, storm events that prevent large amounts of sedimentation filling the proposed dredge berth.

Table 7-2 Bed-shear stresses during spring tide and varying wave conditions

Spring tide cases	Abbrev.	Case 4	Case 5	Case 6	Case 7	Case 8
Mean vel. In current dir	VR (m/s)	0.33	0.33	0.33	0.33	0.5
Significant wave height	H_s (m)	0	0.5	1	1.5	4.5
Peak wave period	T_p (s)	0	5	7	8	10
Angle current and waves	PHI (deg)	0	120	90	90	120
Water temperature	TE (ºC)	25	25	25	25	25
Salinity of fluid (promille)	SA (promille)	35	35	35	35	35
Results						
Critical Bed-Shear Stress	Tau_cr (N/m^2)	**0.30**	**0.27**	**0.30**	**1.52**	**1.52**
Wave-related bed-shear stress	Tau_W (N/m^2)	0.00	0.18	1.09	1.90	5.14
Current-related bed-shear stress	Tau_C (N/m^2)	0.32	0.35	0.35	0.35	0.72
Total bed-shear stress	Tau_b (N/m^2)	**0.32**	**0.53**	**1.45**	**2.25**	**5.86**

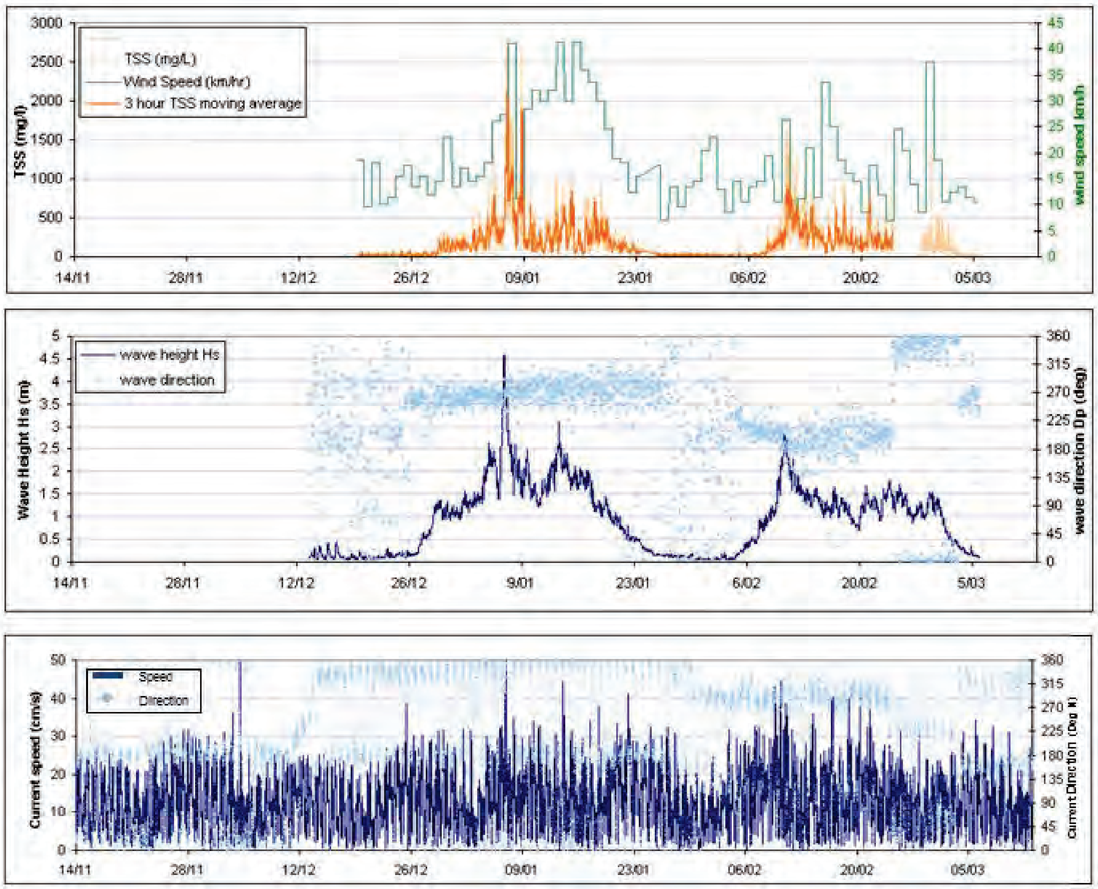

Figure 7-1 (a) Turbidity sensor data TSS (mg/L) (b) wave conditions (c) currents at Boyd Point late 2007 and early 2008

7.2 Siltation Analysis of Proposed Dredged Berth

As shown in Section 7.1 there is a high potential for sediment mobilisation at the dredge site and the majority of this material is mud. The proposed berth pockets are therefore expected to experience siltation. For the purpose of siltation calculations the proposed dredged area has been divided into three areas, as illustrated in Figure 7-2.

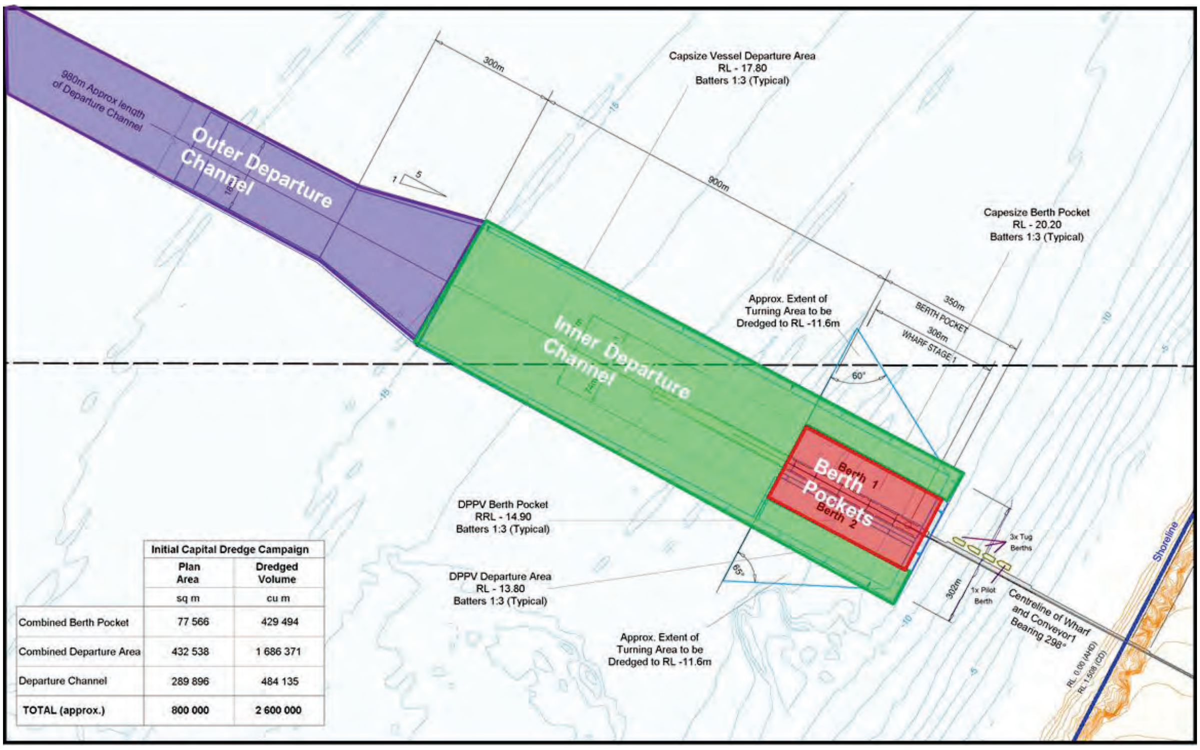

	Initial Capital Dredge Campaign	
	Plan Area	Dredged Volume
	sq m	cu m
Combined Berth Pocket	77 566	429 494
Combined Departure Area	432 538	1 686 371
Departure Channel	289 896	484 135
TOTAL (approx.)	800 000	2 600 000

Figure 7-2 Extract from drawing 25403-501-S0-1721-00100-RevC showing the siltation calculation areas

For the siltation calculations, a representative weighted-average depth was employed at each area as a representation for the various dredge depths. Other parameters that have been assumed for the purpose of siltation calculations are provided in Table 7-3. These parameters are used for the berth pockets, departure areas, and departure channel.

Potential siltation amounts for the proposed berths have been calculated using the percentage exceedance curves for wave heights from records at the Weipa wave buoy. Assumed suspended sediment concentrations for a given wave height are based on recorded data shown in Figure 7-1.

Table 7-3 Parameters assumed for siltation calculations (w_s = fall velocity of sediment)

Parameter	Assumed value
d_{50} of sand fraction	0.00015 (m)
d_{90} of sand fraction	0.0002 (m)
Percentage of sand fraction	20 %
Fluid density	1024 (kg/m^3)
Sediment density	2650 (kg/m^3)
Kinematic viscosity	0.000001 (m^2/s)
W_s suspended clay (< 10 microns)	0.0003 (m/s)
W_s suspended silt (10 to 50 microns)	0.002 (m/s)
W_s suspended sand (> 50 microns)	0.02 (m/s)
Bed Roughness outside	0.02 (m)
Bed roughness in channel	0.02 (m)

Table 7-4 Annual siltation parameters

Significant Wave Height, H_s (m)	*Peak Period,* T_p (s)	% Exceedance	Exceedance (days)	Occurrence of H_s (days)	Concentration (mg/l)
>0.5	5	20.0	73.0	58.40	100
>1	6	4.0	14.6	7.30	200
>1.5	7	2.0	7.3	5.48	400
>2	8	0.5	1.8	1.53	1000
>3	10	0.1	0.3	0.26	1500
>4	12	0.01	0.0	0.04	2000
Total			**73**		

The trapping efficiency and consequent siltation in the proposed berth pockets, and departure areas has been assessed using the SED-PIT model by Van Rijn (2005) for determining trench infilling, as used for previous siltation assessment. This analysis assumes a simplistic 1-D channel shape and considers the current approach velocity and angle, approach depth, approach bed-shear velocity, particle fall velocity, wave height, berth depth and width, and bed roughness.

Based on the results from Table 7-4, the estimated average annual siltation depths are shown in Table 7-5 and the volume of annual infill are provided in Table 7-6.

Table 7-5 Annual siltation (m) based on wave exceedance, metres per year

H_s (m)	Berth Pockets	Inner Departure Channel	Outer Departure Channel
>0.5	0.49	0.33	0.20
>1	0.10	0.07	0.04
>1.5	0.15	0.10	0.06
>2	0.10	0.06	0.04
>3	0.02	0.02	0.01
>4	0.00	0.00	0.00
Total (m)	**0.87**	**0.58**	**0.35**

Table 7-6 Estimated annual average siltation depths and infill volumes

Zone	Annual average siltation depth (m)	Plan Area (m^2)	Infill Volume (m^3)
Berth Pockets	0.87	77,566	67,482
Inner Departure Channel	0.58	432,538	250,870
Outer Departure Channel	0.35	289,896	101,464
Totals		800,000	419,816

Depths of siltation in the proposed berth pockets will vary over the area, and is likely to be higher towards the shoreward end of the berths and channels. This assessment considers only currents of wave and tidal origin; it does not include the actions of propellers from vessel movements in the departure channel. It is likely that propellers would have some impact on local siltation rates and patterns.

The predicted average siltation depth in an average year varies from 0.35 m to 0.87 m (compared with 1.15 m and 0.33 m calculated previously). The predicted total annual volume required for maintenance dredging is 420,000 m^3 for the 2.6 million m^3 case.

The predicted siltation depths and volumes have a high level of uncertainty, primarily due to the number of simplifications and assumptions in relation to the sediment behaviour, wave climate and channel schematisation. The depths adjacent to the proposed departure channel vary and this has a direct impact on the accuracy of determining the amount of siltation that occurs along its length based on only one adjacent depth. The shape of the channel is assumed to be rectangular, although realistically the channel shape will be more rounded, which would result in less siltation than what has been estimated here.

It should be noted that this calculation has been performed for an average year. There will be significant year to year variation in the wave climate based on the frequency of storms, leading to higher or lower siltation. The wave event at Boyd Point in early 2008 is an example of how the annual average deposition derived from the exceedance curves can be exceeded in one storm with a return period greater than one-year. To predict siltation rates for ‘good’ and ‘bad’ years with different return intervals, analysis of the wave climate over a longer period of time is necessary.

8 CONCLUSIONS

The sediment dispersion modelling conducted for this assessment has enabled the prediction of the spatial extent of the sediment plume and deposition characteristics associated with initial capital dredging and soil disposal activities for the proposed Port facility to be investigated and defined. The accuracy of the results obtained in this study has been ensured through detailed interrogation of all datasets utilised in the model development and supported through the high level of skill provided in the hydrodynamic (MIKE3 HD) and wave (MIKE21 SW) model forcing functions.

The entire initial capital dredging program was modelled under two separate dredging options, following the validation of the MIKE 3 MT sediment transport model for the region, inclusive of expected downtime of dredging operations and variable meteorological and oceanographic forcing over the respective dredging programs. Modelling the two separate dredging methodologies has provided a valuable insight into the mobilised material behaviour as a function of the two dredging options.

Key findings from the sediment transport modelling results are presented below.

8.1 Suspended Sediment Concentration

The TSS resulting from the dredging operations were characterised through analysis of the median and 80th percentile maps, time series at sensitive receptor sites, and exceedance of set concentration limits as a percentage of the total dredging duration. This multi-faceted approach to the analysis enabled the plume behavior to be defined and characterised in detail across the two dredging options.

The main findings of the sediment fate model are listed below.

- The turbid plume generated by Port area initial capital dredging extends generally parallel to the coast, from beyond Pera Head and Thud Point in the south (migrating during flood tide) to Boyd Point in the north (migrating during ebb tide).
- The net south-west tidal current direction causes suspended material to accumulate between the proposed Port and Pera Head, with the plume extending up to 27 km south of the proposed development (at concentrations >2 mg/L above background).
- Periods of elevated TSS concentration generally coincide with the TSHD and CSD operating in the inshore area during the dredging of the top layer of sediments, as a result of the higher content of fines in this layer. Whilst the Boyd Point experiences higher instantaneous TSS levels (due to its closer proximity to the dredging operations), Pera Head is predicted to receive more consistently maintained elevated TSS levels due to the net migration south.
- Comparatively, the CSD and TSHD option is shown to produce a larger plume in the nearshore than the CSD and SHB option. This is the result of the multiple discharge sources acting simultaneously and additional discharge from the CSD diffuser contributing to the larger plume present under this dredging methodology.

- The CSD and TSHD option not only produces higher instantaneous and daily average concentrations, but also a more prolonged plume in this vicinity due to the longer dredging operations.
- Offshore at the Nine Mile Reef receptor sites, concentrations are shown to be consistently low under both dredging operations, with the instantaneous depth-averaged TSS less than 5 mg/L, and daily average less than 3 mg/L, under both dredging methodologies.
- Due to the larger volume of material that would be dumped by the TSHD, the instantaneous TSS concentrations at the proposed new spoil ground offshore are higher under the CSD and TSHD case, however, the daily-averaged TSS is comparable amongst both cases due to the more frequent SHB dumping.
- Depth-variation in TSS is significant amongst both dredging options, with peak daily near-seabed TSS concentrations often double those near the surface.

8.2 Total Sedimentation

Sedimentation predicted in the dredge dispersion model was assessed through analysing the mean daily deposition rate over the entire model simulation. In this analysis the deposition rate over the dredging period combining all particle classes was selected as it presented the most indicative level of expected deposition over the dredging program.

Key findings from the analysis of the sedimentation predicted by the model were:

- Areas between Pera Head and Boyd Point are expected to experience the highest deposition rates under both dredging options, with rates outside of this area expected to be negligible compared to the background rates at Pera Head of 17 mg/cm^2/day and 63 mg/cm^2/day in the dry and wet seasons, respectively;
- At both the nearshore and offshore locations the sedimentation is predicted to be lower under the CSD and SHB dredging option;
- Model predictions near the reef areas immediately offshore from Pera Head show the median above-ambient deposition as less than 2.0 mg/cm^2/day under the CSD and TSHD case, and less than 0.8 mg/cm^2/day under the CSD and SHB case;
- The highest sedimentation rates, in excess of 7.5 mg/cm^2/day above background for the CSD and TSHD case, are in the immediate vicinity (within 500 m) of the dredge footprint. Again this is lower at approximately 5.0 mg/cm^2/day under the CSD and SHB option;
- The reef colony immediately south of the dredge area (approximately 1 km to the southwest) is the only sites expected to receive a daily sedimentation rate in excess of 5.0 mg/cm^2/day for more than 80 % of the dredging operation for the CSD and TSHD case, and below 3.0 mg/cm^2/day for the CSD and SHB option;
- Variable conditions at the proposed new spoil ground offshore during the separate SHB disposals result in a low mean daily sedimentation, wheras the TSHD disposal, given its larger load and disposal over a short timeframe, results in a larger level of sedimentation, of up to 3 mg/cm^2/day as depicted in the 80th percentile; and

- Deposition rates above background (0.5 to 2 mg/cm^2/day) would not extend beyond 4km outside the proposed new spoil ground area for either dredging methodologies. The increase in deposition outside the proposed new spoil ground area is expected to be negligible compared to the mean background rates in the area of 47 mg/cm^2/day and 31 mg/cm^2/day for dry and wet season, respectively.

While the suspended sediment concentrations and sedimentation rates are lower for the CSD and SHB compared to the CSD and TSHD method, both methods result in suspended sediment plumes and sedimentation rates that are within the range of the relatively high and variable background at the proposed Port and new spoil disposal sites (refer Section 6.4.4 in RTA, 2011).

8.3 Estimated Maintenance Dredging Requirements

The predicted average siltation depth in the berth pockets, departure area, and departure channel in an average year varies from 0.35 m to 0.87 m. The predicted total annual volume required for maintenance dredging is 420,000 m^3 for the 2.6 million m^3 dredge volume case. This was calculated for a typical year of wave and wind conditions and, as such, it is expected that a potentially significant year to year variation in the wave climate based on the frequency of storms may lead to higher or lower siltation levels.

9 REFERENCES

Andersen, O. B., 1995, "Global ocean tides from ERS 1 and TOPEX/POSEIDON altimetry", J. of Geophys. Res., 100, C12, 25249-25260.

BOM, 2011, National Tide Facility web page: Tide Precitions for Queensland – Weipa (http://www.bom.gov.au/oceanography/tides/MAPS/weipa.shtml#map) [Accessed 22 May 2011]

Booij, N., Ris, R.C., Holthuijsen, L.H., 1999, "A third-generation wave model for coastal regions, Part 1, Model description and validation, J. of Geophys. Res., 104, C4, 7649-7666.

Chung Dang Huu, (2007) "Effects of temperature and salinity on the suspended sand transport", International Journal of Numerical Methods for Heat & Fluid Flow, Vol. 17 Iss: 5, pp.512 - 521

Coffey Geotechnics Pty Ltd, 2009, Rio Tinto Alcan South Of Embley Feasibility Study Nearshore Geotechnical Investigation Interpretative Report, for Bechtel Australia Pty Ltd, GEOTNEWS20261AA BR, 7 April 2009.

Dames & Moore (compiled by), October 1994, The Century Project : draft impact assessment study report, [prepared for] Century Zinc.

Dankers, P.J.T., 2002, "The behavior of fines released due to dredging. A literature review", TU Delft, The Netherlands.

Department of Environment and Heritage, 1998, 'Wave data recording program – Weipa Region For the years 1978 - 1997', Queensland Government, Wave data recording program report No. 13 (W07.2), now the Environmental Protection Agency.

Danish Hydraulic Institute (DHI), 2011, MIKE 3 Flow Model: Hydrodynamic Module Scientific Documentation.

Doorn-Groen, S.M. and Foster, T.M. (2007), Environmental Monitoring and Management of Reclamation Works Close to Sensitive Habitats. Proceedings of the XVIII World Dredging Congress. Orlando, USA (27 May 2007).

Fabricius KE, De'ath G, Poutinen ML, Done T, Cooper TF, Burgess SC (2008). Disturbance gradients on inshore and offshore coral reefs caused by a severe tropical cyclone. Limnol Oceanogr 53: 690-704

GHD 2008, South of Embley Pre-Feasibility Study: Combined Field Data Collection Report (06/07 and 07/08), Prepared for Rio Tinto Alcan, July 2008

Harris, P.T., Heap, A., Marshall, J., Hemer, M., Daniell, J., Hancock, A., Buchanan, C., Brewer, D., Heales, D. (2006) Submerged coral reefs and benthic habitats of the southern Gulf of Carpentaria: Post-Survey Report GA Survey 276, RV Southern Surveyor. Geosciences Australia Record 2007/02, 134 pp.

ICSM, accessed 2008 "The Factors Contributing to the level of Confidence in the Tidal Predictions Accuracy of Tidal Predictions", Permanent Committee on Tides and Mean Sea Level (PCTMSL) and Tidal Interface Working Group (TIWG), from http://www.icsm.gov.au/icsm/tides/

Intergovernmental Panel on Climate Change, 2007, Fourth Assessment Report: Climate Change 2007: Synthesis Report, Summary for Policymakers.

Jones, G., Baban, S., and Pathirana, S. 2008, Coastal Erosion Issues in the East Point and Nightcliff areas of Darwin, Report prepared for Darwin City Council, School of Environmental Science and Management, Southern Cross University, Lismore, NSW. Accessed 2008, from http://www.google.com/search?q=documents%2fCou1stagn05ColouredAttachmenttoItem12_2forweb.pdf

Jones, M. R., 1986, "Surficial sediments of the central Gulf of Carpentaria. Geological Survey of Queensland, Report 1986/40.

L.C. van Rijn, A.G. Davies, J.S. Ribberink, J. van de Graaff, eds., 2001, Sediment Transport Modelling in Marine Coastal Environments, Aqua Publications, 2001

National Committee on Coastal and Ocean Engineering, 2004, Guidelines for Responding to the Effects of Climate Change in Coastal and Ocean Engineering, 2004 Update, Engineers Australia.

Pennekamp, JGS and Quaak, MP (1990). "Impact on the Environment of Turbidity Caused by Dredging". Terra et Aqua, nr. 42, April, pp. 10-20.

Queensland Government, 1998, 'Wave data recording program, Weipa Region, for the years 1978-1997', Wave data recording program report No. 13 (W07.2), Environmental Protection Agency.

Roelofs, A.J., Rasheed, M.A., Thomas, R., McKenna, S. and Taylor, H. (2006). Port of Weipa Long Term Seagrass Monitoring, 2003 - 2005. Ecoports Monograph Series No. 23 Ports Corporation of Queensland. 31pp.

RTA. 2011. Queensland EIS for South of Embley Project.

SKM, 2008, "Draft SoE Feasibility Study – Dredging".

Somers I.F. and Long B.G. 1994. Short communication: Note on the sediments and hydrology of the Gulf of Carpentaria, Australia. Australian Journal of Marine & Freshwater Science, 45(3): 282-292.

State of Queensland (Department of Natural resources and Mines), 2004, Queensland Climate Change and Community Vulnerability to Tropical Cyclones, Project Synthesis Report – August 2004.

Sudusta, J. A., 1988, 'Non-linear interaction of wind and tide driven currents in the Gulf of Carpentaria', M.Sc. Thesis, Dep. Geol. Geophys, Univ. Sydney, 123 pp.

TOLMAN, H. L. 2002. Testing of WAVEWATCH III Version 2.22 in NCEP's NWW3 Ocean Wave Model Suite, Technical Note No. 214.

Whitehouse, R., Soulsby, R., Roberts, W., Mitchener, H., 2000, Dynamics of estuarine muds, HR Wallingford. Thomas Telford Publishing, London, UK.

Wolanski, E. 1993, 'Water circulation in the Gulf of Carpentaria', J. of Mar. Sys., 4., 401-420.

Worley Parsons, 2011. South of Embley Project: Revised capital dredge results and maintenance dredging requirements. Prepared for Rio Tinto Alcan (Doc No. 301001-01069-00-EN-REP-0006)

Van Rijn, L. 2005, Principles of Sedimentation and Erosion Engineering in Rivers, Estuaries and Coastal Seas, Aqua Publications, Netherlands (pp.580)